# Analyses of the Substrate-Selective Ubiquitination of Mitotic Regulators and its Involvement in Silencing the Spindle Assembly Checkpoint

Yasunori Horikoshi

# Contents

# List of Figures



# List of Tables

# Abstract

During ordered mitotic progression, various proteins are quantitatively regulated by an identical ubiquitin ligase, the anaphase-promoting complex or cyclosome (APC/C)-dependent ubiquitination and subsequent proteasomal degradation with the respective appropriate timings. To date, it has been revealed that in order to deal with the orchestrated proteolysis APC/C sequentially alters its substrate specificity during mitosis, and one of the regulatory mechanisms for it is the spindle assembly checkpoint (SAC). The SAC targets Cdc20, an APC/C coactivator required for substrate recognition, to incorporate it into mitotic checkpoint complex (MCC) and form APC/C bound to MCC (APC/C$^{MCC}$), and inhibits ubiquitination catalyzed by APC/C bound to Cdc20 (APC/C$^{Cdc20}$). Intriguingly, current studies have implied that the activity of APC/C also contributes to the disassembly of APC/C$^{MCC}$ in the process of silencing the SAC.

In the present research, I first describe a fission yeast temperature-sensitive *ubc11-P93L* mutant in which cell cycle progression is arrested at mitosis. The *ubc11*$^{+}$ gene encodes one of the two E2 enzymes required for progression through mitosis in fission yeast. The temperature-sensitivity could be suppressed in the absence of the functional SAC, suggesting that the arrest is not due to abnormal spindle assembly, but rather due to prolonged activation of this checkpoint. Supporting this notion, MCCs remain bound to APC/C even when the SAC is satisfied. It is remarkable that Slp1 (a fission yeast homolog of Cdc20), which is degraded in an APC/C-dependent manner, stays stable throughout the cell cycle in the *ubc11-P93L* mutant lacking the functional SAC. Other APC/C substrates, in contrast, were degraded on schedule. I have also found that a defect of Ubc4, the other E2 required for progression through mitosis, does not affect the stability of Slp1. I further attempted to analyze the *cut23-Y395H* mutant. The *cut23*$^{+}$ gene encodes one of the fission yeast APC/C subunits, and the mutant also exhibited the SAC-dependent temperature-sensitivity and abnormal mitotic phenotypes at the restrictive temperature. In these cells, as is the case in *ubc11-P93L* mutants, Slp1 became stable independently of the SAC.

I propose that each of the two E2 enzymes is responsible for collaborating with APC/C for a specific set of substrates, and that in addition, some kind of subunits can be utilized as a determinant of a specific set of substrates. Besides, I propose that Ubc11 is responsible for regulating Slp1 with APC/C for silencing the SAC.

# Introduction

## The cell cycle progression and ubiquitin-dependent proteolysis

### The cell theory

As well as the theory of evolution or the double-helix structure of DNA encoding genetic information (Avery et al., 1944; HERSHEY and CHASE, 1952; WATSON and CRICK, 1953), the cell theory is a well-known scientific theory that is one of the foundations of biology. According to this, all living organisms are composed of one or more cells, cells are the most basic unit for function and structure of all organisms, and *"Omnis cellula e cellula"*: the concept that all cells come from cells that already exist. A cell reproduces by performing an orderly sequence of events in which it duplicates its contents and then divides in two. This cycle of duplication and division is known as the cell cycle, and its most fundamental task is to pass on of the genetic information to the next generation of cells.

### Four phases of the cell cycle

The eucaryotic cell cycle is traditionally divided into four sequential phases and each of them is generally defined as $G_1$ phase, S phase, $G_2$ phase and M phase, respectively (Figure 1). During S phase (S for synthesis), the DNA in each chromosome, the structure composed of a DNA molecule and associated proteins, is faithfully replicated to produce two complete copies. After DNA replication the duplicated chromosomes are distributed to the two daughter cells so that each receives a copy of the entire genome. This period is termed M phase (M for mitosis). Since it takes much more time for most cells to grow and double their mass of proteins and organelles other than DNA replication and cell division, extra gap phases are inserted in most cell cycles: a $G_1$ phase between M phase and S phase, and a $G_2$ phase between S phase and M phase. In addition, $G_1$, S and $G_2$ together are called interphase.

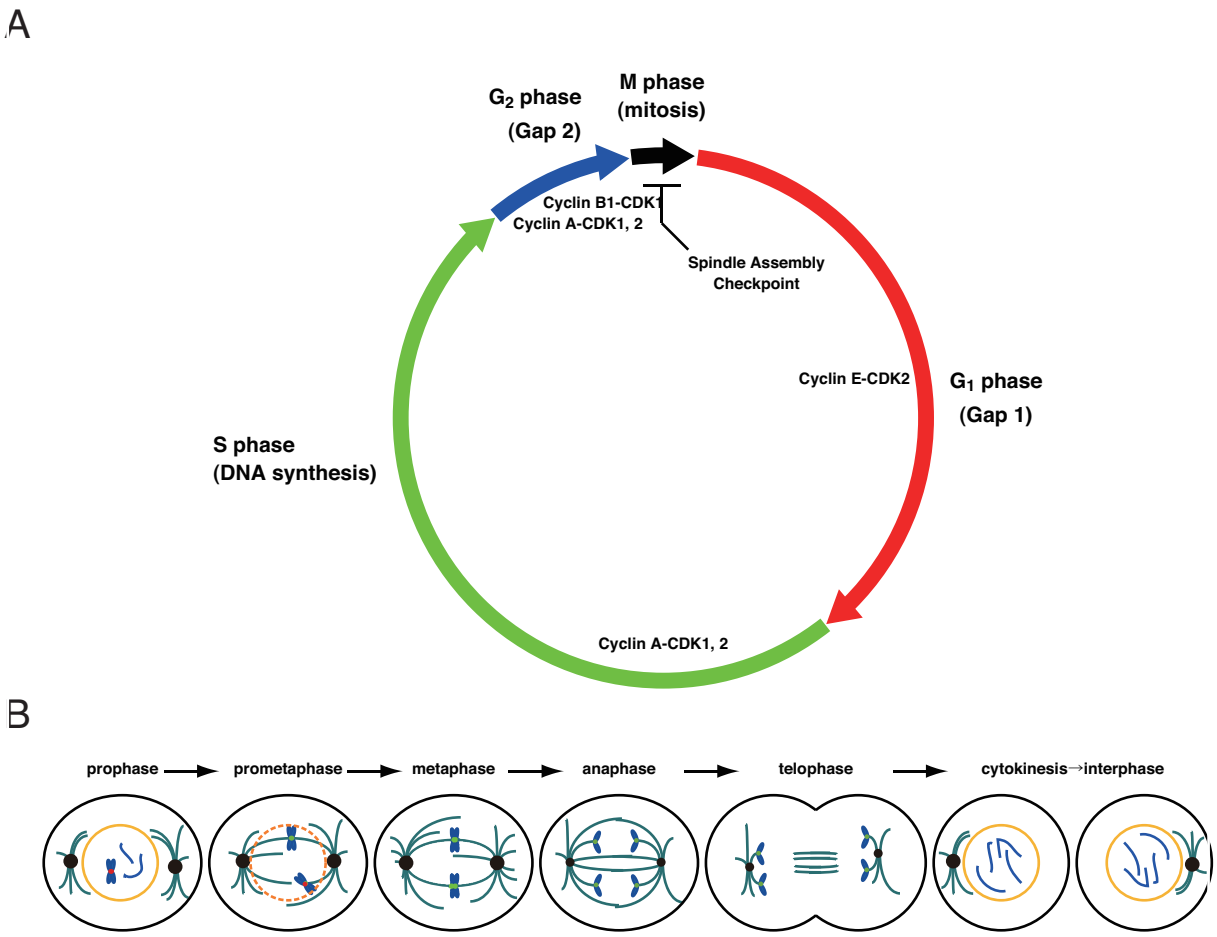


Figure 1 The cell cycle and mitosis.

(A) The eukaryotic cell cycle is traditionally divided into four sequential phases. Each of the phases is regulated by the indicated cyclin-dependent kinases respectively. (B) M phase is further divided into six stages. Each component is stained as follows; chromosomes are blue, centrosomes are black, nuclear envelope is orange and microtubules are green. See text for details.

## The cell cycle and checkpoint mechanisms

For orderly progression through the cell cycle, the initiation of many cycle-specific events requires the successful execution of some previous events. Preparing to the case of incompletion of previous events, cells are equipped with surveillance-feed-back mechanisms, called "checkpoints", and the cycle can be arrested at appropriate phases (Hartwell and Weinert, 1989). Well-known examples are the DNA damage checkpoint and DNA replication checkpoint. The former monitors DNA damage as implied by the name and in the presence of the damaged DNA, delays the cycle to provide time for the DNA to be repaired. Likewise, the latter also surveys the completion of DNA replication and treatments that block the event cause arrest at the S phase owing to the activation of this checkpoint. Including other checkpoints that aren't mentioned above, all of them are the essential mechanisms that ensure the fidelity of "the blueprint of life".

## The ubiquitin-dependent proteasomal degradation

Proper cell cycle progression is a collective phenomenon, which can be brought about by an orderly sequence of intricate reactions among various regulators. It is remarkable that most of the individual enzymatic activities are strictly limited to only when required. The quantitative control by ubiquitin-dependent proteasomal degradation is an essential one of such regulatory mechanisms. For a drastic example, the programmed destruction of B-type cyclin results in the irreversible inactivation of cyclin-dependent kinase (Cdk) in late mitosis (Glotzer et al., 1991; Hershko et al., 1991). Together with the existence of inhibitors or regulation of gene expression, this proteolytic system contributes to oscillation of the activity of this "cell cycle engine".

Ubiquitination is nowadays commonly-recognized as one of the most biologically significant posttranslational modifications. This modification is carried out in a series of reactions: ubiquitin activation, conjugation and ligation (Figure 2). These processes are mediated by ubiquitin-activating enzymes (E1s), ubiquitin-conjugating enzymes (E2s) and ubiquitin ligases (E3s). In the first reaction, ubiquitin activation, the carboxyl terminus of ubiquitin is activated through its high-energy thioester linkage to the sulfhydryl group of a cysteine in the active site of the E1 molecule (Ciechanover et al., 1981, 1982; Haas and Rose, 1982; Haas et al., 1983). This reaction requires ATP hydrolysis, and it proceeds via a covalent AMP-ubiquitin intermediate. The E1-ubiquitin conjugate subsequently interacts with one of a family of E2s and the activated ubiquitin on E1 is transferred to an active-site cysteine in the E2 molecule (Hershko et al., 1983; Pickart and Rose, 1985). The E2 and substrate are brought together by a target-specific E3, which then catalyzes the formation of a peptide bond between the activated carboxy-terminal glycine of ubiquitin from the E2-ubiquitin conjugate and the

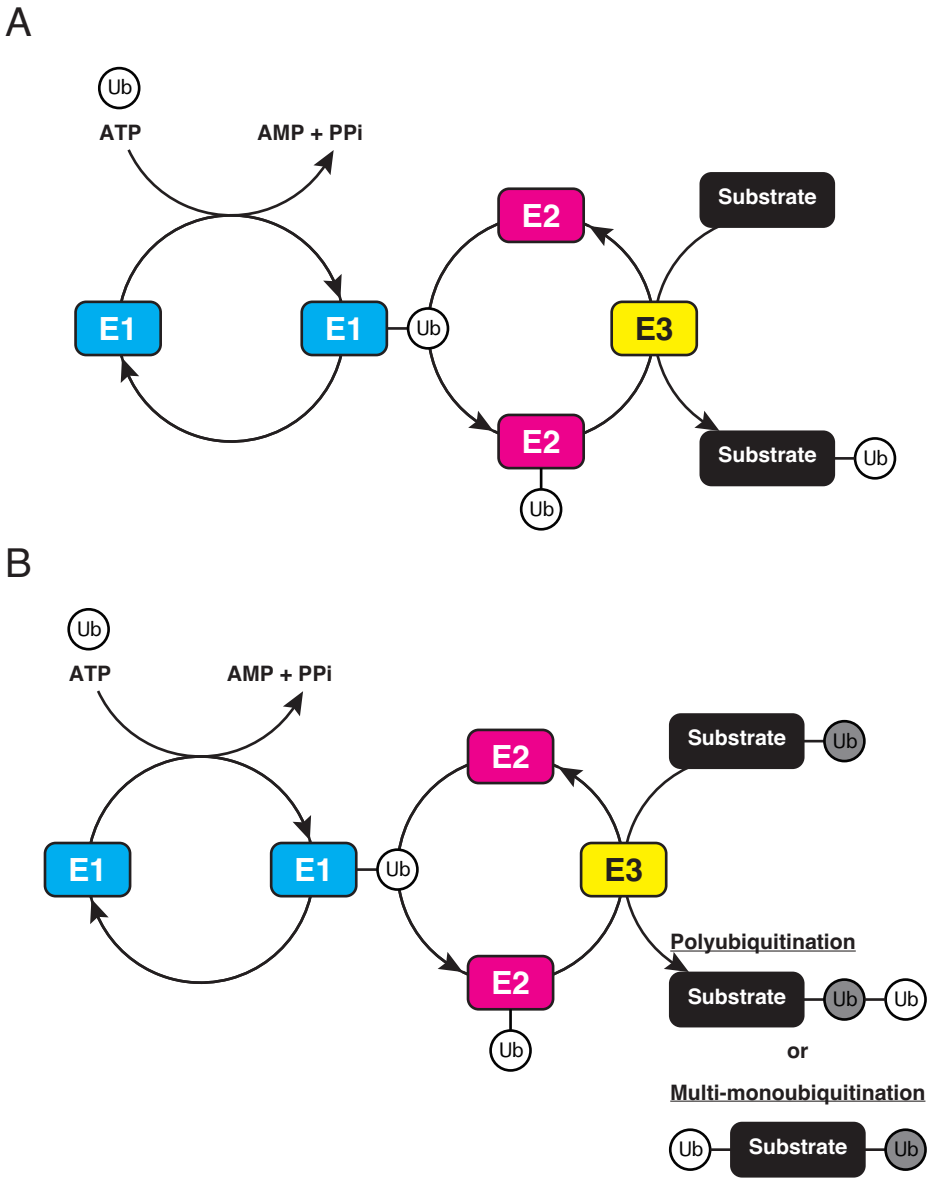


Figure 2 Steps in protein ubiquitination.
Schematic overview of monoubiquitination (A) and polyubiquitination or multi-monoubiquitination (B). See text for details.

amino group of a lysine side chain in the target protein (Goldknopf and Busch, 1977; Hershko et al., 1980, 1983, 1984, 1986). In principle, proteasomal proteolysis requires long polyubiquitin chains on the substrate as a degradation signal, and they are formed by transferring additional ubiquitins to lysine residues within ubiquitins themselves (Hough and Rechsteiner, 1984; Hershko et al., 1984; Hough et al., 1986; Deveraux et al., 1994; Thrower et al., 2000). On the other hand, however, by recent discoveries there has been an increase in the number of the exceptions (Hershko et al., 1984; Shaeffer, 1994; De Domenico et al., 2006; Boutet et al., 2007; Kravtsova-Ivantsiv et al., 2009; Yin et al., 2010; Carvallo et al., 2010; Dimova et al., 2012).

# The mitotic progression and the Anaphase Promoting Complex/Cyclosome

## The six stages of mitosis

Mitosis is further divided into six stages traditionally: prophase, prometaphase, metaphase, anaphase, telophase and cytokinesis, respectively (Figure 1B). At prophase, chromosome condensation occurs and subsequently nuclear envelope breaks down at prometaphase. The duplicated chromosomes simultaneously become attached to the microtubules of the mitotic spindle. At metaphase, the chromosomes are aligned at the equator of the mitotic spindle. The abrupt segregation of sister chromatids marks the beginning of anaphase, and during this phase the chromosomes move to opposite poles of the spindle. Undergoing the decondensation of chromosomes and rearrangement of nuclei, the cell is pinched in two by cytokinesis, and cell division is completed.

## The Anaphase Promoting Complex/Cyclosome

### Architectural map of the APC/C

The quantitative regulation of proteins can be also observed during the orderd mitotic progression. The central component of the ubiquitin-proteasome pathway in mitosis is the anaphase-promoting complex or cyclosome (APC/C) (Hershko et al., 1994; Sudakin et al., 1995). The APC/C is a high-molecular mass of over 1-MDa complex composed of more than a dozen different subunits, most of which are well conserved in evolution (Table 1 and Figure 3). Each of them can be roughly classified into four groups: a component of the catalytic subcomplex, tetratricopeptiderepeat (TPR) subunit, scaffolding protein or the others (Thornton et al., 2006).

The catalytic subcomplex is comprised of APC2, a cullin subunit, and APC11, a RING-finger protein (Zachariae et al., 1998b; Yu et al., 1998; Yoon et al., 2002). This subcomplex has an ability to cooperate with E2 enzymes and support ubiquitination reaction (Leverson et al., 2000; Gmachl et al., 2000; Tang et al., 2001).

Table 1 Subunits and regulators of the mitotic APC/C

| | Vertebrate | *S.cerevisiae* | *S.pombe* | Structural motifs | Function and properties |
|---|---|---|---|---|---|
| Subunits | | | | | |
| | APC1/Tsg24 | Apc1 | cut4 | PC repeats | Scaffolding |
| | APC2 | Apc2 | apc2 | Cullin homology | Catalytic |
| | APC3/CDC27* | Cdc27* | nuc2* | TPR motifs | Binds APC10 and Coactivators |
| | APC4 | Apc4 | cut20/lid1 | Unclear | Scaffolding |
| | APC5 | Apc5 | apc5 | TPR motifs | Scaffolding |
| | APC6/CDC16* | Cdc16* | cut9* | TPR motifs | Scaffolding? |
| | APC7 | | | TPR motifs | Unclear |
| | APC8/CDC23* | Cdc23* | cut23* | TPR motifs | Binds CDC20 |
| | | Apc9 | | Unclear | Unclear |
| | APC10 | Doc1 | apc10 | DOC domain | Part of degron receptor |
| | APC11 | Apc11 | apc11 | RING finger | Binds E2 enzyme |
| | APC12/CDC26* | Cdc26* | hcn1* | Unclear | Unclear |
| | APC13 | Swm1 | apc13 | Unclear | Unclear |
| | | | apc14 | Unclear | Unclear |
| | APC15 | Mnd2 | apc15 | Unclear | Releases MCCs from the APC/C |
| | APC16 | | | Unclear | Unclear |
| E2 enzymes | | | | | |
| | UBE2C/UbcH10 | | ubc11 | UBC | Initiates ubiquitin chains |
| | UBE2D1/UbcH5 | Ubc4, Ubc5 | ubc4 | UBC | Initiates ubiquitin chains** |
| | UBE2S | Ubc1 | | UBC | Elongates ubiquitin chains |
| Coactivators | | | | | |
| | CDC20 | Cdc20 | slp1 | WD40 and IR | Mitotic regulator |
| | CDH1 | Cdh1/Hct1 | ste9/srw1 | WD40 and IR | $G_1$ phase and endoreplication |
| Inhibitors | | | | | |
| | MAD2/MAD2L1 | Mad2 | mad2 | HORMA domain | Inhibits APC/$C^{CDC20}$ |
| | BUBR1 | Mad3 | mad3 | TPR KEN box | Inhibits APC/$C^{CDC20}$ |
| | CDK1 | Cdc28 | cdc2 | | Inhibits APC/$C^{CDH1}$ |
| | EMI1 | | | F box and zinc binding | Inhibits APC/$C^{CDC20}$, APC/$C^{CDH1}$ |

*Present in two copies. **Fission yeast Ubc4 elongates ubiquitin chains.

The APC/C uses at least two or three kinds of E2s, UBE2C/UbcH10 (fission yeast Ubc11), UBE2D1/UbcH5 (fission yeast Ubc4) and UBE2S (Seufert and Jentsch, 1990; Damagnez et al., 1995; Yu et al., 1996; Aristarkhov et al., 1996; Osaka et al., 1997; Seino et al., 2003; Garnett et al., 2009; Williamson et al., 2009; Wu et al., 2010). Recent studies have proposed that each of these three E2s has a different function; the first two initiate ubiquitin chains and the rest elongates (Garnett et al., 2009; Williamson et al., 2009; Wu et al., 2010). Additionally, there is a report that UBE2C/UbcH10 binds to APC2 whereas UBE2D1/UbcH5 interacts directly with APC11 (Tang et al., 2001).

APC3/Cdc27 (fission yeast Nuc2), APC6/Cdc16 (fission yeast Cut9), APC7 and APC8/Cdc23 (fission yeast Cut23) contain protein-protein interaction domains of the TPR family (Hirano et al., 1988; Lamb et al., 1994; Samejima and Yanagida, 1994; Tugendreich et al., 1995; Irniger et al., 1995; King et al., 1995; Peters et al., 1996; Yamada et al., 1997; Yu et al., 1998; Yamashita et al., 1999). These TPR subunits comprise the other subcomplex, which provides sites for the recruitments of substrates and coactivators (Vodermaier et al., 2003;

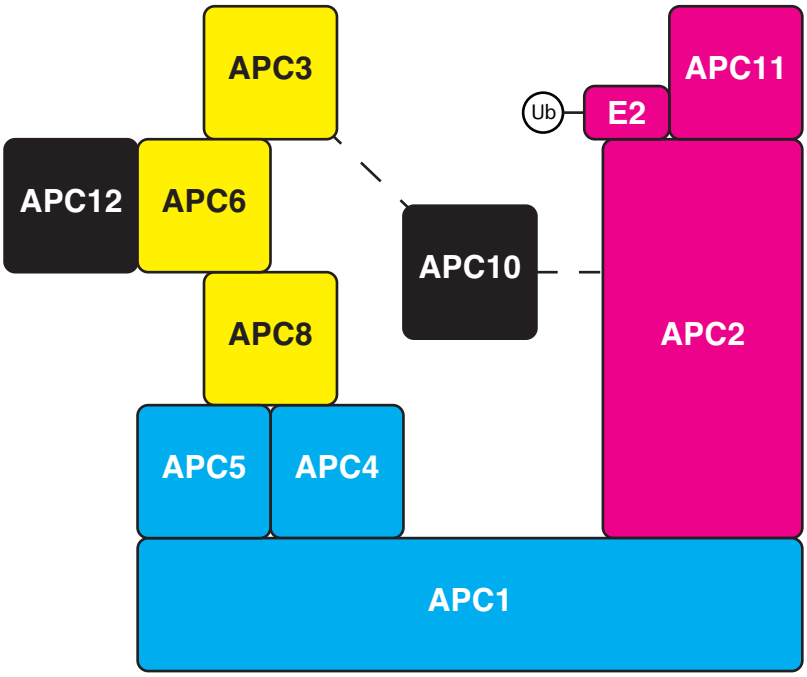


Figure 3 An architectural map of the APC/C.
Each component is stained as follows; scaffolding proteins are cyan, components of the catalytic subcomplex (and E2 enzyme) are magenta, the TPR subunits are yellow and the others are black. The dotted lines indicates the suggested physical interaction of APC10 with both APC2 and APC3. See text for details.

Thornton et al., 2006; Matyskiela and Morgan, 2009; Izawa and Pines, 2011).

Although APC5 also contains TPR motifs, this subunit can be categorized into the scaffolding proteins. Together with APC4 (fission yeast Cut20/Lid1), it forms the link between the subcomplex composed of TPR subunits and the largest subunit, APC1 (fission yeast Cut4), which holds two subcomplexes together (Peters et al., 1996; Zachariae et al., 1996; Yamashita et al., 1996; Zachariae et al., 1998b; Yu et al., 1998; Yamashita et al., 1999; Berry et al., 1999; Yoon et al., 2002; Vodermaier et al., 2003; Thornton et al., 2006).

Although there are not enough studies on the other subunits (Zachariae et al., 1996; Yamada et al., 1997; Zachariae et al., 1998b; Gmachl et al., 2000; Yoon et al., 2002; Passmore et al., 2003; Hall et al., 2003; Dube et al., 2005; Kops et al., 2010; Mansfeld et al., 2011), APC10 is the only exception (Hwang and Murray, 1997; Zachariae et al., 1998b; Kominami et al., 1998; Grossberger et al., 1999). This small subunit has been implicated in substrate recognition and APC/C processivity (Carroll and Morgan, 2002; Passmore et al., 2003; Carroll et al., 2005; Passmore and Barford, 2005; Matyskiela and Morgan, 2009; Buschhorn et al., 2011; da Fonseca et al., 2011). Besides, it seems to interact with both two subcomplex via binding to APC2 and APC3 (Vodermaier et al., 2003; Thornton et al., 2006).

Quite a few key mitotic regulators are targeted by an identical ubiquitin ligase, this APC/C, and it is notable that the individual timing of destruction is strictly contolled (Table 2). To date, a number of studies have been revealed that in order to deal with the orchestrated proteolysis APC/C sequentially alters its substrate specificity during mitosis, and suggested that at least two factors contribute to this algorithm: multiple coactivators and inhibitors.

**APC/C coactivators**

Previous studies have indicated that APC/C-mediated ubiquitination requires a member of the WD40 family as a coactivator (as an example, human Cdc20 is taken in Figure 4). These proteins contain a C-terminal WD40 domain, which adopts a propeller-like structure and plays a key role in substrate recognition: direct interacting with specific amino acid sequences in targets (Sørensen et al., 2001; Hilioti et al., 2001; Kraft et al., 2005). The most common sequence is the destruction box (D box), RxxLxxxxN (R is arginine, x is any amino acid, L is leucine and N is asparagine) (Glotzer et al., 1991). Another well-known motif is the KEN box, KENxxxN (K is lysine and E is glutamate) (Pfleger and Kirschner, 2000). In addition, coactivators have a conserved isoleucine-arginine (IR) dipeptide motif at their C-terminus and the C-box. These sequence elements mediate their binding to TPR subunits of the APC/C (Schwab et al., 2001; Vodermaier et al., 2003; Passmore et al., 2003; Thornton

Table 2 Mitosis-related APC/C substrates

| coactivator | substrate | Timing of destruction | Function | References |
|---|---|---|---|---|
| Cdc20 | A-type Cyclin | Prometaphase | Regulatory subunit of protein kinase | (den Elzen and Pines, 2001)<br>(Geley et al., 2001) |
| | Nek2A | Prometaphase | Centrosome regulator/Protein kinase | (Hames et al., 2001) |
| | B-type Cyclin | Metaphase | Regulatory subunit of protein kinase | (Clute and Pines, 1999)<br>(Yamano et al., 1996)/*Sp*Cdc13 |
| | Securin | Metaphase | Separase inhibitor | (Zou et al., 1999)<br>(Funabiki et al., 1997)/Cut2<br>(Cohen-Fix et al., 1996)/Pds1 |
| Cdh1 | Plk1 | Anaphase | Mitotic regulator/Protein kinase | (Lindon and Pines, 2004)<br>(Shirayama et al., 1998)/*Sc*Cdc5 |
| | Aurora A | Anaphase | Mitotic regulator/Protein kinase | (Honda et al., 2000) |
| | Aurora B | Anaphase/Telophase | Mitotic regulator/Protein kinase | (Stewart and Fang, 2005) |
| *,** | Cdc20 | Prometaphase | APC/C coactivator | (Nilsson et al., 2008)<br>(Pan and Chen, 2004)/*Sc*Cdc20* |
| | | Anaphase | | (Pfleger and Kirschner, 2000)**<br>(Prinz et al., 1998)/*Sc*Cdc20** |
| Unclear | UBE2C/UbcH10 | Anaphase/Telophase | APC/C cognate E2 | (Rape and Kirschner, 2004) |

*Coactivator-independnet manner (Foe et al., 2011). **APC/$C^{Cdh1}$-dependent manner.

et al., 2006).

Among all coactivators, Cdc20 (fission yeast Slp1) and Cdh1 (fission yeast Ste9) are responsible for destruction of mitotic regulators (Schwab et al., 1997; Visintin et al., 1997). In general, the difference between the two is the timing of interaction with APC/C: the former is assigned to activate from early mitosis to metaphase/anaphase transition, whereas the latter after that (Fang et al., 1998b; Kramer et al., 1998). Besides, there is a difference in the ability to recognize degrons. APC/C bound to Cdc20 (APC/$C^{Cdc20}$) seems to be able to recognize substrates only with D box, while APC/C bound to Cdh1 (APC/$C^{Cdh1}$) with both D box and KEN box (Burton and Solomon, 2001; Hilioti et al., 2001; Burton et al., 2005; Kraft et al., 2005). This coactivator switching produces diversity of the substrate specificity (Pfleger and Kirschner, 2000), and accordingly main targets of APC/$C^{Cdc20}$ are anaphase inhibitor securin (fission yeast Cut2) and B-type cyclin (fission yeast Cdc13).

**APC/C inhibitors**

As noted above, the active APC/$C^{Cdh1}$ forms only after metaphase/anaphase transition. This regulation is achieved by phosphorylation of Cdh1 by Cdk, and the modification prevents efficient interaction of Cdh1 with

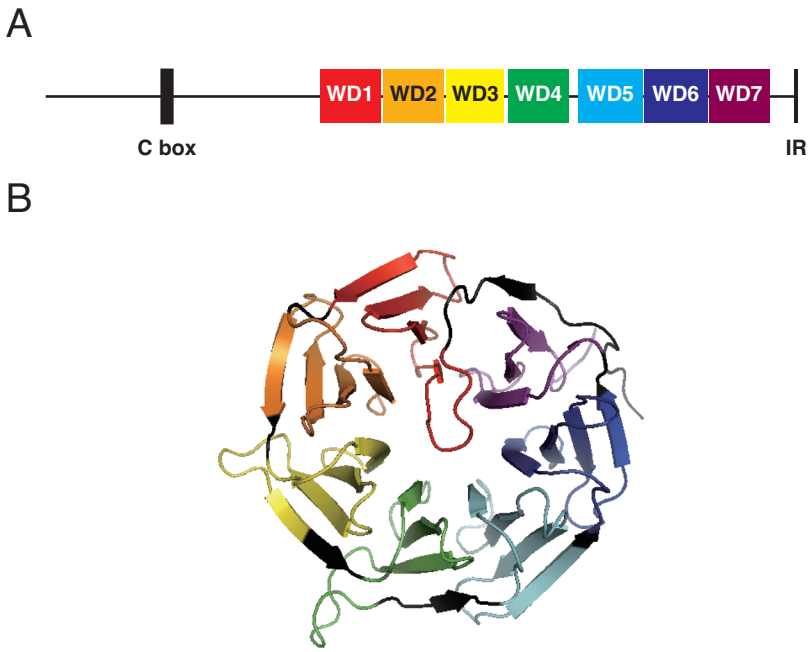


Figure 4 Domains and motifs of human Cdc20.
(A) Domain structure of human Cdc20 with its seven WD40 repeats, C box and IR motif. (B) A structure model of the WD40 domain of human Cdc20, PDB ID code 4GGA (Tian et al., 2012). Each of the seven blades of the WD40 $\beta$ propeller is stained in the respective colors indicated in (A). All structure figures in this thesis are generated with PyMOL (www.pymol.org).

APC/C (Zachariae et al., 1998a; Jaspersen et al., 1999; Kramer et al., 2000; Blanco et al., 2000; Yamaguchi et al., 2000). In vertebrates, Emi1 is also identified as an APC/C inhibitor (Reimann et al., 2001a,b; Hsu et al., 2002; Miller et al., 2006). And more than anything else, the mitotic checkpoint complex (MCC) is the key regulator of APC/C (Figure 5).

APC/C$^{Cdc20}$ can catalyze the ubiquitination of securin, which result in its proteasomal degradation (Funabiki et al., 1996b; Cohen-Fix et al., 1996; Funabiki et al., 1997). Throughout most of the cell cycle this protein functions as the separase (fission yeast Cut1) inhibitor via tight binding to block its active site (Funabiki et al., 1996a; Ciosk et al., 1998; Zou et al., 1999). The protease activity of separase is required for the cleavage of Scc1 (fission yeast Rad21), a component of the cohesin complexes that maintains the link between the sister chromatids (Guacci et al., 1997; Michaelis et al., 1997; Uhlmann et al., 1999, 2000). This therefore means that the activation of APC/C$^{Cdc20}$ triggers sister-chromatid separation, and in order to complete it accurately eukaryotic cells are equipped with an APC/C$^{Cdc20}$ inhibitory mechanism, termed the spindle assembly checkpoint (SAC). When there exists even one kinetochore unattached to spindle microtubules, the SAC senses it to block disruption of substrates and the following premature sister chromatid separation and mitotic exit (Rieder et al., 1994, 1995; Clute and Pines, 1999; Hagting et al., 2002). This preventation is fulfilled by APC/C$^{MCC}$ formation, direct binding of checkpoint components Mad2, BubR1 (fission yeast Mad3) and Bub3 to Cdc20 and subsequent interaction with APC/C (Hardwick et al., 2000; Sudakin et al., 2001; Burton and Solomon, 2007; Herzog et al., 2009; Chao et al., 2012).

## Silencing the Spindle Assembly Checkpoint

Compared with its activation, the silencing mechanism of this checkpoint has been far less understood. Recent studies, however, have soundly unveiled details about this issue. Among the most important is the discovery that Cdc20, but not the other components of MCCs, is continuously synthesized and degraded in SAC-active cells (Pan and Chen, 2004; Nilsson et al., 2008; Ge et al., 2009; Foster and Morgan, 2012; Uzunova et al., 2012). These results indicate that the disassembly of MCCs *per se* can occur independently of the kinetochore-spindle attachment, and enable to consider this event, silencing the SAC, as a consequence of two separate processes: the SAC satisfaction and MCCs disassembly (Figure 6).

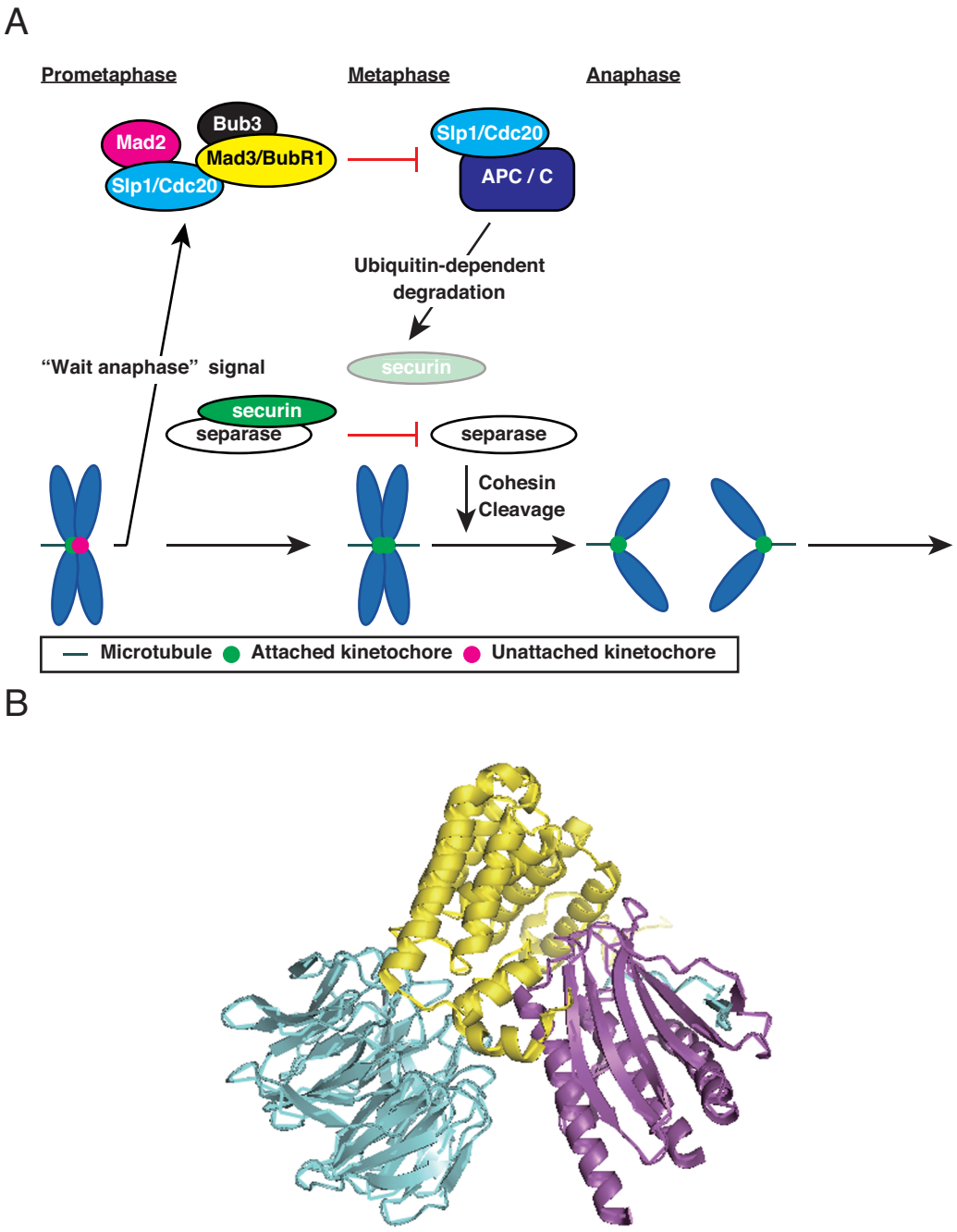


Figure 5 Mitotic progression and the spindle assembly checkpoint.
(A) During prometaphase, unattached kinetochores activate the spindle assembly checkpoint (SAC) and mitotic checkpoint complexex (MCCs), which inhibit the APC/C-dependent ubiquitination of securin, are formed. In metaphase, when all kinetochores are attached to spindle, the SAC is silenced and APC/$C^{Cdc20}$ ubiquitinates securin. Separase then cleaves cohesin complexes and thereby initiates sister-chromatid separation. (B) The crystal structure of fission yeast MCC, PDB ID code 4AEZ (Chao et al., 2012). Slp1 is indicated in cyan, Mad2 is indicated in magenta and Mad3 is indicated in yellow.

### SAC satisfaction

The "wait-anaphase" SAC signal is generated at unattached kinetochores, and there target the core components of the SAC including Mad2, BubR1 and Bub3 (Chen et al., 1996; Li and Benezra, 1996; Taylor and McKeon, 1997; Fang et al., 1998a; Taylor et al., 1998; Jablonski et al., 1998; Chen et al., 1998; Abrieu et al., 2001). Consistent with these observations, several lines of evidence suggests that they provide a catalytic platform for the continuous assembly of Mad2-Cdc20 complexes and the following MCCs production, and therefore, conversely it has been proposed that by the depletion of checkpoint proteins from kinetochores can be halted this cycle (Luo et al., 2000; Howell et al., 2000; Luo et al., 2002; Sironi et al., 2002; Kallio et al., 2002; Luo et al., 2004; Shah et al., 2004; Howell et al., 2004; De Antoni et al., 2005; Vink et al., 2006; Mapelli et al., 2007).

The SAC signals at kinecothores are hardly observed after the microtubule end-on attachment. At present it has been thought that this extinction is achieved through two behaviors: the transporting existing proteins from kinetochores to spindle poles and the prevention of further recruitment of SAC components. And the state "SAC is satisfied" is indicated by the completion of both these events. A previous report has shown that the former can be mediated by the dynein/dynactin complex, a minus-end-directed microtubule moter (Howell et al., 2001). On the other hand, recent studies have provided evidence that the latter is dependent on the recruitment of protein phosphatase 1, PP1, to kinetochores (Vanoosthuyse and Hardwick, 2009; Pinsky et al., 2009; Rosenberg et al., 2011; Meadows et al., 2011; Espeut et al., 2012). Considering that the protein phosphorylation catalyzed by several kinases is required for the SAC activation, it is reasonable that in contrast dephosphorylation contributes to the SAC silencing (Lampson et al., 2004; Tang et al., 2004; Pinsky et al., 2006; King et al., 2007; Kang et al., 2008; Liu et al., 2009; Kawashima et al., 2010; Liu et al., 2010; Welburn et al., 2010; Posch et al., 2010; Salimian et al., 2011; Zich et al., 2012; Shepperd et al., 2012; London et al., 2012; Yamagishi et al., 2012; Suijkerbuijk et al., 2012).

### MCCs disassembly

Despite its robustness — resistant to washing with a high salt concentration of 0.4 M KCl, around the transition from metaphase to anaphase MCCs are indeed disassembled and only Cdc20 is degraded (Fang et al., 1998a; Wassmann and Benezra, 1998; Pan and Chen, 2004; Nilsson et al., 2008; Ge et al., 2009; Foster and Morgan, 2012; Uzunova et al., 2012). Here arises a serious question; how Cdc20 can be released from MCCs and activate APC/C?

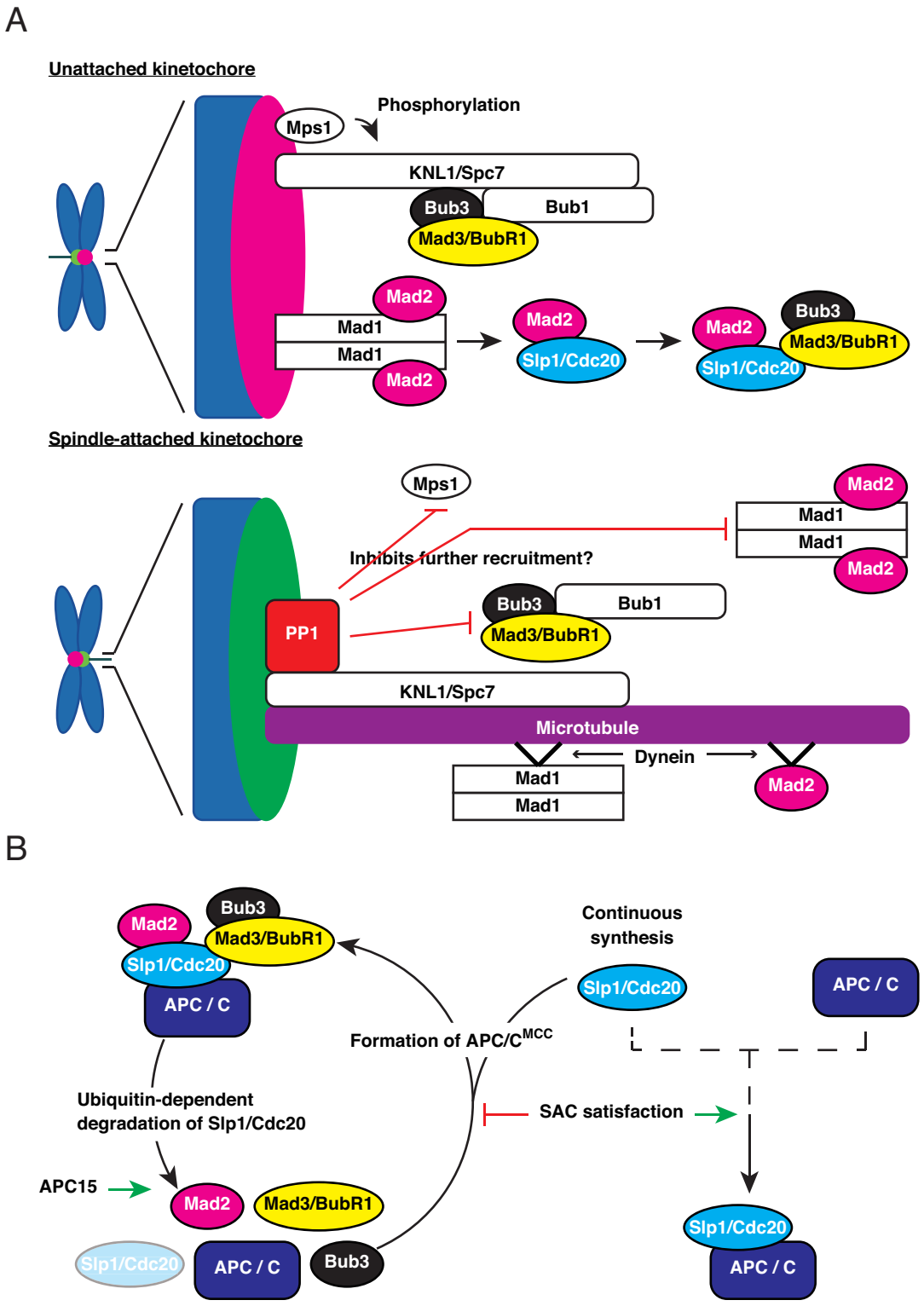


Figure 6 Silencing the Spindle Assembly Checkpoint.
(A) The SAC satisfaction. During the SAC activation, SAC components are recruited to unattached kinetochores and it induces the MCCs assembly (top panel). After kinetochore-spindle attachment, existing SAC components are transported from the kinetochore and their further recruitments are prevented (bottom panel). (B) The disassembly of MCCs. Unless the SAC is satisfied, APC/C$^{MCC}$ is continuously assembled and therefore APC/C$^{Slp1/Cdc20}$ can not be formed.

This most critical issue still remains controversial. One group has proposed that a cognate E2 of APC/C, UBE2C/UbcH10-dependent Cdc20 ubiquitylation and the subsequent conformational change causes its dissociation from MCCs (Reddy et al., 2007). By contrast, later researches have reported that MCCs containing Cdc20 lacking ubiquitination sites can be also disassembled, suggesting that this posttranslational modification is just a degradation signal (Nilsson et al., 2008; Mansfeld et al., 2011; Jia et al., 2011). Current studies further have indicated that the APC/C subunit APC15 mediates Cdc20 autoubiquitination by APC/C$^{MCC}$, release of MCCs from APC/C and is required for MCCs disassembly (Mansfeld et al., 2011; Foster and Morgan, 2012; Uzunova et al., 2012). The conflict of opinion about the proposition can be also seen among them. However, all of them reached an agreement that APC/C-mediated ubiquitylation reactions are involved in MCCs disassembly.

**Candidates of the Checkpoint Silencer in higher eukaryotes**

As a candidate responsible for silencing the SAC, p31$^{comet}$ was initially identified through a screen of a HeLa cell cDNA library by the yeast two-hybrid system with Mad2 as bait (Habu et al., 2002). It has been reported that this protein binds to Mad2 *in vivo* and formation of the complex coincides with dissociation of Mad2 from the target, Cdc20 (Habu et al., 2002; Xia et al., 2004; Mapelli et al., 2006; Yang et al., 2007). Although its mechanism of action is debatable, several studies have demonstrated that the disassembly of MCCs can be indeed accelerated by p31$^{comet}$ (Reddy et al., 2007; Teichner et al., 2011; Westhorpe et al., 2011; Mansfeld et al., 2011; Jia et al., 2011; Miniowitz-Shemtov et al., 2012). Other than p31$^{comet}$, Rod (Rough deal)/ZW10 (Zeste White-10)/Zwilch complex (RZZ complex) and Spindly have been suggested as candidates of the SAC silencer, which are involved in stripping SAC proteins from kinetochores (Williams et al., 1992; Starr et al., 1998; Scaërou et al., 2001; Griffis et al., 2007; Gassmann et al., 2008; Yamamoto et al., 2008; Chan et al., 2009; Gassmann et al., 2010; Barisic et al., 2010).

Homologs mentioned above, however, have been identified only in higher eukaryotes. Besides, even dynein is not essential for spindle checkpoint inactivation in fission yeast (Courtheoux et al., 2007). These facts imply that such silencing mechanisms are unlikely to be conserved in evolution.

## Analyses of mitotic progression in *Schizosaccharomyces pombe*

In this study I used the fission yeast *Schizosaccharomyces pombe*, which is one of the single-celled organisms. Together with the budding yeast *Saccharomyces cerevisiae*, this fungi has been generally used in studies of the cell cycle for the reason that the basic mechanisms are remarkably similar from yeast to human, except for the "closed mitosis": mitotic progression without break down of nuclear envelope (Figure 7). In the case of the fission yeast, the microtubules of the mitotic spindle form inside the nucleus and are attached to spindle pole bodies (SPB) at its periphery. The cell divides by the forming of a septum, or partition known as the cell plate and splitting in two at the middle of the cell (Funabiki et al., 1993).

For genetic analysis, the employment of yeasts has an obvious advantage over using mammalian cells; their ability to proliferate in a haploid state, in which only a single copy, or homolog, of each chromosome is present in the cell. This means that when cells are haploid we can readily isolate and analyze recessive mutations that inactivate a gene without considering the influence of a second copy of the gene. Additionally, it is relatively easy to delete specific genes, replace with defined mutant versions or express under the inducible promoters that are responsive to chmicals added to the medium. In particular the yeast SAC genes are non-essential, unlike metazoan, and this character has contributed to quite a few significant findings about the mechanism of SAC (Hardwick and Murray, 1995; He et al., 1997; Bernard et al., 1998; Chen et al., 1999; Hardwick et al., 2000; Dobles et al., 2000; Millband and Hardwick, 2002; Ikui et al., 2002). On the other hand, when it came to biochemical analyses of APC/C, researchers using the fission yeast are imposed to have relatively more technical difficulties.

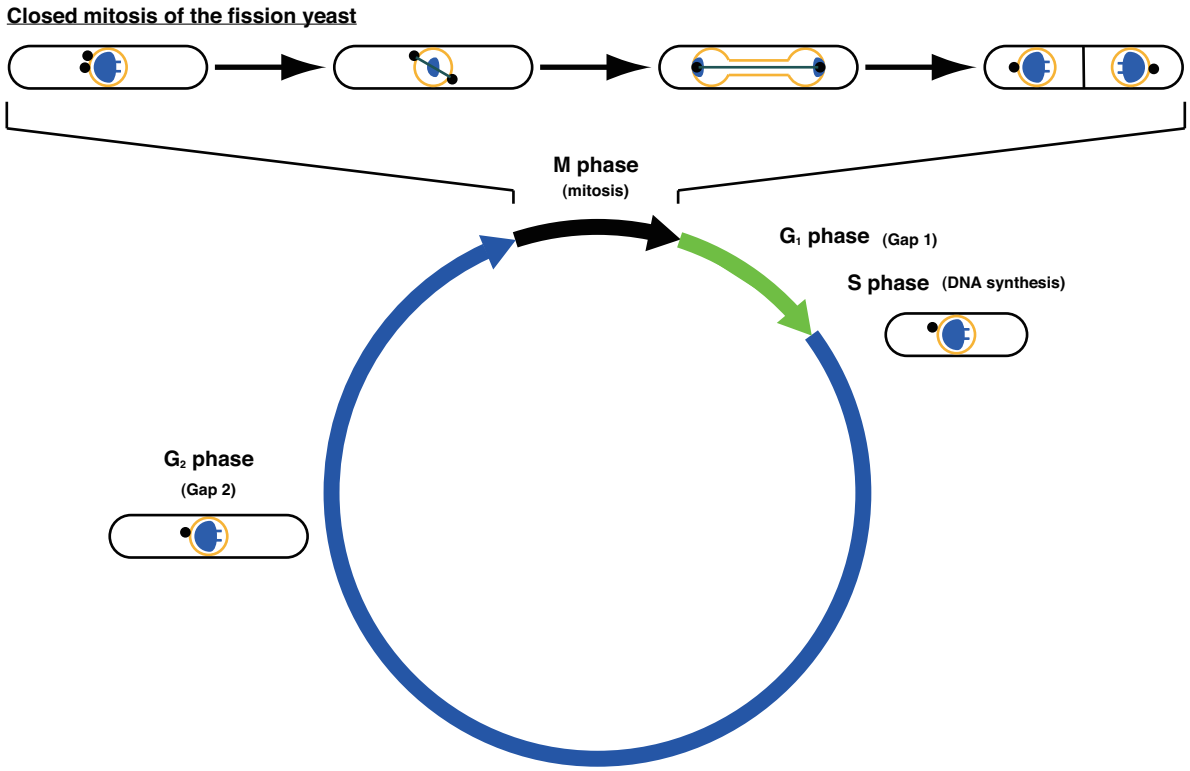


Figure 7 Closed mitosis of the fission yeast.
Each component is stained as follows; chromosomes are blue, spindle pole bodies are black, nuclear envelope is orange and microtubules are green. See text for details.

# Materials and Methods

## Strains, media and transformation

The strains used in this study are derivatives of *Schizosaccaharomyces pombe* $h^-$ 972 and $h^+$ 975 (Beach et al., 1985) and listed in Table 3. The Δ*mad2*, *slp1-mr63* (Kim et al., 1998), Δ*mad3*, Δ*bub3* (Millband and Hardwick, 2002), *mts3-1* (Gordon et al., 1996), *GFP-cnp1* (Takayama et al., 2008), *slp1-362* (Matsumoto, 1997), *nda3-KM311* (Hiraoka et al., 1984), *cdc25-22* (Fantes, 1979), *cut4-533* (Yamashita et al., 1996), *cut9-665* (Hirano et al., 1986), *his5-303* and *lys1-131* (Cottarel, 1995), all of which were previously reported, are our laboratory stock. The mutant *ubc4-P61S* (*$h^-$ ade6-M216 leu1-32 ura4-D18 ubc4-P61S::ura4$^+$*) was a generous gift from Dr. Hiroaki Seino (Seino et al., 2003). EMM[1] was used as a minimal medium, and YEA[2] (Beach et al., 1985) as a rich medium except for *nda3-KM311* mutant strains, which were grown in YPAD[3] medium. Unless mentioned below, strains were constructed by crossing and tetrad dissection. Crosses were performed on SPAS[4] media or MEA[5] media. All yeast transformations were carried out by lithium acetate methods (Okazaki et al., 1990; Gietz et al., 1992). Total RNAs were prepared from fission yeast culture as previously described (Jensen et al., 1983).

[1] 3 g/l potassium hydrogen phthallate, 5.5 g/l $Na_2HPO_4 \cdot 12H_2O$, 5 g/l $NH_4Cl$, 20 g/l glucose, 1.05 g/l $MgCl_2 \cdot 6H_20$, 14.7 mg/l $CaCl_2 \cdot 2H_20$, 1 g/l KCl, 40 mg/l $Na_2SO_4$, 1 mg/l pantothenic acid, 10 mg/l nicotinic acid, 10 mg/l inositol, 10 $\mu$g/l biotin, 0.5 mg/l boric acid, 0.4 mg/l $MnSO_4$, 0.4 mg/l $ZnSO_4 \cdot 7H_2O$, 0.2 mg/l $FeCl_2 \cdot 6H_2O$, 40 $\mu$g/l molybdic acid, 0.1 mg/l KI, 40 $\mu$g/l $CuSO_4 \cdot 5H_2O$ and 1 mg/l citric acid (plus 225 mg/l supplements — adenine, histidine, leucine, uracil and/or lysine hydrochloride — when needed)

[2] 30 g/l glucose, 5 g/l yeast extract, 75 mg/l adenine

[3] 5 g/l yeast extract, 10 g/l glucose, 10 g/l polypeptone and 40 mg/l adenine

[4] 10 g/l glucose, 1 g/l $KH_2PO_4$, 1 mg/l pantothenic acid, 10 mg/l nicotinic acid, 10 mg/l inositol, 10 $\mu$g/l biotin and 45 mg/l supplements

[5] 30 g/l Bacto-malt extract, 225 mg/l adenine, histidine, leucine and uracil, adjusted to pH 5.5 with NaOH

Table 3 Strains used in this study

| Strains | Genotype | Source/Reference |
|---|---|---|
| AE147 | *h*$^{-}$ *leu1-32 ura4-D18 mad2::ura4*$^{+}$ | Laboratory stock |
| AE202 | *h*$^{-}$ *leu1-32 slp1-362* | Laboratory stock |
| AE204 | *h*$^{-}$ *leu1-32 mts3-1* | Laboratory stock |
| AE243 | *h*$^{-}$ *leu1-32 slp1-mr63* | Laboratory stock |
| RBC115 | *h*$^{-}$ *leu1-32 mad2::ura4::nmt1-mad2* | Laboratory stock |
| RBC116 | *h*$^{+}$ *leu1-32 mad2::ura4::nmt1-mad2* | Laboratory stock |
| SP6 | *h*$^{-}$ *leu1-32* | Laboratory stock |
| SP628 | *h*$^{-}$ *leu1-32 cdc25-22* | Laboratory stock |
| SP858 | *h*$^{+}$ *leu1-32 nda3-KM311* | Laboratory stock |
| SP1047 | *h*$^{-}$ *leu1-32 cut4-533* | Laboratory stock |
| SP1049 | *h*$^{-}$ *leu1-32 cut9-665* | Laboratory stock |
| *cut23-Y395H* | *h*$^{-}$ *leu1-32 cut23-Y395H* | This work |
| *cut23-Y395H-5FLAG* | *h*$^{-}$ *leu1-32 his5-303 cut23-Y395H-5FLAG-HIS3MX6* | This work |
| *cut23-Y395H GFP-Cnp1* | *h*$^{-}$ *leu1-32 cut23-Y395H GFP-Cnp1-hph* | This work |
| *cut23-Y395H* Δ*mad2* | *h*$^{-}$ *leu1-32 ura4-D18 cut23-Y395H mad2::ura4*$^{+}$ | This work |
| *cut23-Y395H-5FLAG* Δ*mad2* | *h*$^{-}$ *leu1-32 ura4-D18 his5-303 cut23-Y395H-5FLAG-HIS3MX6 mad2::ura4*$^{+}$ | This work |
| *cut23-Y395H* Δ*mad2 GFP-Cnp1* | *h*$^{-}$ *leu1-32 ura4-D18 cut23-Y395H mad2::ura4*$^{+}$ *GFP-Cnp1-hph* | This work |
| *cut23-Y395H slp1-mr63* | *h*$^{-}$ *leu1-32 cut23-Y395H slp1-mr63* | This work |
| *cut9-665 mts3-1 Ptif51-6His-Ub* | *h*$^{-}$ *leu1-32 cut9-665 mts3-1 lys1-131::lys1*$^{+}$*-Ptif51-6His-Ub* | This work |
| *mts3-1* Δ*mad2* | *h*$^{?}$ *leu1-32 ura4-D18 mts3-1 mad2::ura4*$^{+}$ | This work |
| *mts3-1 Ptif51-6His-Ub* | *h*$^{-}$ *leu1-32 mts3-1 lys1-131::lys1*$^{+}$*-Ptif51-6His-Ub* | This work |
| *mts3-1 Ptif51-HA-Ub* | *h*$^{-}$ *leu1-32 mts3-1 lys1-131::lys1*$^{+}$*-Ptif51-HA-Ub* | This work |
| *nda3-KM311 Cut23-5FLAG* | *h*$^{-}$ *leu1-32 his5-303 nda3-KM311 cut23-5FLAG-HIS3MX6* | This work |
| *nda3-KM311 Ptif51-6His-Ub* | *h*$^{-}$ *leu1-32 nda3-KM311 lys1-131::lys1*$^{+}$*-Ptif51-6His-Ub* | This work |
| *nda3-KM311 ubc4-P61S* | *h*$^{-}$ *leu1-32 ura4-D18 nda3-KM311 ubc4-P61S::ura4*$^{+}$ | This work |
| *nda3-KM311 ubc11-P93L* | *h*$^{-}$ *leu1-32 nda3-KM311 ubc11-P93L* | This work |
| *nda3-KM311 ubc4-P61S ubc11-P93L* | *h*$^{?}$ *leu1-32 ura4-D18 nda3-KM311 ubc4-P61S::ura4*$^{+}$ *ubc11-P93L* | This work |
| *slp1-362* Δ*mad2* | *h*$^{-}$ *leu1-32 ura4-D18 slp1-362 mad2::ura4*$^{+}$ | This work |
| *ubc11-P93L* | *h*$^{-}$ *leu1-32 ubc11-P93L* | This work |
| *ubc11-P93L Cut23-5FLAG* | *h*$^{-}$ *leu1-32 his5-303 ubc11-P93L cut23-5FLAG-HIS3MX6* | This work |
| *ubc11-P93L* Δ*bub3* | *h*$^{-}$ *leu1-32 ura4-D18 ubc11-P93L bub3::ura4*$^{+}$ | This work |
| *ubc11-P93L* Δ*mad2* | *h*$^{-}$ *leu1-32 ura4-D18 ubc11-P93L mad2::ura4*$^{+}$ | This work |
| *ubc11-P93L* Δ*mad2 Cut23-5FLAG* | *h*$^{-}$ *leu1-32 ura4-D18 his5-303 ubc11-P93L mad2::ura4*$^{+}$ *cut23-5FLAG-HIS3MX6* | This work |
| *ubc11-P93L* Δ*mad3* | *h*$^{-}$ *leu1-32 ura4-D18 ubc11-P93L mad3::ura4*$^{+}$ | This work |
| *ubc11-P93L GFP-Cnp1* | *h*$^{-}$ *leu1-32 ubc11-P93L GFP-Cnp1-hph* | This work |
| *ubc11-P93L mts3-1* | *h*$^{-}$ *leu1-32 ubc11-P93L mts3-1* | This work |
| *ubc11-P93L mts3-1 Ptif51-6His-Ub* | *h*$^{-}$ *leu1-32 ubc11-P93L mts3-1 lys1-131::lys1*$^{+}$*-Ptif51-6His-Ub* | This work |
| *ubc11-P93L Ptif51-6His-Ub* | *h*$^{-}$ *leu1-32 ubc11-P93L lys1-131::lys1*$^{+}$*-Ptif51-6His-Ub* | This work |
| *ubc11-P93L slp1-mr63* | *h*$^{-}$ *leu1-32 ubc11-P93L slp1-mr63* | This work |
| *mad2*$^{+}$/Δ*mad2* | *h*$^{+}$/*h*$^{-}$ *ade6-210/ade6-216 ura4-d18/ura4-d18 leu1-32/leu1-32 mad2*$^{+}$*/mad2::ura4*$^{+}$ | This work |
| *mad2*$^{+}$/Δ*mad2 ubc11*$^{+}$/Δ*ubc11* | *h*$^{+}$/*h*$^{-}$ *ade6-210/ade6-216 ura4-d18/ura4-d18 leu1-32/leu1-32 mad2*$^{+}$*/mad2::ura4*$^{+}$ *ubc11*$^{+}$*/ubc11::LEU2* | This work |

## Strain construction

### Deletion of *ubc11*$^{+}$ gene

A plasmid to delete the *ubc11*$^{+}$ gene, pBS_Δ*ubc11::LEU2*, was constructed by PCR amplification of about 500-bp DNA fragment upstream of the start codon of the *ubc11*$^{+}$ gene and about 700-bp DNA fragment downstream of the stop codon. The primers used in the PCR were as follows: for amplification of the upstream sequence, the forward primer was *Xho*I-*ubc11*us[6] and the reverse primer was *ubc11*us-*Hin*dIII[7]; for the down-

[6][5′-GGGGCTCGAG(*Xho*I)CACTAGCCATCCTTC-3′]
[7][5′-GGGGAAGCTT(*Hin*dIII)TCCTCAAGTTGTTAC-3′]

stream sequence, the forward primer was *Hin*dIII-*ubc11*ds[8] and the reverse primer was *ubc11*ds-*Xba*I[9]. The resulting DNA fragments were digested with combinations of appropriate restriction enzymes and then ligated into pBS plasmid to create pBS_Δ*ubc11*. This plasmid was digested with (*Hin*dIII) and ligated with a DNA fragment that contained *LEU2* sequence isolated from pREP1 (Maundrell, 1990, 1993). Digestion of the resulting plasmid, pBS_Δ*ubc11::LEU2*, with *Spe*I generated about 3.4-kbp DNA fragment containing the *LEU2* gene flanked by the 500-bp upstream and the 700-bp downstream sequences of the *ubc11* gene, which was used for transformation to delete the *ubc11* gene in the $h^+/h^-$ *ade6-210/ade6-216 ura4-d18/ura4-d18 leu1-32/leu1-32* $mad2^+/mad2::ura4^+$ diploid strain.

**5FLAG tagging of C-terminus region of Cut23**

An about 0.4-kbp DNA fragment of C-terminus region of $cut23^+$ was amplified by PCR using the forward primer *Pvu*II-*cut23*C[10] and the reverse primer *cut23*C-*Bgl*II[11]. The resulting DNA fragment was digested with combinations of appropriate restriction enzymes and then inserted into *Pvu*II-*Bam*HI site of pFA6a-5FLAG-kanMX6 (generously provided by Dr. Jun-ichi Nakayama). The sequence was verified by sequencing.

On the other hand, an about 1.2-kbp DNA fragment downstream of the stop codon of $cut23^+$ was also amplified by PCR using the forward primer *Sac*I-*cut23*ds[12] and the reverse primer *cut23*ds-*Spe*I [13]. The resulting DNA fragment was digested with combinations of appropriate restriction enzymes and then inserted into *Sac*I-*Spe*I site of pFA6a-3HA-His3MX6 (Longtine et al., 1998). The sequence was verified by sequencing.

Both of resultant plasmids were digested with *Pvu*II and *Bgl*II. An about 0.8-kbp DNA fragment derived from the former and an about 4.9-kbp DNA fragment derived from the latter were ligated. The resulting plasmid, pFA6a-Cut23-5FLAG-His3MX6, was digested with *Bam*HI and introduced into wild-type *his5-303* or *cut23-Y395H his5-303* strains. $His^+$ transformants were isolated. The gene replacement was confirmed by PCR and immunoblotting.

**Strains expressing tagged ubiquitins**

For construction of strain expressing His-tagged ubiquitin, two plasmids, Ptif51(HA-Ubi)-LEU2 and pREP1 (6His-Ubi) (generously provided by Dr. Kenji Kitamura), were digested with *Pst*I and *Bgl*II. An about 8.5-

[8] [5′-GGGGAAGCTT(*Hin*dIII)TTAGGCCGGTCTATT-3′]
[9] [5′-GGGGTCTAGAA(*Xba*I)CTAGTCATTCGCAG-3′]
[10] [5′-GGGGCAGCTG(*Pvu*II)TCAACGAGCTACTGC-3′]
[11] [5′-GGGGAGATCT(*Bgl*II)GATCATATGAATGCT-3′]
[12] [5′-GGGGGAGCTC(*Sac*I)TATAAATTTTATGAC-3′]
[13] [5′-GGGGACTAGT(*Spe*I)TGTGACGTGGTTAGC-3′]

kbp DNA fragment derived from the former and an about 1.3-kbp DNA fragment derived from the latter were ligated. This plasmid was digested with *Pst*I and *Bam*HI, and the resulting DNA fragment was cloned into *Pst*I-*Bam*HI site of pBS SK+ (Agilent). The resultant plasmid and pREP1 were digested with *Bam*HI and *Sac*I. An about 4.5-kbp DNA fragment derived from the former and an about 1-kbp DNA fragment derived from the latter were ligated. This plasmid and Ptif51(HA-Ubi)-LEU2 were digested with *Pst*I and *Nde*I. An about 4.3-kbp DNA fragment derived from the former and an about 0.8-kbp DNA fragment erived from the latter were ligated. The resulting plasmid, pBS-P*tif51*-His-Ub, was digested with *Kpn*I and *Sac*I. An about 2.5-kbp DNA fragment was inserted into *Kpn*I-*Sac*I site of pYAT1, an integration vector containing a part of C-terminus region of *lys1*$^+$ gene as a selection marker (Laboratory stock). The resultant plasmid was introduced into wild-type *lys1-131* strain and Lys$^+$ transformants were isolated. The gene replacement was confirmed by immunoblotting.

For construction of strain expressing HA-tagged ubiquitin, two plasmids, Ptif51(HA-Ubi)-LEU2 and the above-mentioned pBS-P*tif51*-His-Ub, were digested with *Pst*I and *Bam*HI. An about 1-kbp DNA fragment derived from the former and an about 4-kbp DNA fragment derived from the latter were ligated. The resulting plasmid was digested with *Kpn*I and *Sac*I. An about 2.1-kbp DNA fragment was inserted into *Kpn*I-*Sac*I site of pYAT1. The resultant plasmid was introduced into wild-type *lys1-131* strain and Lys$^+$ transformants were isolated. The gene replacement was confirmed by immunoblotting.

### Temperature-sensitive mutants and their derivatives

Cells were first cultured at the permissive temperature of 26°C and then shifted to the restrictive temperature of 36°C.

### *nda3-KM311* strains

For synchronization, *nda3-KM311* mutant cells were first cultured at permissive temperature (26 or 32°C) before being shifted down to the restriction temperature (20°C) for 6 hours.

### Spot assay

Exponentially growing cultures were washed twice with distilled water and then 5-fold diluted serially. Each dilution was spotted onto agar plates.

## Immunofluorescence microscopy

Fluorescence from GFP, mCherry or Alexa Fluor 594 was visualized with a laser-scanning microscope (Leica). At least 200 cells in each sample were examined for nuclear morphology. Images were processed with IP lab (BD) and Photoshop version 12.0.4 (Adobe).

### Methanol fixation

PEM buffer[14] was added to the fixed cells at 30% (v/v) of the final methanol concentration. Cells were fixed with methanol as described above and were treated with 1 mg/ml zymolyase 100T in PEMS buffer[15] at 37°C for 30 minutes. The cells were then washed with PEMS containing 1% TritonX-100 for 2 minutes and washed with PEM three times. For blocking, PEMBAL buffer[16] was used. After 30 minutes of blocking, cells were stained with the primary antibody (TAT1; generously provided by Dr. Andrea Baines) and incubated over night. Cells were washed with PEMBAL three times, followed by incubation with Alexa Fluor 594 Goat Anti-mouse (1:1000; Molecular Probes) for hours. Finally cells were washed with PEMBAL three times and stained with 0.2 $\mu$g/ml of 4′,6′-diamidino-2-phenyl-indole (DAPI). All steps were performed at room temperature. The GFP-Cnp1 signal was observed under the microscope using the same cells as was used for tubulin immunostaining.

### Formaldehyde fixation

Cells were first fixed by formaldehyde alone at the final concentration of 3% for 1 hour. After performing three wash steps with PEM, the cells were treated with 1 mg/ml zymolyase 100T in PEMS buffer at 37°C for 70 minutes. The cells were then washed with PEMS containing 1% TritonX-100 for 2 minutes and washed with PEM three times. For blocking, PEMBAL buffer was used. After 30 minutes of blocking, cells were stained with the primary antibody (TAT1) and incubated over night. Cells were washed with PEMBAL three times, followed by incubation with Alexa Fluor 594 Goat Anti-mouse (1:1000; Molecular Probes) over night. Finally cells were washed with PEMBAL three times and stained with 0.2 $\mu$g/ml of DAPI. All steps were performed at room temperature. The GFP-Cnp1 signal was observed under the microscope using the same cells as was used for tubulin immunostaining.

[14] 100 mM PIPES, 1 mM EGTA, 1 mM $MgCl_2$, pH 6.9
[15] PEM, 1.2 M sorbitol
[16] PEM, 0.1% bovine serum albumin

# Protein analyses

## Ubiquitin transfer assay

### Plasmids and construction

Ptr3, fission yeast ubiquitin activating enzyme E1, mRNA was reverse-transcribed by use of ReverTra Ace (TOYOBO) and then the resultant cDNA was amplified by PCR. The primer sequences used in the PCR were as follows; the forward primer was *Bam*HI-*ptr3* [17] and the reverse primer was *ptr3-Not*I [18]. The resulting DNA fragment was digested with combinations of appropriate restriction enzymes and then inserted into *Bam*HI-*Not*I site of PinPointXa-1 vector (Promega) in-frame with biotinylated purification protein tag sequence. The biotinylated purification tagged Ptr3 or biotylated purification tagged protein were expressed in *E.coli* BL21(DE3) strain at 20°C. The fusion protein was directly purified with SoftLink soft release avidin resin according to the manufacturers protocol.

Ubc11 mRNAs were also reverse-transcribed by use of ReverTra Ace and then the resultant cDNA was amplified by PCR. The primer sequences used in the PCR were as follows; the forward primer was *Eco*RI-*ubc11* [19] and the reverse primer was *ubc11-Xho*I [20]. The resulting DNA fragment was digested with combinations of appropriate restriction enzymes and then inserted into *Eco*RI-*Xho*I site of pET30a vector (Promega) in-frame with Histidine tag sequence. The His-tagged Ubc11 was expressed in *E.coli* BL21(DE3) strain by IPTG induction and directly purified with TALON Metal Affinity Resin according to the manufacturers protocol.

To obtain $^{32}$P-labeled ubiquitin protein, Protein kinase A phosphorylation site (Arg-Arg-Ala-Ser-Val) was introduced into pET30a in-frame with 6xHistidine tag sequence (pET30a KT). Yeast ubiquitin was amplified by PCR using the plasmid Ptif51(HA-Ubi)-LEU2 as a template. The primer sequences used in the PCR were as follows; the forward primer was *Eco*RV-Ub [21] and the reverse primer was Ub-*Sac*I [22]. The resulting DNA fragment was digested with combinations of appropriate restriction enzymes, and then cloned into pET30a KT in-frame with 6xHistidine and PKA phosphorylation site. The His-PKA site tagged ubiquitin was expressed in *E.coli* BL21(DE3) strain by IPTG induction and directly purified with TALON Metal Affinity Resin according to the manufacturers protocol.

[17] [5′-GGGGGGATCC(*Bam*HI)GGATGAGTAATAACATGAAC-3′]
[18] [5′-GGGGGCGGCCGC(*Not*I)TTACAACTTGATACAAAT-3′]
[19] [5′-GGGGGAATTC(*Eco*RI)ATGGATTCTGATATG-3′]
[20] [5′-GGGGCTCGAG(*Xho*I)CTAAATTTCATCGAT-3′]
[21] [5′-GGGGGATATC(*Eco*RV)ATGCAGATCTTCGTC-3′]
[22] [5′-GGGGGAGCTC(*Sac*I)TCAACCACCTCTTAG-3′]

### *in vitro* phosphorylation reaction

*in vitro* phosphorylation reaction was performed by cAMP-dependent kinase-catalytic subunit (20 mM Tris-HCl, 100 mM NaCl, 12 mM MgCl2, 1 mM DTT, 25%(v/v) glycerol, pH7.4, 2.4 units/$\mu$l cAMP-dependent kinase-catalytic subunit (Promega), 1.5$\mu$Ci/$\mu$l ($\gamma$-$^{32}$P)ATP, 0.5 $\mu$g/$\mu$l His-Ubc11 purified protein) at 25°C for 30 min. The labeling mixture was directly loaded onto BioSpin-P6 column (Bio-Rad) pre-equilibrated with incubation buffer (20 mM Tris-HCl, 100 mM NaCl, 12 mM MgCl2, 1 mM DTT, 25%(v/v) glycerol, pH7.4), and the flow-through fraction was collected and calibrated with autoradiography. Two hundred cpm/protein $\mu$g were used for thioester formation reaction.

### Thioester formation reaction

Thioester formation reactions contained 0.5 $\mu$g of $^{32}$P-labeled His ubiquitin, 0.1 $\mu$g of Pinpoint-Ptr3 or PinPoint tag protein and 0.5 $\mu$g of His Ubc11$^{WT}$ or Ubc11$^{P93L}$ in 4 mM Tris-HCl, 0.5 mM MgCl, 0.2 mM ATP, pH7.6) at 25°C, for 30 min. Reactions were terminated by incubating the mixtures for 10 min at 25°C in 50 mM Tris-HCl pH6.8, 2% SDS, 10% glycerol, and 0.5% BPB or boiling the mixtures for 3 min in 50 mM Tris-HCl pH6.8, 2% SDS, 10% glycerol, 1 mM DTT, and 0.5% BPB. The duplicated gels were stained by Silver-staining protocol or take the autoradiogram on X-ray film.

## Yeast cell extracts

Cells were collected, washed once with PBS, rapidly frozen by liquid nitrogen, and kept at -80°C. Cells were thawed, washed once with below-mentioned buffers and thereafter suspended in such buffers including protease/proteasome inhibitors[23]. Cells were lysed by glass beads and centrifuged at 13,000 rpm for 15 min. Supernatants were used for analyses.

### Western blot analysis

Cells were thawed and suspended in modified HB buffer[24] containing Laemmli sample buffer and boiled for 5 min before cell disruption.

[23] 1 mM PMSF, 10 $\mu$M MG132 and 1% (v/v) of the final concentration of protease inhibitor cocktail (nacalai tesque) containing 100 mM 4-(2-Aminoethyl)benzenesulfonyl fluoride hydrochloride, 80 $\mu$M Aprotinin, 1.5 mM E-64, 2 mM Leupeptin, 5 mM bestatin and 1 mM pepstatin A

[24] 25 mM Tris-HCl, [pH7.5], 15 mM EGTA, 15 mM $MgCl_2$, 60 mM $\beta$-glycerophosphate, 15 mM $\rho$-nitrophenylphosphate, 0.5 mM $Na_3VO_4$, 10 mM N-ethylmaleimide (NEM, Sigma), 0.1% NP-40, 0.1 mM NaF

### Immunoprecipitation

Cells were thawed and suspended in modified HB buffer, disrupted by glass beads and centrifuged. Supernatants were used for SDS-PAGE followed by immunoblotting. Anti-FLAG M2 Affinity Gel (Sigma) or Slp1 antibodies mixed with protein A-sepharose beads (Pharmacia) were shaking for 2 hr at 4°C, followed by washing. Supernatants of extracts were added and incubated at 4°C for 2 hr with shaking, followed by three cycles of washing and SDS-PAGE after boiling for 3 min.

### Detection of Slp1 ubiquitylation

Ubiquitylation analysis was performed as described (Takayama et al., 2010). Cells expressing 6His-tagged (6His-Ub) or HA-tagged ubiquitin (HA-Ub) under the *tif51* promoter (Matsuyama et al., 2008) integrated at the *lys1* locus were grown to log phase at the permissive temperature and then shifted to the restrictive temperature. For preparation of cell lysates, the cells were washed with buffer I[25] and broken by vortexing with glass beads, and the lysates were cleared by centrifugation. Six milligrams of cell lysates were incubated for 4 hr at room temperature with the TALON beads (BD bioscience Clontech, Palo Alto, CA), and washed twice with buffer I and four times with buffer II[26]. Slp1 protein pulled down with the beads was diluted in 5x sample buffer and boiled for 3 min, and ubiquitinated forms were detected by immunoblotting with Slp1 antibody.

### Antibodies

As primary antibodies, anti-Slp1 (1:500), anti-Mad2 (1:50), anti-FLAG M2 (1:1000; Sigma), anti-Cdc13 (1:200; Santa Cruz Biotechnology), anti-Cut2 (1:3000; generously provided by Dr. Mitsuhiro Yanagida), anti-Ubc11 (1:200; generously provided by Dr. Fumiaki Yamao) and anti-$\beta$-actin (1:8000; Abcam) were employed, respectively. As secondary antibodies, goat HRP-conjugated anti-mouse (1:10000; GE Healthcare), anti-rabbit (1:10000; GE Healthcare) or anti-rat (1:50000; Invitrogen) antibody were employed, respectively.

[25] 10 mM Tris-HCl [pH 7.5], 100 mM Na phosphate, 0.1% NP-40, 10 mM Imidazole, 6 M Guanidine-HCl
[26] 10 mM Tris-HCl [pH 7.5], 100 mM Na phosphate, 0.1% NP-40, 10 mM Imidazole, 1 mM PMSF

# Results

## Isolation of the *ubc11-P93L* mutant

As previous studies have shown, constitutive activation of the SAC leads to mitotic arrest, yet the SAC components are non-essential in fission yeast (He et al., 1997; Bernard et al., 1998; Millband and Hardwick, 2002; Ikui et al., 2002). Taking this fact as advantage, we designed a genetic screen for mutants defective in silencing the SAC with an assumption that perturbation of mitotic progression by a defect in silencing SAC can be suppressed by loss of the functional SAC. A strain conditionally expressing Mad2 was mutagenized, and the survivors were screened for mutants whose temperature sensitivity was dependent on expression of Mad2.

### Strains in which Mad2 is expressed under control

Initially, we constructed a strain whose native *mad2* promoter is displaced by the inducible *nmt41* promoter (Figure 8A). In such cells, expression of Mad2 depends on the absence of thiamine, and this was confirmed by western blot analysis (Figure 8B). Although the level of Mad2 expression was higher in this strain than the wild-type strain, it was found that the expression didn't cause a growth defect and could be regulated when they were cultured in thiamine-free EMM media.

### Temperature-sensitive mutants only in the presence of Mad2

We subsequently screened a large number of colonies arising from chemically mutagenized *RBC115* (*h*$^{-}$ *leu1-32 mad2::ura4::nmt1-mad2*) cells. At this stage, we selected candidates that exhibited a temperature-sensitivity in the absence of thiamine, which means that these cells displayed a growth defect at the restrictive temperature (36°C) only when Mad2 was expressed. Mad2 is known as a crucial activator of the SAC, and accordingly it is commonly assumed that a lack of this protein causes inactivation of the checkpoint. It has been reported that *mad2*$^{+}$ isn't an essential gene in *S.pombe* and its genetic deletion doesn't cause noticeable defects under

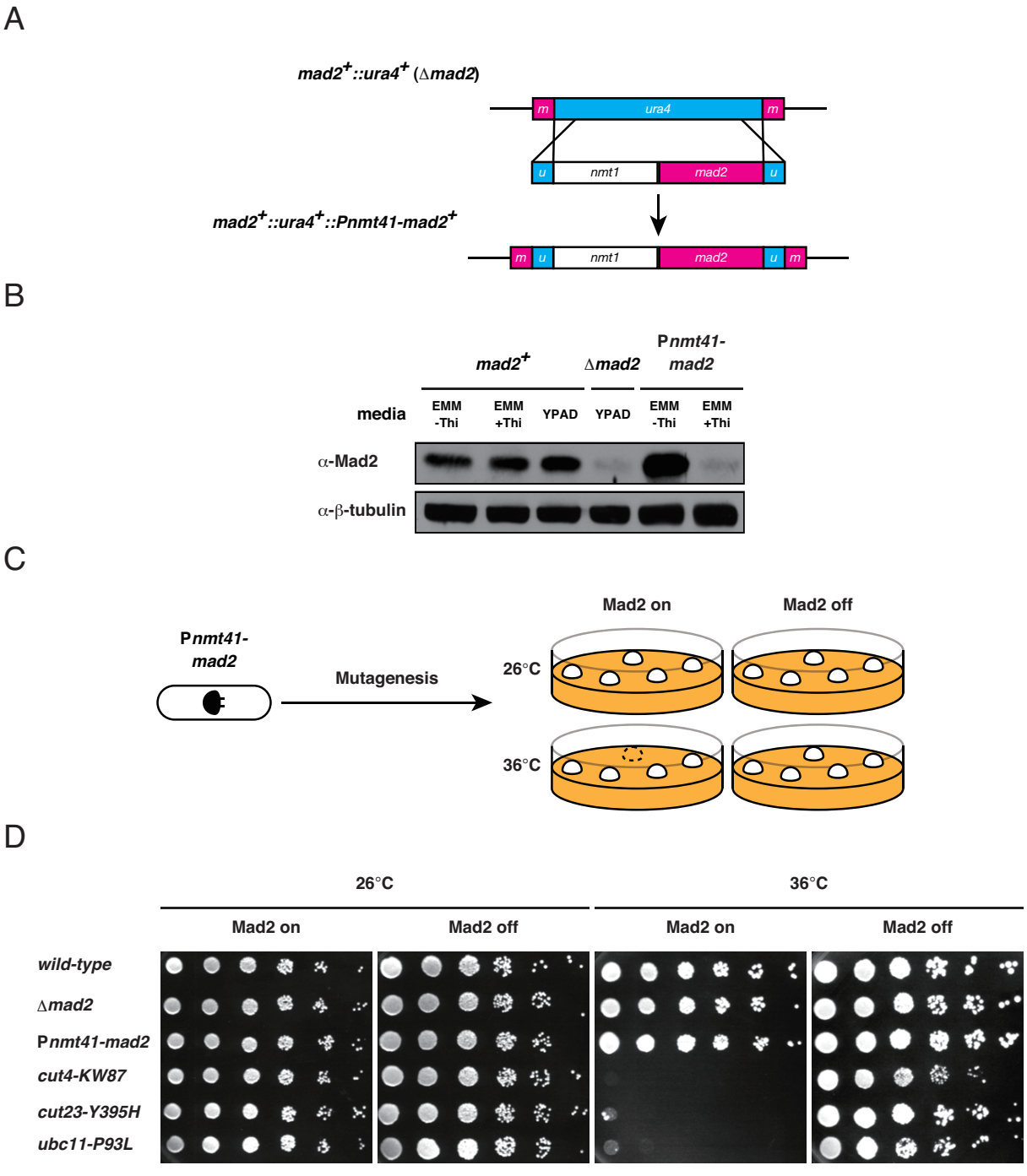


Figure 8 Isolation of mutants in which expression of Mad2 is inducible.
(A) Construction of a strain in which expression of Mad2 is inducible. (B) Levels of Mad2 expression. (C) Strategy of this screening. (D) Temperature-sensitive mutants only in the presence of Mad2.

normal growth conditions (Kim et al., 1998), and intriguingly, our mutants could also grow adequately in the absence of Mad2 even at the restrictive temperature (Figure 8D). Thus this temperature-sensitivity is possibly due to the failure to silence the checkpoint signal. Consequently, we obtained twenty-eight candidates that met the above criteria.

### Delay in chromosome segregation

Although the twenty-eight mutants exhibited the temperature-sensitivity, it was necessary to examine if they were appropriate candidates for involvement in silencing the SAC; it was likely that some of them might be simply thiamine auxotroph at a high temperature, for instance. Hence, further analyses were made to rule out those false-positives.

As a first step to this approach, each mutant was incubated at the restrictive temperature for 4 hours, which was thought of as one cell cycle period under this condition, and stained with DAPI to observe the nuclear morphology. In general, condensed chromosomes, aberrant segregation of chromosomes or *cut* (cell untimely torn; undivided nucleus is intersected by the septum and torn into two parts by the subsequent cytokinesis) phenotype (Figure 9A) are known as the typical instances involved in mitotic defects.

Consequently, nineteen out of the twenty-eight strains were selected as the appropriate candidates. These cells had one or more of the above features (Figure 9B), whereas the rest mostly showed a normal nuclear morphology and at most merely small cells.

### Intracellular accumulation of Slp1

Moreover, it was required to obtain evidence that selected mutants were precisely arrested in mitosis. To confirm this, the level of Slp1 was examined. Slp1 is strictly regulated in a cell cycle-dependent manner; it begins to accumulate intracellularly as cells enter M phase and is proteolytically degraded after mitosis (Yamada et al., 2000). This fact leads to the suggestion that mitotic-arrested mutants could accumulate Slp1. Sixteen out of the nineteen candidates, in which cellular accumulation of Slp1 could be observed at the restrictive temperature, were chosen for further study.

### Intracellular accumulation of Slp1-Mad2 complexes

The intracellular accumulation of Slp1 *per se* actually was also not an sufficient condition for the activation of the SAC, and therefore the state of the Slp1-Mad2 complex was examined (Ikui et al., 2002).

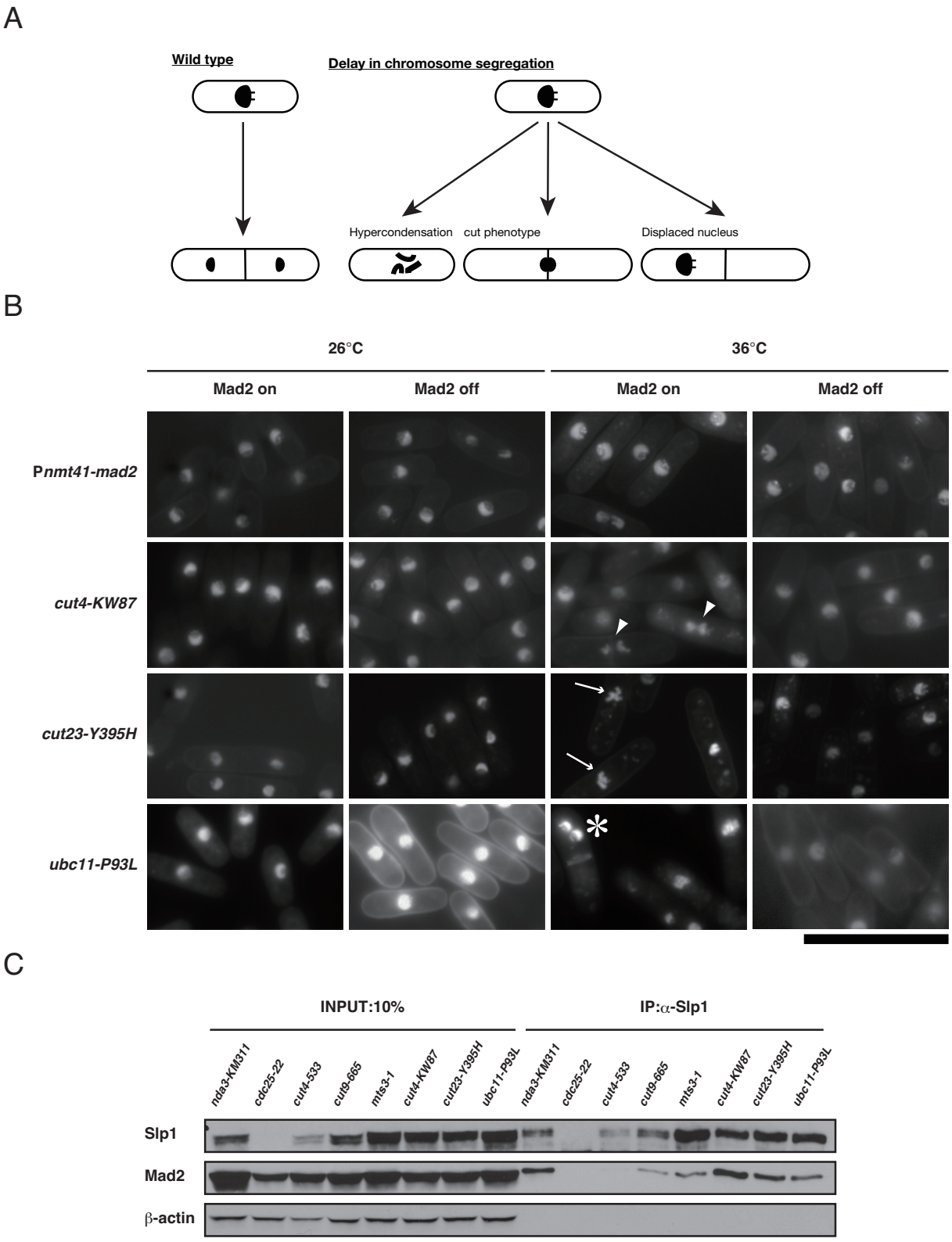


Figure 9 Screening for Mad2-dependent temperature sensitive mutants.
(A) Typical phenotypes of mitotic defect mutants. (B) Nuclear morphology. (C) Intracellular accumulation of Slp1 and immunoprecipitation of the Slp1-Mad2 complex.

Immunoprecipitation with the antibody to Slp1 with cell extracts prepared from mutants was performed. Extracts from the folloing mutant strains were also used as controls: the *nda3-KM311*, which is unable to form a spindle because of a mutation in the $\beta$-tubulin gene at the restrictive temperature of 20°C, as a positive control, the *cdc25-22*, which arrests at the boundary of G2/mitosis at the restrictive temperature of 36°C, as a negative control, and the *cut4-533*, *cut9-665* and *mts3-1* as controls of mutation involved in events after the checkpoint silencing. In six out of the sixteen candidates, respective bands of Mad2 from each extracts were the same or stronger than that from *nda3-KM311* mutant strain (Figure 9D), and thus they were selected for genetic analysis.

## Back-cross

The six strains were backcrossed with the parental strains $h^-$ *RBC115* or $h^+$ *RBC116 ($h^+$ leu1-32 mad2::ura4::nmt1-mad2)* twice and the segregation pattern of the ts marker was examined for each cross by tetrad analysis. When $ts^+$:$ts^-$ was 2:2 in $>$ 10 tetrads, the ts phenotype was judged to be due to a mutation at a single locus.

Five strains showed $2^+$:$2^-$ segregation for temperature sensitivity, indicating that each of their temperature-sensitive phenotypes was caused by a single genetic defect. These five strains were selected as candidates for further analysis.

## Linkage analysis

10 pairwise crosses were carried out among the five candidates, and the results indicated that the five mutants fall into three linkage groups. A group containing *KW88* strain has three members, and *KW87* strain and *KW89* strain each have one. These three mutants were selected as the final candidates.

## Gene cloning

In this study, one of the mutants, which was identified as the *KW89* strain through the screen, was further analyzed. By using the temperature-sensitivity in the presence of the functional SAC as a selection marker, a genomic DNA fragment complementing the temperature sensitivity was isolated from a fission yeast genomic DNA library (Tanaka et al., 2000; Nakamura et al., 2001). The integration mapping proved that this fragment originated from the *ubc11* locus encoding a cognate ubiquitin-conjugating enzyme of APC/C.

To determine the mutation sites, genomic DNA of the above-mentioned *ubc11* mutant strain was isolated and used to amplify the *ubc11* mutant gene by the PCR, and then its nucleotide sequence was determined. Only

one nucleotide substitution was found in the whole coding region: the 521st cytosine was altered to thymine. This mutation led one amino acid substitution, the 93rd prorine to leucine, and hence this mutant allele was designated as *ubc11-P93L* (Figure 10).

A

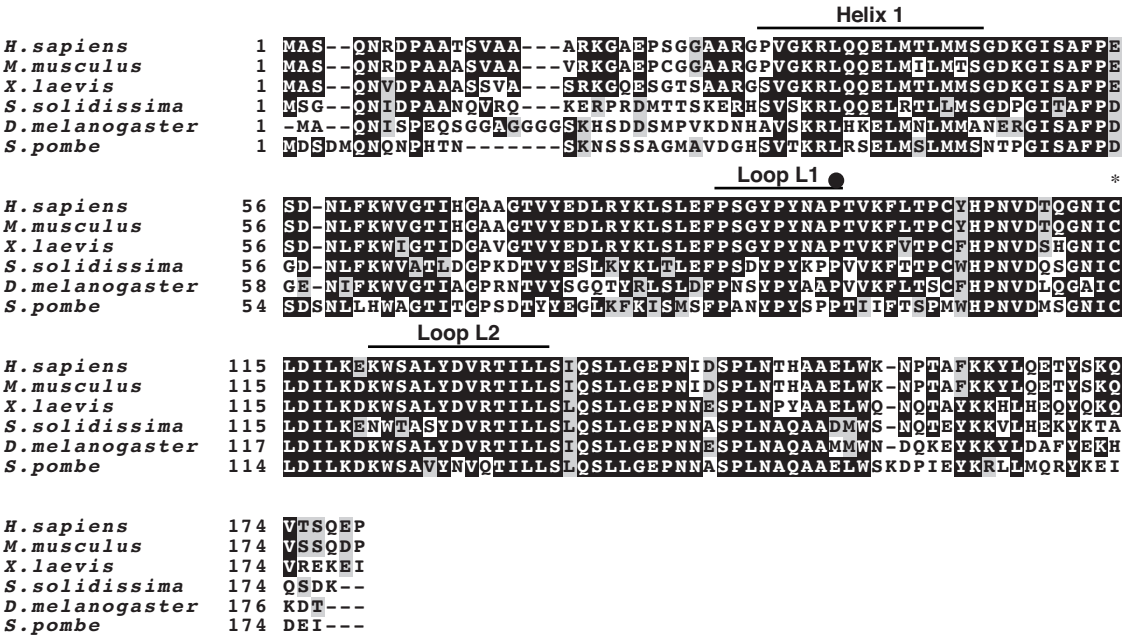


B

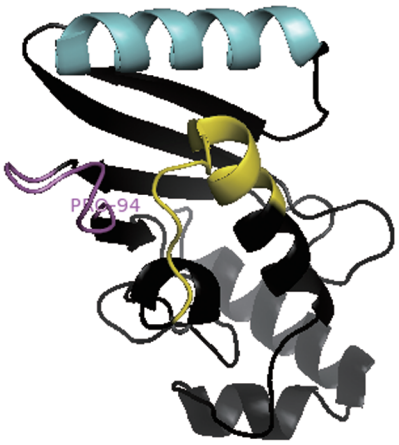


Figure 10 Multiple alignment of the amino acid sequences of *Sp*Ubc11 and its homologues.
(A) Multiple alignment of amino acid sequences of human UbcH10/UBE2C, mouse Ube2C, frog UBCx, clam E2-C, fruitfly Vihar and fission yeast Ubc11. A closed circle indicates the mutation site of Ubc11$^{P93L}$, where Pro is mutated to Leu. A cysteine residue in UBC domain for thiolester formation with ubiquitin is marked by an asterisk. (B) The crystal structure of human UbcH10$^{C114S}$, PDB ID code 1I7K (Lin et al., 2002). The E1-interacting Helix 1 is shown in cyan, and the two E3-interacting loops are shown in magenta (Loop L1) and yellow (Loop L2).

# Analyses of the *ubc11-P93L* mutant

## Inadequate Ubc11-mediated ubiquitination in *ubc11-P93L mutant cells*

### Suppression of the temperature-sensitivity in the absence of the functional SAC

As above noted, the temperature-sensitivity of the *ubc11-P93L* mutant was dependent on expression of Mad2 (Figure 11A). In order to confirm that the immediate cause was the functional SAC, further genetic analyses were performed. As indicated in Figure 11B, the temperature sensitivity could be also suppressed by deletion of the *mad3* gene as well as by introduction of *slp1-mr63*, an allele defective in binding to Mad2, suggesting that physical interaction between Slp1 and Mad2, not additional unknown functions of Mad2, might cause the growth defect in the *ubc11-P93L* mutant (Kim et al., 1998).

Meanwhile the *ubc11-P93L* $\Delta$*bub3* strain remained temperature-sensitive (Figure 11B). It has been presumed that *Sp*Bub3, as well as its homologs, is a component of MCCs, and indeed indicated that it can be co-immunoprecipitated with Mad3 in fission yeast cells (Millband and Hardwick, 2002). Recent studies, however, have proposed that *Sp*Bub3 is more likely to be dispensable for the SAC activation (Tange and Niwa, 2008; Vanoosthuyse et al., 2009; Windecker et al., 2009; Heinrich et al., 2012).

### Biochemical analysis of Ubc11$^{P93L}$ *in vitro*

In ubiquitination, E2s are well known to play two key roles; primarily receive an activated forms of ubiquitin from E1 ubiquitin-activating enzyme and subsequently catalyze ubiquitination of the substrates through interaction with E3 ubiquitin-protein ligases (Hershko et al., 1983). To examine whether Ubc11$^{P93L}$ mutant protein maintained the general functions, an *in vitro* ubiquitin transfer assay, by which we could investigate whether the Ubc11$^{P93L}$ had the ability to receive an activated forms of ubiquitin from E1, was performed. Each component was prepared from *E.coli* as a recombinant protein (Figure 12). In the positive control reaction using wild-type Ubc11 (Ubc11$^{WT}$), band at approximately 45 kDa corresponding to the sum of His-tagged Ubc11$^{WT}$ and His-tagged ubiquitin, and slower migrated band could be detected (Figure 12, lane 12). Because these bands were sensitive to boiling in the presence of DTT (data not shown), they were protein complexes consisting of Ubc11 and ubiquitins linked via the thiolester bond. In the case of Ubc11$^{P93L}$, by contrast, band at approximately 45 kDa and slower migrated band could not be detected, suggesting that the mutant was defective in transfer of activated ubiquitins from E1 (Figure 12, lane 13).

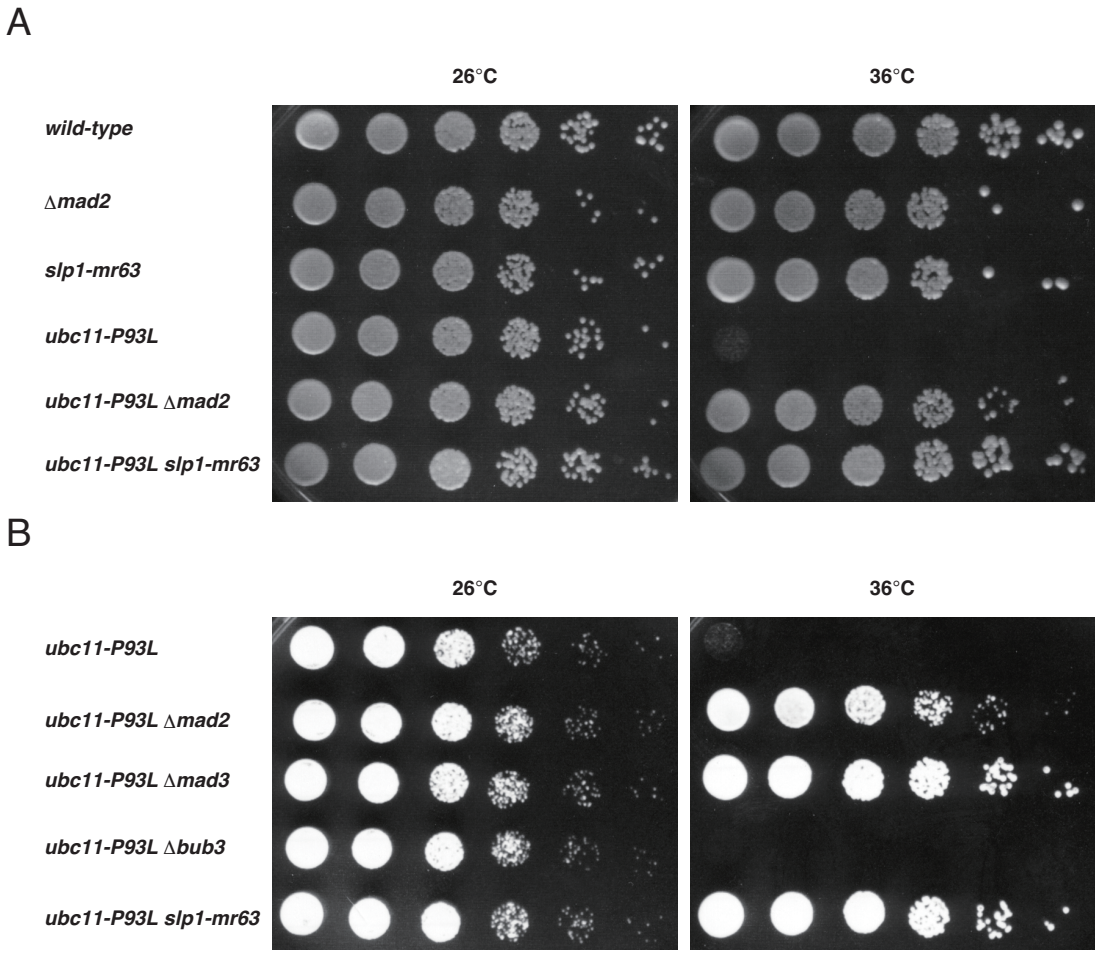


Figure 11 Suppression of the temperature-sensitivity in the absence of the functional SAC.
(A) A wild-type strain, a strain deleted for *mad2*$^{+}$ gene, Δ*mad2*, a strain expressing the mutant form of Slp1 incapable of binding to Mad2, *slp1-mr63*, *ubc11-P93L*, *ubc11-P93L* Δ*mad2*, *ubc11-P93L slp1-mr63* for their temperature-sensitivity by spot test. They were grown in liquid YEA and spotted on YEA media. The plates were incubated at 26°C or 36°C for 3 days. (B) The *ubc11-P93L*, *ubc11-P93L* Δ*mad2*, *ubc11-P93L* Δ*mad3*, *ubc11-P93L* Δ*bub3* and *ubc11-P93L slp1-mr63* strains were examined for their temperature-sensitivity by spot test. They were grown in liquid YEA and spotted on YEA media. The plates were incubated at 26°C or 36°C for 3 days.

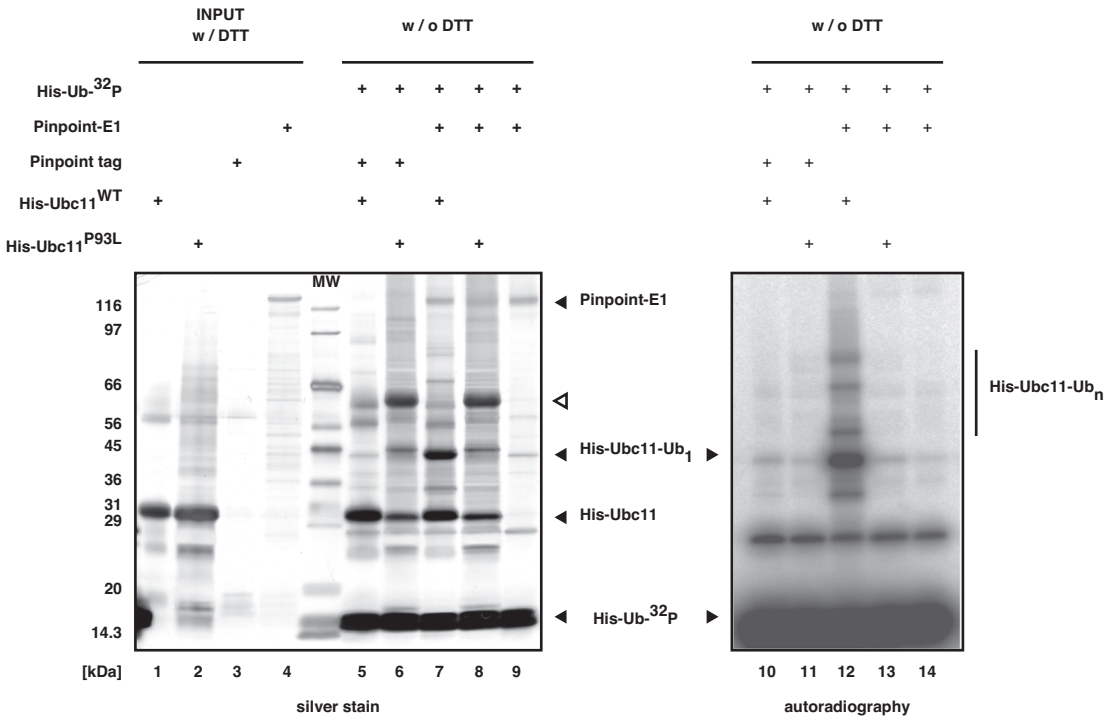


Figure 12 *in vitro* ubiquitin transfer assay of Ubc11$^{P93L}$.

The reaction mixtures for the *in vitro* ubiquitin transfer assay were run on SDS-PAGE and silver-stained (left panel) or dried and exposed to the X-ray film (right panel). Note that the His-tagged Ubc11$^{P93L}$ mutant proteins run on SDS-PAGE slower when incubated without DTT. The position on the gel (shown with open triangle) suggests that they may form a dimer. This assay was performed by Dr. Habu.

**Biochemical analysis of Ubc11$^{P93L}$ *in vivo***

We noticed that the His-tagged Ubc11$^{P93L}$ mutant proteins prepared from *E.coli* run on SDS-PAGE slower when incubated without DTT. The position on the gel, shown with the open triangle in Figure 12, suggested that they may form a dimer. Western blot analysis of cell extracts, however, revealed that the Ubc11$^{P93L}$ mutant protein existed as a monomer (Figure 13A). We speculated that the mutant protein would be protected by a cellar factor from dimerization. In addition, western blot analysis revealed that Ubc11$^{P93L}$ became extremely unstable in yeast cells (Figure 13B). Taken together, these results indicated that the level of the Ubc11-dependnet ubiquitination would be extremely low in the *ubc11-P93L* mutant cells.

**The *ubc11*$^{+}$ gene is essential even in the absence of the functional SAC**

The instability of Ubc11$^{P93L}$ could be observed even in *ubc11-P93L* Δ*mad2* cells, and the fact allowed a postulation that the essential *ubc11*$^{+}$ gene could be knocked out in the absence of the functional SAC (Osaka et al., 1997). To address this hypothesis, the *mad2*$^{+}$*/mad2::ura4*$^{+}$ *ubc11*$^{+}$*/ubc11::LEU2* heterozygous diploid strain was constructed and then tetrad analysis was performed (Figure 14A and B). All 10 tetrads dissected gave rise to two viable and two inviable spores (Figure 14C). These survivors were all leucine auxotrophic mutants and the segregation patterns were independent on uracil auxotrophy, suggesting that activities of Ubc11 are required for cell proliferation regardless of the SAC.

Taken together, these results suggested that the level of the Ubc11-mediated ubiquitination would be extremely low, but not completely-lost, in the *ubc11-P93L* mutant cells.

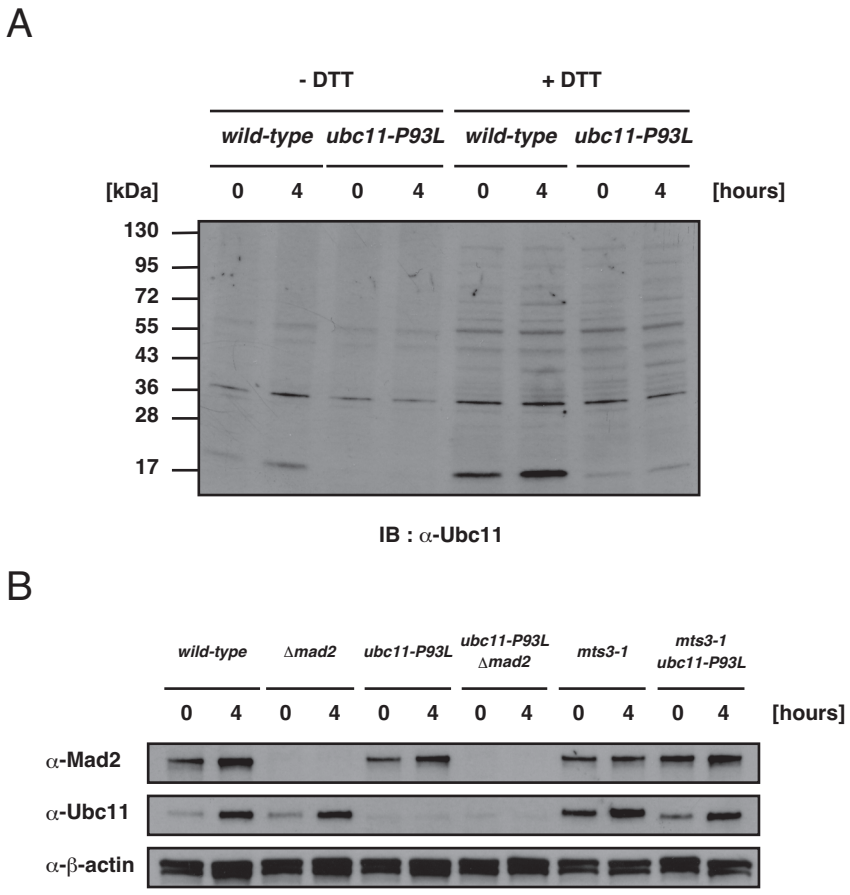


Figure 13 Biochemical analysis of Ubc11$^{P93L}$ *in vivo*.
(A and B) Western blot was performed with extracts prepared from cells incubated at 26°C or 36°C for 4 hours. The genotype of each strain is indicated on the top.

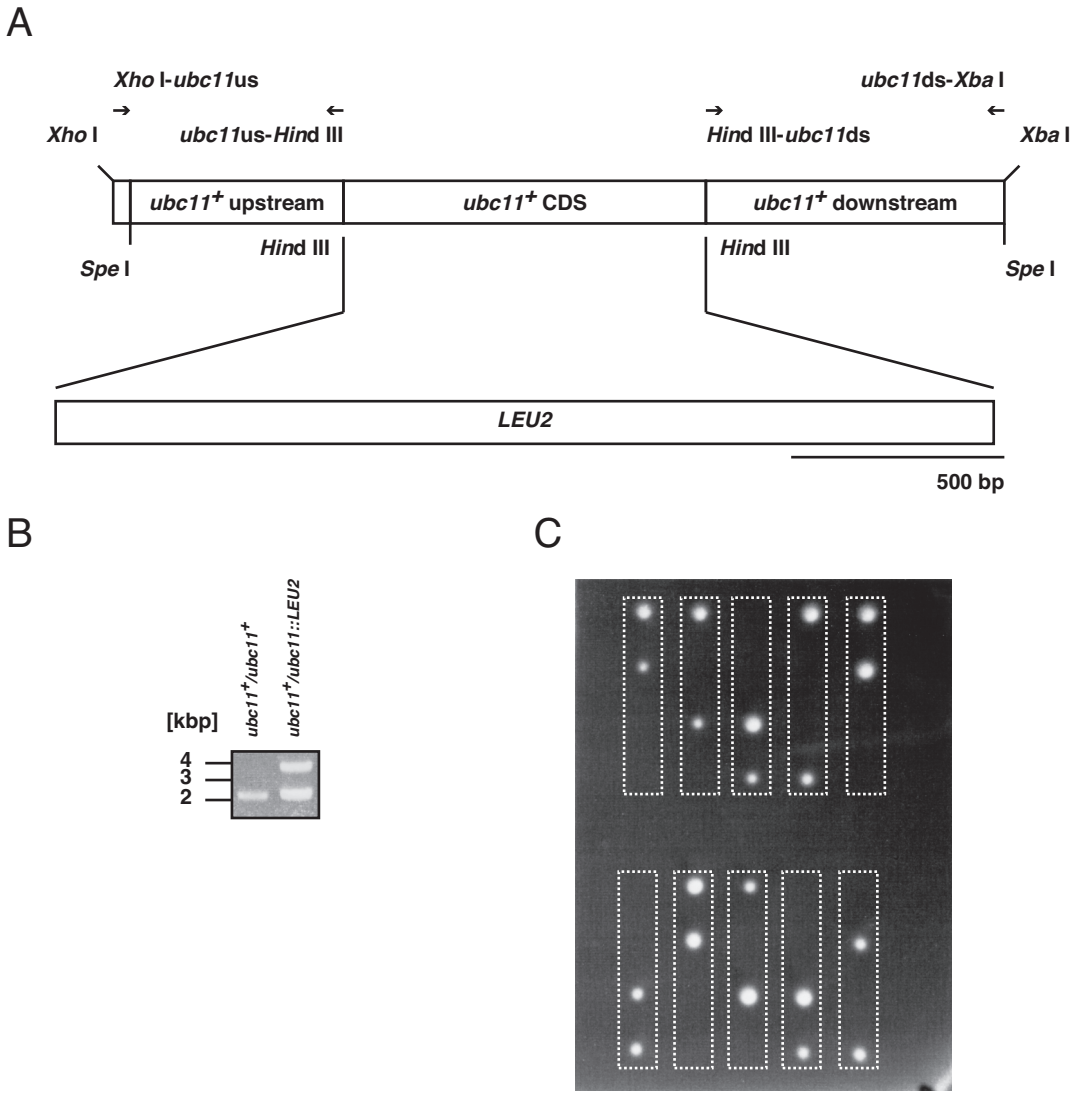


Figure 14 The *ubc11*$^+$ gene is essential even in the absence of the functional SAC.
(A) A partial restriction enzyme map of the *ubc11*$^+$ genomic locus. *ubc11*$^+$ fragment was constructed by replacing the CDS of *ubc11*$^+$ with the *LEU2* sequence isolated from pREP1. (B) Colony PCR fragments amplified by using the forward primer *Xho*I-*ubc11*us and the reverse primer *ubc11*ds-*Xba*I, from *ubc11*$^+$*/ubc11*$^+$ homozygote (left lane) or *ubc11*$^+$*/ubc11::LEU2* heterozygote (right lane). (C) The *mad2*$^+$*/mad2::ura4*$^+$ *ubc11*$^+$*/ubc11::LEU2* heterozygous diploids were induced to sporulate and the resulting tetrad were dissected. The four spores from a single tetrad are contained within each vertical column.

## Ubc11 is required for APC/C$^{MCC}$ disassembly

### Mitotic arrest in the *ubc11-P93L* mutant

Considering the prerequisites for its growth defect, *ubc11-P93L* cells were most likely to have difficulty in mitotic progression. In order to determine at which stage of the cell cycle the *ubc11-P93L* mutant was arrested, first the nuclear morphology were examined. Two hours after the shift to the restrictive temperature, the mutant cells exhibited condensed chromosomes (Figure 15) and short spindle (Figure 16), indicating that they were arrested around metaphase. The arrest was not tight as the mutant cells thereafter exhibited *cut* phenotype or aberrant septation (Figure 15).

### SAC can be Satisfied in the *ubc11-P93L* mutant

To further analyze which events the defect of Ubc11 could influence, and first whether kinetochore-spindle attachment was established properly was investigated. GFP-Cnp1 signals, an indicator of the position of centromere/kinetochore, were found as multiple foci no more than six, which overlapped with microtubules in 45% of the *ubc11-P93L* mutants shifted to the restrictive temperature for 2 hours (Figure 16), suggesting that SAC was satisfied with establishment of kinetochore-spindle attachment in these cells.

### Stable APC/C$^{MCC}$ in the *ubc11-P93L* mutant

Finally, whether APC/C$^{MCC}$ was disassembled was examined. Co-immunoprecipitation was performed with cell extracts prepared from a strain expressing a component of APC/C, Cut23, tagged with FLAG epitope to precipitate APC/C. As shown in Figure 17, both Slp1 and Mad2 were bound to APC/C in cells shifted to the restrictive temperature for 2 to 3 hours. The level of Slp1 both in cell extracts and immunoprecipitates with APC/C thereafter decreased. This reduction was partly due to its residual activity of the Ubc11$^{P93L}$, not complete loss-of-function mutant (Figure 13 B), or alternatively, due to decreased expression of Slp1 by cell cycle progression.

Considering together with these observations, it was concluded that the activity of Ubc11 was required for SAC silencing through MCCs disassembly, but not for its satisfaction.

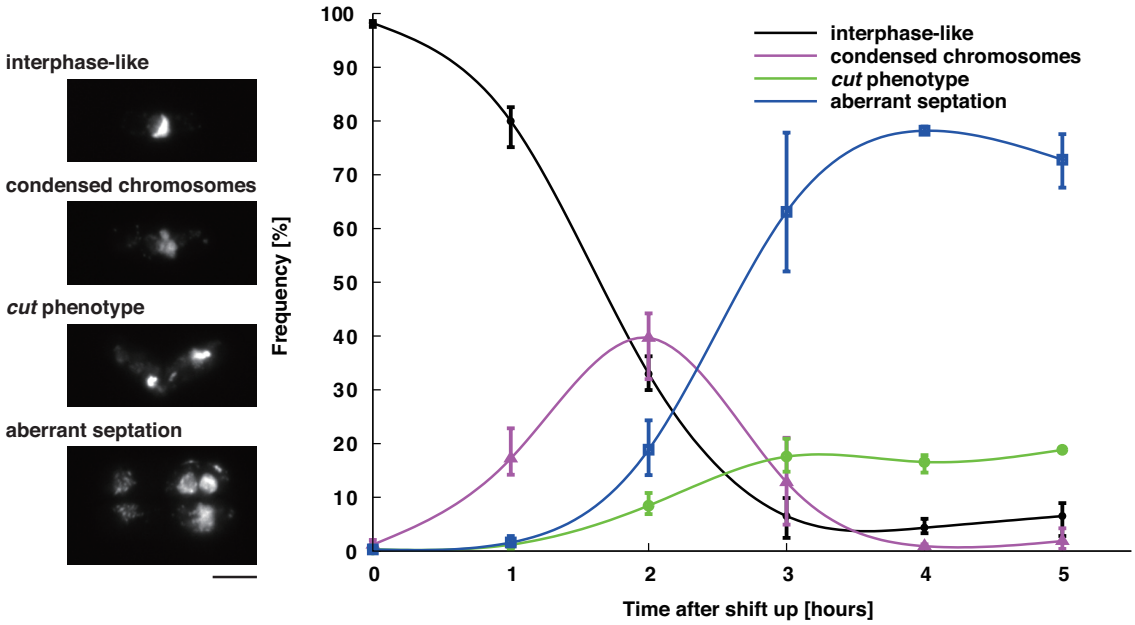


Figure 15 Mitotic arrest in the *ubc11-P93L* mutant.
The frequency of respective phenotypes of nuclear morphology; inter-phase like normal phenotype, condensed chromosomes, the *cut* phenotype and aberrant septation are shown at each time point after the shift to the restrictive temperature.

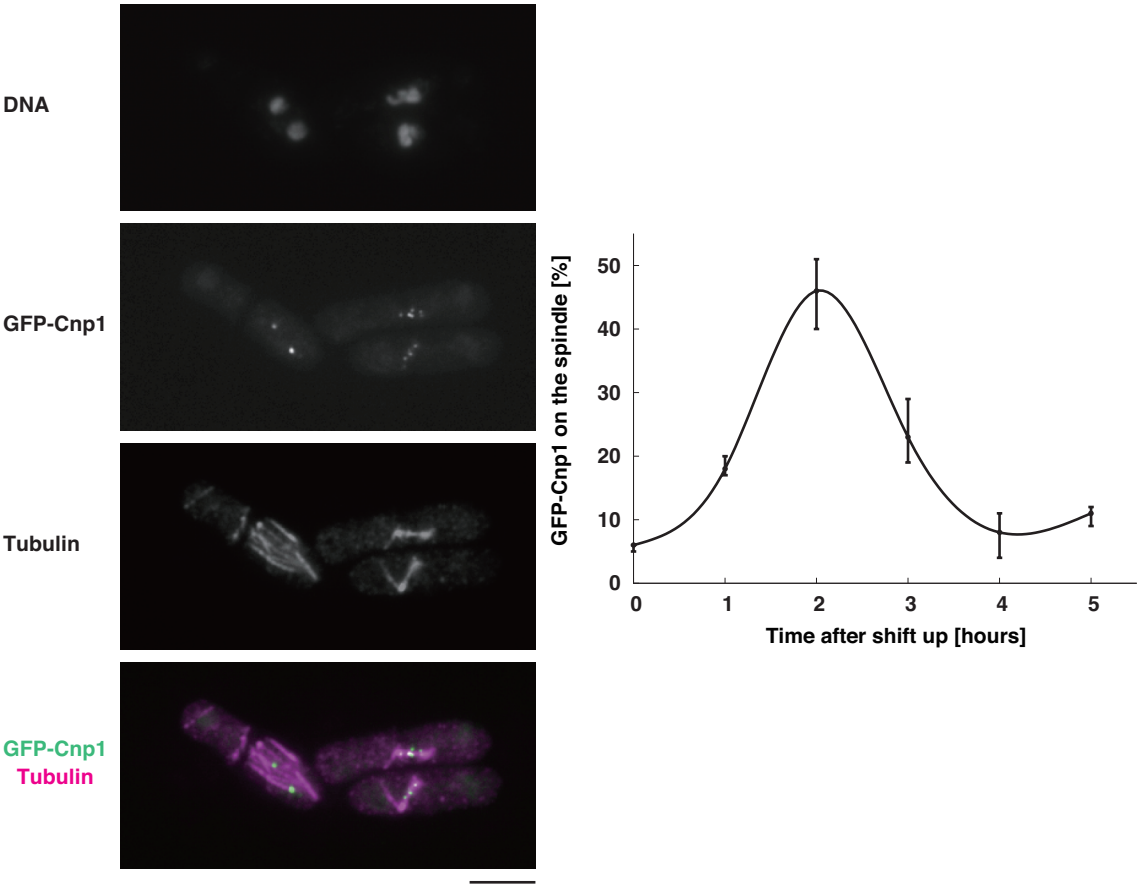


Figure 16 SAC can be Satisfied in the *ubc11-P93L* mutant.
The *ubc11-P93L* mutant cells were incubated for up to 5 hours at the restrictive temperature. The sample taken at 2 hour after the shift was processed for indirect immunofluorescent staining with the aniti-tubulin antibody (magenta). DNA was visualized by staining with DAPI. The position of the centromere (Cnp1-GFP, green) was also examined. The scale bar indicates 5 $\mu$m. The frequency of the cells with Cnp1-GFP on the spindle was also shown at each time point after the shift to the restrictive temperature.

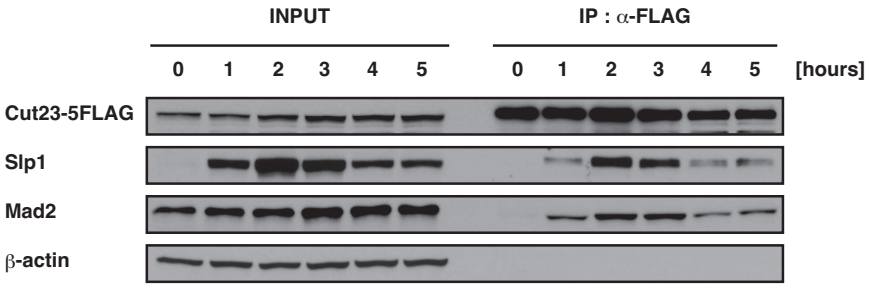


Figure 17 Stable APC/C$^{MCC}$ in the *ubc11-P93L* mutant.
Immunoprecipitation with the anti-FLAG antibody was performed with extracts prepared from the *ubc11-P93L* cells incubated at 26°C or 36°C for up to 5 hours.

## Specific requirement of Ubc11 for Slp1 destruction

### APC/C substrate stabilities in *ubc11-P93L* and *ubc11-P93L* Δ*mad2* cells

It has been previously reported that the B-type cyclin/*Sp*Cdc13 and securin/Cut2 cause a mitotic arrest if not properly degraded in the APC/C-dependent manner (Glotzer et al., 1991; Yamano et al., 1996; Funabiki et al., 1996a, 1997). Now here arises a question: Regardless of harboring the defect of Ubc11, why and how can the SAC-defective *ubc11-P93L* strains overcome the temperature-sensitivity and promote cell cycle progression? Therefore how the Ubc11$^{P93L}$ mutation affected the stability of proteins normally degraded in the APC/C-dependent manner was examined, and first the cellular levels of Slp1, Cdc13 and Cut2 in the *ubc11-P93L* mutants were monitored. As shown in Figure 18A, the level of Slp1 began to increase and reached a peak 2 hours after the shift to the restrictive temperature. The other two proteins, Cdc13 and Cut2, transiently accumulated after the shift, but were degraded much more rapidly than Slp1. Remarkably, Slp1 also accumulated in the *ubc11-P93L* Δ*mad2* double mutant, which could grow at the restrictive temperature.

### APC/C substrate stabilities in *slp1-362* and *mts3-1* cells

The above-descrived finding remained, however, equivocal and the result could be also interpreted that the degradations of Cdc13 and Cut2 observed in the *ubc11-P93L* cells were caused by an APC/C- or even proteasome-independent proteolytic system, which could be triggerd by prolonged mitotic arrest. Indeed, in the *ubc11-P93L* Δ*mad2* cells an association of Slp1 with APC/C could not be detected by coimmunoprecipitation, raising the possibility that in these cells APC/C$^{Slp1}$ could not be assembled and therefore was dispensable for the ubiquitination of Cdc13 and Cut2 (Figure 18B). To address this, two temperature-sensitive mutants were further analyzed: *mts3-1* strain defective in 26 S proteasome function and *slp1-362* strain defective in the formation of APC/C$^{Slp1}$ due to a 113 amino acid truncation of the C-terminus including IR-motif, which is required for binding of Slp1 to APC/C (Gordon et al., 1996; Matsumoto, 1997; Yamada et al., 2000; Ohi et al., 2007).

First, genetic analysis revealed that their temperature-sensitivity could not be suppressed in the absence of the functional SAC (Figure 19A). This was a cleary distinguishable characteristic from the *ubc11-P93L* strain, and next the cellular levels of Cdc13 and Cut2 in these mutants were monitored. In the *mts3-1* cells, the level of Cdc13 increased immediately after the shift to the restrictive temperature and subsequently, 3 hours after the shift, Cut2 began to accumulate (Figure 19B). A similar tendency was also observed in the case of the *mts3-1* Δ*mad2* mutant, except that the individual signal intensities were slightly lower. On the other hand,

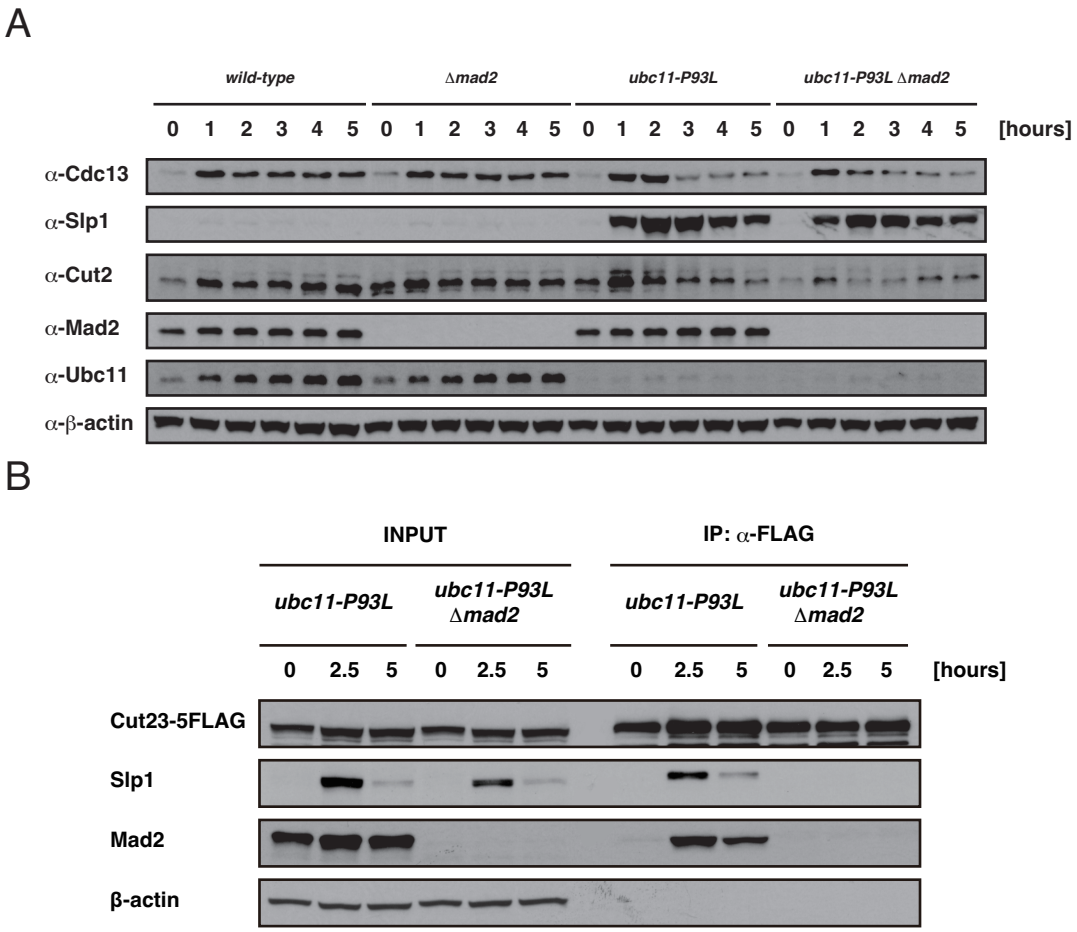


Figure 18 APC/C substrate stabilities in *ubc11-P93L* and *ubc11-P93L* Δ*mad2* cells.
(A) Western blot was performed with extracts prepared from cells incubated at 26°C or 36°C for up to 5 hours. The genotype of each strain is indicated on the top. (B) Immunoprecipitation with the anti-FLAG antibody was performed with extracts incubated at 26°C or 36°C for up to 5 hours. The genotype of each strain is indicated.

in the *slp1-362* cells the respective levels of Cdc13 and Cut2 gradually and almost simultaneously began to increase after the shift. In the absence of the functional SAC, each of them accumulated more rapidly. Albeit more or less differences in signal intensities, both Cdc13 and Cut2 remained stable in these four mutant cells, suggesting that the two substrates could be ubiquitinated by APC/C$^{Slp1}$ and thereafter degraded by proteasome in the *ubc11-P93L* mutants whereas Slp1 could not.

**Comparison of APC/C substrate stabilities in *ubc4-P61S* and *ubc11-P93L* cells**

A previous study proposed that fission yeast APC/C cooperated with at least two E2s, Ubc11 and Ubc4, each of which had an essential and incompatible role in polyubiquitin-chain formation (Seino et al., 2003). The above-mentioned findings, however, provided a novel hypothesis that APC/C$^{Slp1}$-dependent ubiquitination of Cdc13 and Cut2 could take place in the absence of Ubc11. To address this, here analyses using strains with a point mutation in Ubc4, *ubc4-P61S* mutant (Seino et al., 2003), were performed. The temperature-sensitivity caused by this mutation could not be suppressed by *mad2*$^{+}$ deletion (Figure 20A), suggesting that the function of Ubc4 could be different from that of Ubc11.

To test the above noted hypothesis more rigorously, the cellular levels of the three proteins at the transition from prophase to anaphase were compared. The cold-sensitive *nda3-KM311* mutation defective in the spindle formation (Hiraoka et al., 1984) was introduced into the *ubc11-P93L*, *ubc4-P61S* and *ubc4-P61S ubc11-P93L* double mutants, respectively.

In the *nda3-KM311* single mutant after incubation at its restrictive temperature of 20°C, the three proteins accumulated. Upon the shift to 36°C, they were mostly degraded within 9 minutes (Figure 20B). The level of Cdc13, which gradually declined in each of the *ubc4-P61S nda3-KM311* and *ubc11-P93L nda3-KM311* double mutants, was stably maintained in the *ubc4-P61S ubc11-P93L nda3-KM311* triple mutant. While decreased in the *ubc4-P61S nda3-KM311* double mutant, the level of Slp1 rather continued to increase in *ubc11-P93L* mutants. In the *nda3-KM311* single mutant at time point 0, the band representing Cut2, which was observed as a ladder, rapidly disappeared after the shift up. In the *ubc4-P61S nda3-KM311* double mutant, Cut2 was stable largely as a single band, indicated with a white arrow in Figure 20B. The Cut2-ladder persisted in the *ubc11-P93L nda3-KM311* double mutant, though it was degraded to some extent at later time points. In the triple mutant, both of the two forms, the ladder and the single band, of Cut2 remained stable.

These results would suggest the substrate specific roles of the two E2s. First, only either one of these two E2s can induce degradation of Cdc13. This reaction, however, can be synergistically enhanced. On the other

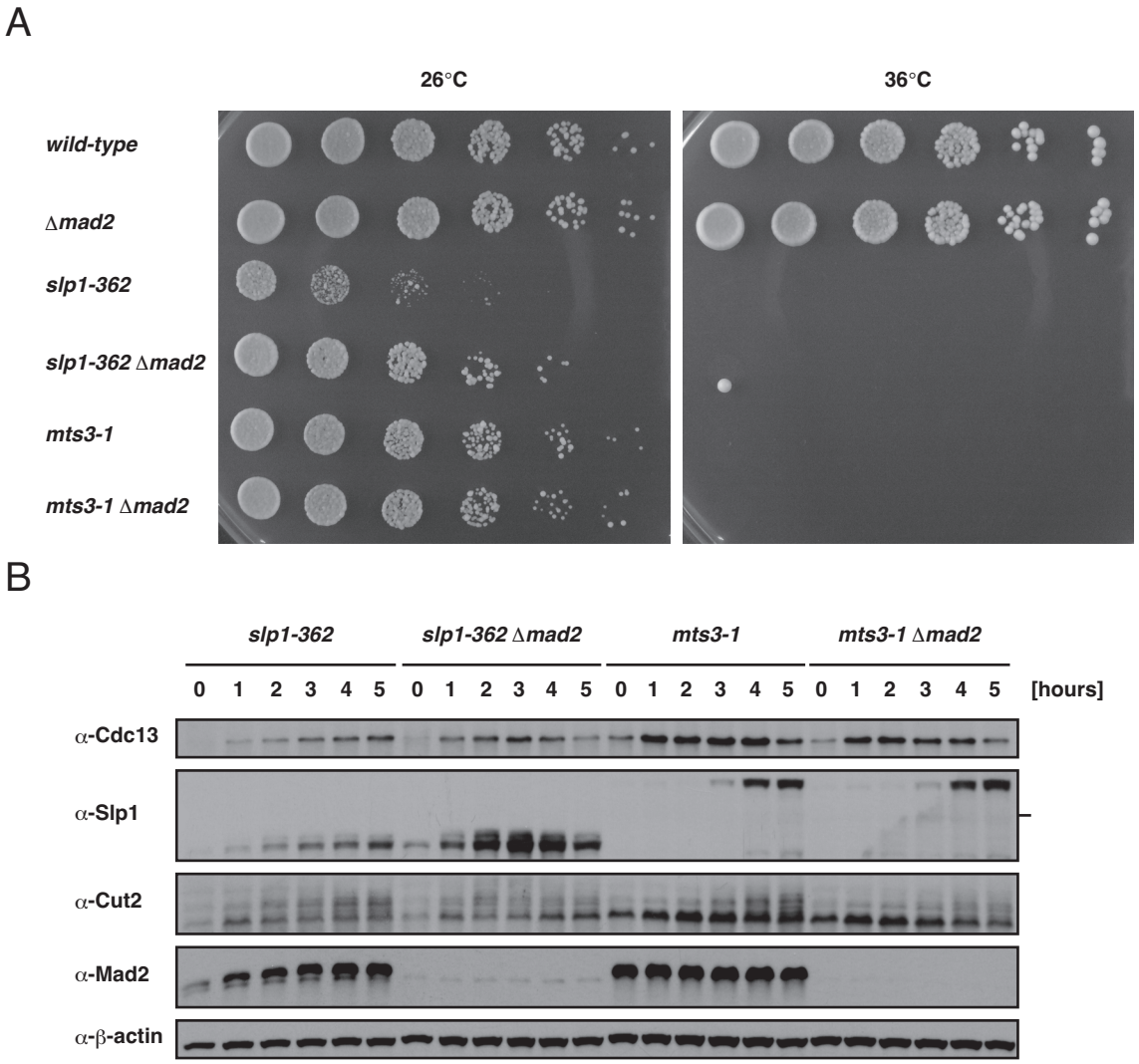


Figure 19 APC/C substrate stabilities in *slp1-362* and *mts3-1* cells.
(A) A wild-type, Δ*mad2*, *slp1-362*, *slp1-362* Δ*mad2*, *mts3-1* and *mts3-1* Δ*mad2* strains were examined for their temperature-sensitivity by spot test. They were grown in liquid YEA and spotted on YEA media. The plates were incubated at 26°C or 36°C for 4 days. (B) Western blot was performed with extracts prepared from cells incubated at 26°C or 36°C for up to 5 hours. The genotype of each strain is indicated on the top.

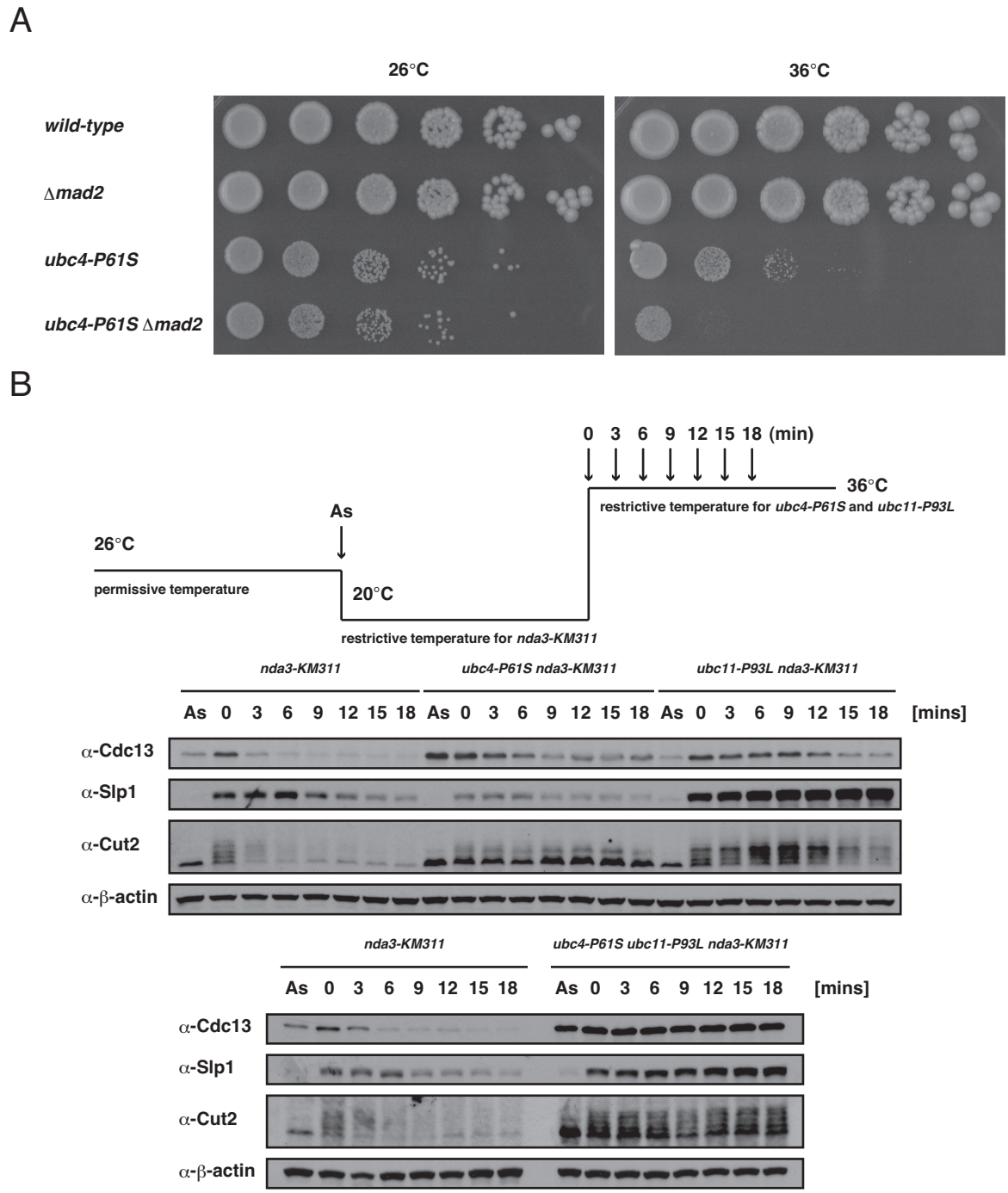


Figure 20 Comparison of APC/C substrate stabilities in *ubc4-P61S* and *ubc11-P93L* cells.
(A) A wild-type, Δ*mad2*, *ubc4-P61S*, *ubc4-P61S* Δ*mad2* strains were examined for their temperature-sensitivity by spot test. They were grown in liquid YEA and spotted on YEA media. The plates were incubated at 26°C or 36°C for 4 days. (B) Each strain was arrested by the shift to the restrictive temperature for the *nda3-KM311* mutation, 20°C, for 6 hours and released to 36°C at time 0. Cell extracts were prepared at indicated time points and processed for western blotting with each antibody. The genotype of each strain is indicated on the top. Extracts prepared from an asynchronous culture (As) were also examined in the same way.

hand, each of them seems to take a separate responsibility for destruction of Cut2. Besides, these data would depict the specific requirement of Ubc11 for degradation of Slp1; this E2 is almost exclusively responsible for the stability of Slp1.

## Ubc11-dependent ubiquitination of Slp1

### Ubc11- and APC/C-dependent Slp1 ubiquitylation

Although previous studies showed that Cdc13 and Cut2 could be ubiquitinated dependently on APC/C (Yamashita et al., 1996; Berry et al., 1999; Yoon et al., 2002), no evidence was presented for ubiquitination of Slp1, unlike its homologs. Therefore whether Slp1 was ubiquitinated was tested by following an assay previously reported (Takayama et al., 2010). His6-tagged ubiquitin (His-Ub) was ectopically expressed in the following three strains, the wild-type, *mts3-1* mutant and *cut9-665 mts3-1* double mutant defective in APC/C and 26 S proteasome function (Hirano et al., 1986).

Four hours after the shift to the restrictive temperature of 36°C for the *mts3-1* and *cut9-665* mutations, His-Ub and its conjugates were purified from the respective cell extracts with the metal beads, and the presence/status of Slp1 was examined by immunoblot with the anti-Slp1 antibody. The *mts3-1* mutant expressing HA-tagged ubiquitin (HA-Ub) was also examined as a negative control. As shown in Figure 21A lane 3, in the extracts of the *mts3-1* mutant expressing His-Ub, a smearing band above 95 kDa could be detected. This band could not be detected in the *cut9-665 mts3-1* double mutant expressing His-Ub, suggesting it was produced dependently on the functional APC/C (Figure 21A lane 5). In order to examine the identity of the band appeared at the position slightly above 55 kDa, indicated by the asterisk in Figure 21, cell extracts from the *slp1-362* mutant were prepared, and the metal beads-bound fraction was analyzed by immunoblot with the anti-Slp1 antibody. As shown in Figure 21 lane 2, in this mutant cell extracts, a band at the position of 43 kDa, but not around 55 kDa in the metal beads-bound fraction, could be detected, indicating that the asterisk in Figure 21 represented the wild-type Slp1. Furthermore, the smearing band above 95 kDa was not detectable in the metal beads-bound fraction of extracts prepared from the *slp1-362* mutant. It was also found that in the extracts of the *ubc11-P93L mts3-1* double mutant signal intensity of the smearing band above 95 kDa was weakened (Figure 21 lane 6). On the other hand, two bands specific to this condition could be observed in the molecular weight range from 72 to 95 kDa. These modifications were probably due to a residual activity of Ubc11$^{P93L}$ or other E2 enzymes with a low activity/specificity, rather highlighting a crucial role of Ubc11 for efficient polyubiquitination of Slp1.

Taken together, these results would suggest that Slp1 can be ubiquitinated by APC/C- and primarily Ubc11-dependent manner and subsequently degraded by the 26 S proteasome.

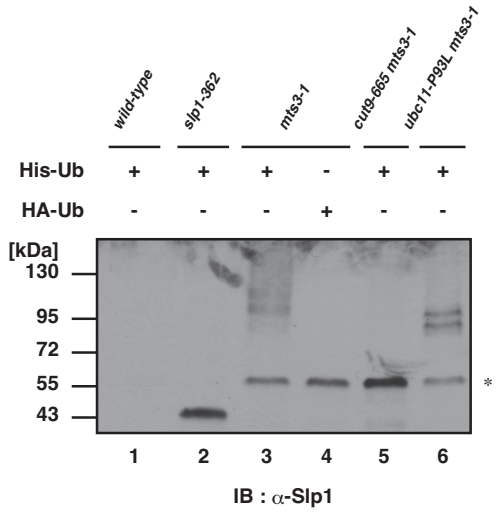


Figure 21 Ubc11- and APC/C-dependent Slp1 ubiquitylation.
Cell extracts were prepared from cultures first incubated at 26°C and then shifted up to 36°C for 4 hours. Ubiquitinated proteins were purified and analyzed by immunoblotting with the Slp1 antibody. Note that the band likely representing nonubiquitinated Slp1, indicated by asterisk, can also be detected in the pull-down samples, likely due to a His-residue cluster within the Slp1 protein.

**Kinetochore-spindle attachment-independent Slp1 ubiquitination**

Previous studies provided evidence that APC/C-mediated ubiqutination and the following proteasomal degradation of Cdc20 occurred even during the SAC activation (Pan and Chen, 2004; Nilsson et al., 2008). To test whether this was also the case for fission yeast Slp1, its stability was examined in the *nda3-KM311* mutant cells arrested at the restrictive temperature due to SAC. In the presence of 100 $\mu$g/ml cycloheximide, an inhibitor of protein synthesis, the cellular level of Slp1 rapidly decreased, while other proteins, including Cdc13 and Cut2, were more stable (Figure 22A). Besides, in the extracts of the arrested *nda3-KM311* mutant cells expressing His-Ub, a smearing band above 95 kDa could be also detected (Figure 22B). These results indicate that as well as its homologs, Slp1 could be quantitatively regulated via the ubiquitin-dependent proteasomal proteolysis during the SAC activation.

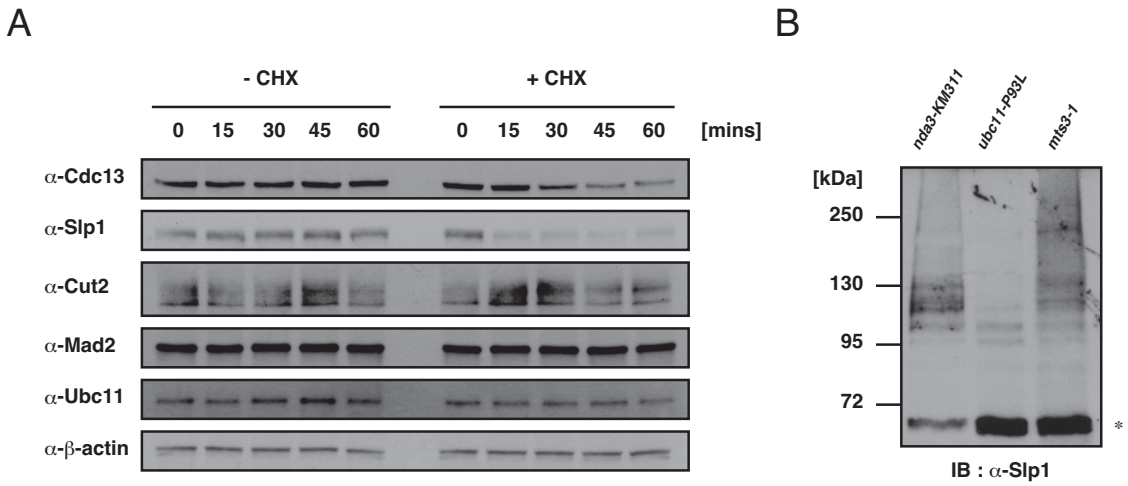


Figure 22 Kinetochore-spindle attachment-independent Slp1 ubiquitination.
(A) The *nda3-KM311* mutant cells were first incubated at 20°C for 6 hours. Cycloheximide was added to the media at time 0, and continuously incubated for up to 60 minutes. Cell extracts were processed for immunoblot at each time point. (B) The *nda3-KM311* mutant cell extracts were prepared from cultures first incubated at 32°C and then shifted down to 20°C for 6 hours. Other cell extracts were prepared and processed as in Figure 21.

## Analyses of the *cut23-Y395H* mutant

### Isolation of the *cut23-Y395H* mutant

In this study, another mutant strain isolated by the same procedures was also analyzed. Genetic analysis indicated that the mutation was on the *cut23*$^{+}$ gene, encoding the fission yeast homolog of Apc8/Cdc23, a subunit of APC/C. Sequencing of the mutated gene identified an amino acid residue substitution, the 395th tyrosine by histidine, and thereby this allele was designated *cut23-Y395H* (Figure 23 A). As was the case for the *ubc11-P93L* strains, the temperature-sensitivity could be suppressed by deletion of the *mad2* gene as well as by introduction of *slp1-mr63*, suggesting that physical interaction between Slp1 and Mad2 might cause the growth defect in the *cut23* mutant (Figure 23 B).

### MCCs disassembly requires its binding to APC/C through Cut23

Preceding analyses in budding yeast and mammal indicated that a point mutation in one TPR motif of this subunit, *Sc*Cdc23$^{N405A}$ or *Hs*APC8$^{N338A}$, reduced binding to the coactivators (Matyskiela and Morgan, 2009; Izawa and Pines, 2011). The 395th tyrosine of Cut23 was not identical to this amino acid residue and contained in the neighboring TPR motif, but was located relatively close (Figure 21 A), leading to the presumption that the similar defect would be seen in this mutant. To examine, co-immunoprecipitation was performed with cell extracts prepared from a strain expressing FLAG-tagged wild-type Cut23 or Cut23$^{Y395H}$ mutant protein. As shown in Figure 24, in the *cut23-Y395H-5FLAG* cells Slp1 coimmunoprecipitated with anti-FLAG antibody was obviously less than the positive control, the extract prepared from the arrested *nda3-KM311* mutant cells expressing FLAG-tagged Cut23. The signal intensity of the coimmunoprecipitated Mad2 was correspondingly weaker, suggesting that Cut23$^{Y395H}$ mutant form also reduced affinity for MCCs. On the other hand, as was the case for the *ubc11-P93L* Δ*mad2* mutant (Figure 18B), an association of Slp1 with APC/C in the *cut23-Y395H-5FLAG* Δ*mad2* cells could not be detected by coimmunoprecipitation.

It was noticeable that there remained Slp1 incorporated into MCCs in the *cut23-Y395H-5FLAG* cells. As mentioned below, the SAC could be satisfied in this mutant cells (Figure 25B), suggesting that the disassembly of MCCs required its binding to Cut23 — APC/C. This observation supports the prevailing hypothesis that APC/C-mediated ubiquitylation reactions are involved in MCCs disassembly.

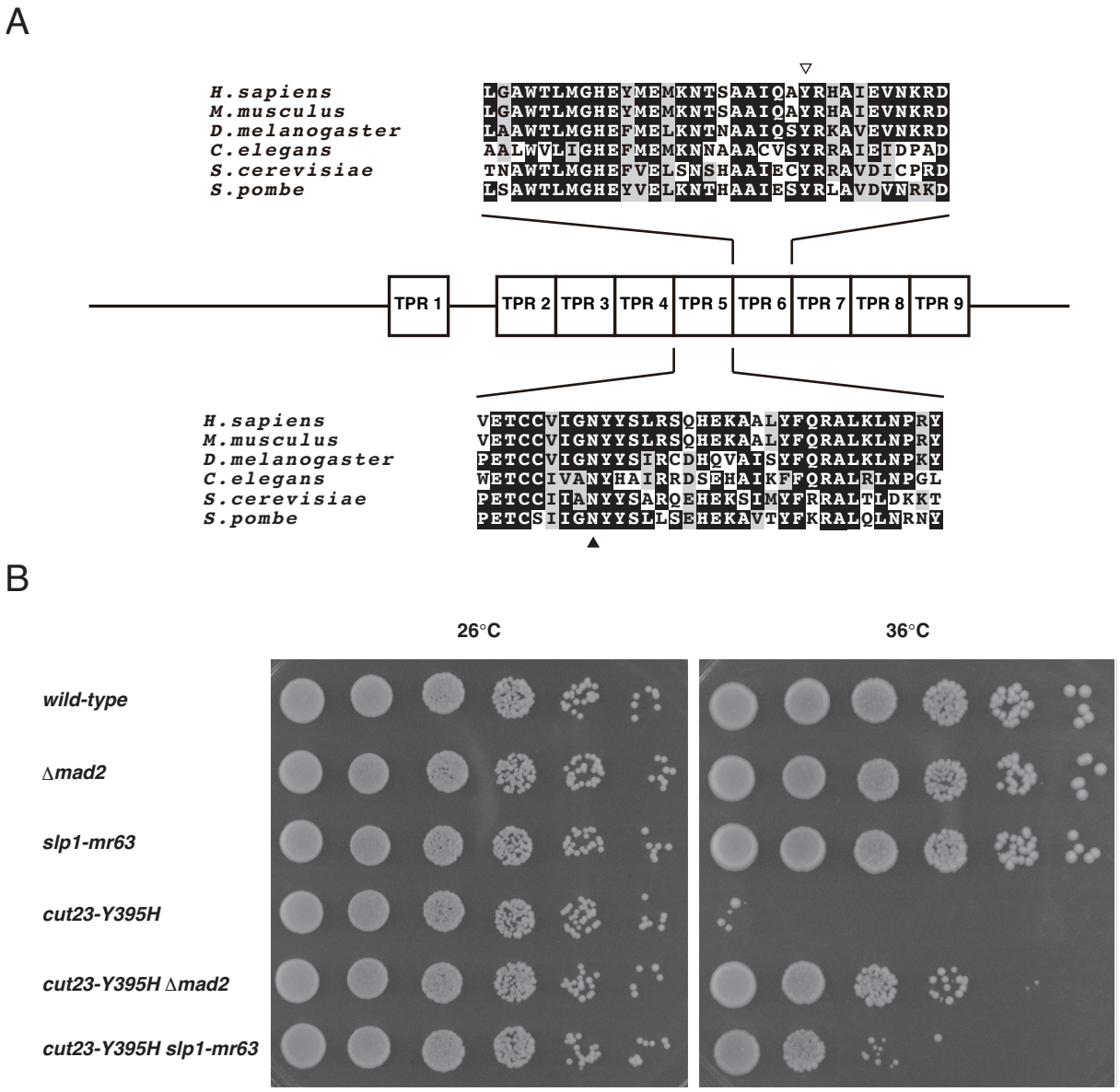


Figure 23 Isolation of the *cut23-Y395H* mutant.
(A) Multiple alignment of partial amino acid sequences of human APC8/CDC23, mouse Cdc23, fruitfly Cdc23, budding yeast Cdc23 and fission yeast Cut23. An open triangle indicates the mutation site of Cut23$^{Y395H}$, where Tyr is mutated to His. Previously known mutation site, *Sc*Cdc23$^{N405A}$ or *Hs*APC8$^{N338A}$, is marked by a closed triangle. (B) A wild-type, Δ*mad2*, *slp1-mr63*, *cut23-Y395H*, *cut23-Y395H* Δ*mad2*, *cut23-Y395H slp1-mr63* for their temperature-sensitivity by spot test. They were grown in liquid YEA and spotted on YEA media. The plates were incubated at 26°C or 36°C for 3 days.

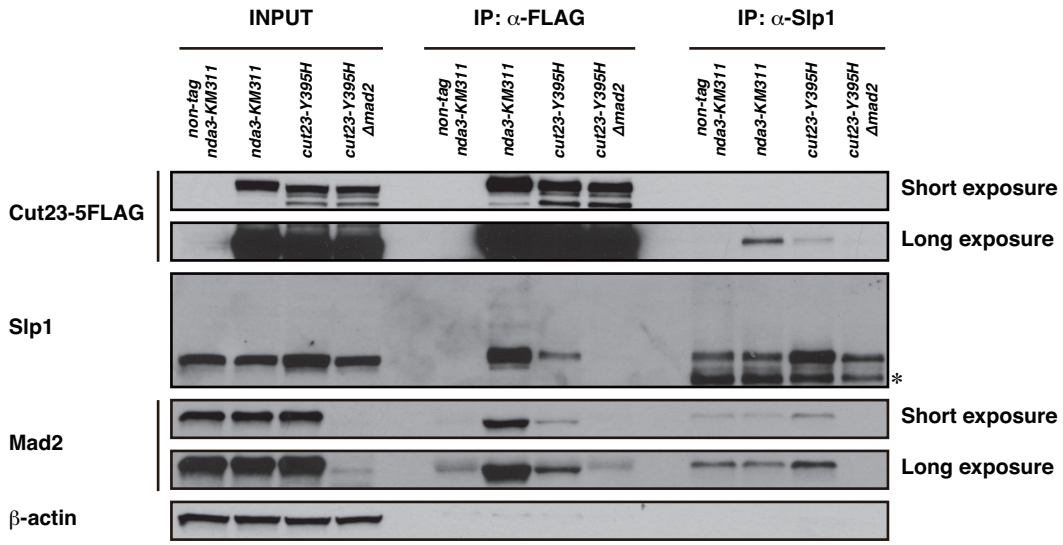


Figure 24 MCCs disassembly requires its binding to APC/C through Cut23.
Immunoprecipitation with the anti-FLAG antibody or anti-Slp1 antibody were performed with extracts prepared from the cells, each of whose genotypes is indicated on the top. The *nda3-KM311* cells were first cultured at 32°C and then incubated at 20°C for 6 hours. The *cut23-Y395H* cells were initially cultured at 26°C and thereafter shifted up to 36°C for 4 hours.

### Specific requirement of Cut23 for Slp1 destruction

Further the cellular levels of the three proteins, Cdc13, Cut2 and Slp1 in the *cut23-Y395H* or *cut23-Y395H-5FLAG* Δ*mad2* cells were investigated.

As shown in Figure 25A, the level of Slp1 in the *cut23-Y395H* cells began to increase and reached a peak 4 hours after the shift to the restrictive temperature of 36°C. The signal intensity of Cdc13 after the shift up was almost constant and a drastic drop seen in the case of the *ubc11-P93L* mutants (Figure 18A) could not be detected. Cut2 remained stable and was observed as a ladder 3 or more hours after the shift. The increase of GFP-Cnp1 signals on the spindle coincided with this, suggesting that they undergo tight mitotic arrest after the SAC satisfaction compared with the *ubc11-P93L* mutant (Figure 24 and Figure 25B).

On the other hand, also in the *cut23-Y395H* Δ*mad2* cells, after the shift the obvious decrease of Cdc13 could not be observed. Compared with wild-type or Δ*mad2* cells, there seemed not to be striking difference in the cellular level/state of Cut2 — at most slightly increase of non-phosphorylated form. Considering the results in Figure 19, it was conceivable that APC/C$^{Slp1}$ containing Cut23$^{Y395H}$ had the potential ability to ubiquitinate these substrates and promote cell cycle progression. By contrast, Slp1 accumulated in this mutant cells. The peak value was, however, less than the case in the *mad2*$^{+}$ cells probably due to cell cycle-related oscillation of expression of Slp1.

These results imply the specific requirement of Cut23, in addition to Ubc11, for degradation of Slp1.

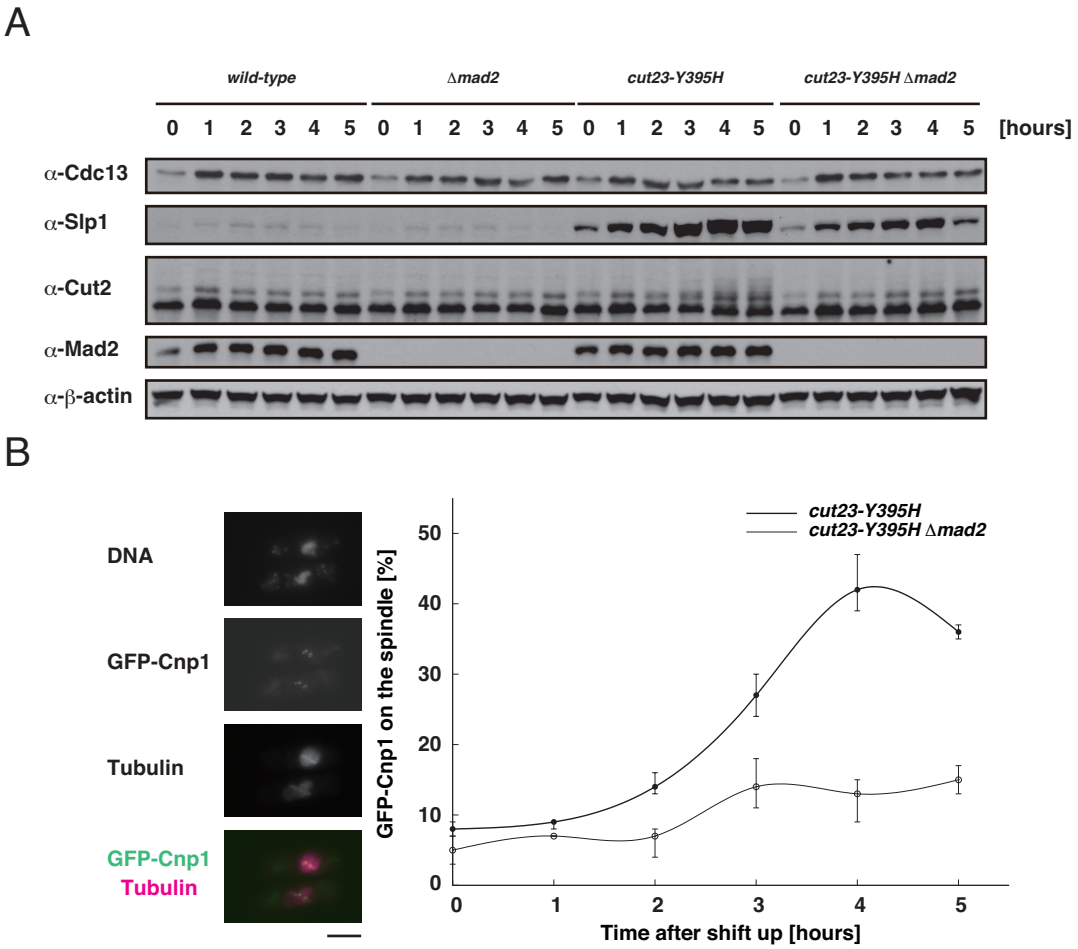


Figure 25 Specific requirement of Cut23 for Slp1 destruction.
(A) Western blot was performed with extracts prepared from cells incubated at 26°C or 36°C for up to 5 hours. The genotype of each strain is indicated on the top. (B) The *cut23-Y395H* mutant cells were incubated for up to 5 hours at the restrictive temperature. The sample taken at 4 hour after the shift was processed for indirect immunofluorescent staining with the aniti-tubulin antibody (magenta). DNA was visualized by staining with DAPI. The position of the centromere (Cnp1-GFP, green) was also examined. The scale bar indicates 5 $\mu$m. The frequency of the cells with Cnp1-GFP on the spindle was also shown at each time point after the shift to the restrictive temperature.

# Discussion

## Multiple E2s and binding modes of Slp1 to APC/C

The present work suggested the specific requirement of Ubc11 and Cut23 for ubiquitination of Slp1. This leads to the conclusion that a kind of cognate E2 or subunit have an additional feature: a selection of substrates for APC/C. As discussed below, in any case, it is probable that the competition and/or collaboration between the two E2s and multiple binding modes of coactivator can result in producing diversity of ubiquitination kinetics and apparent substrate specificity (Figure 26).

### APC/C structure

To date it has been proposed that APC/C cooperates with at least two ubiquitin-conjugating enzymes, Ubc11 and Ubc4 in fission yeast, both of which are individually required for polyubiquitin-chain formation at different steps; the former for initiation, while the latter for elongation (Seino et al., 2003). Based on this prevailing model, a defect of either of the two E2s can be sufficient for stabilization of APC/C substrates including B-type cyclin/*Sp*Cdc13, securin/Cut2 and Cdc20/Slp1. However, this thesis showed that a loss of Ubc11 could inhibit the degradation of Slp1 among the three substrates. Here arises a simple but significant question; What makes the difference between Ubc11- and Ubc4-dependent ubiquitination? One hypothesis follows structural and/or biochemical analyses of APC/C.

To begin with, a previous study reported that UBE2C/UbcH10 binds to APC2 whereas UBE2D1/UbcH5 interacts directly with APC11 (Tang et al., 2001). This divergence is likely to produce the differeince in spatial arrangements, which restricts the respective interaction surfaces, and as a consequence limit the scope for substrate ubiquitinations. Intriguingly, it has been shown that Slp1 can be recruited closer to *Sp*Apc2 than *Sp*Apc11 (Ohi et al., 2007). This can be interpreted that Slp1 is located at the distance that only Ubc11 can interact with and catalyze at least the initiation of ubiquitination. Although the first finding was obtained

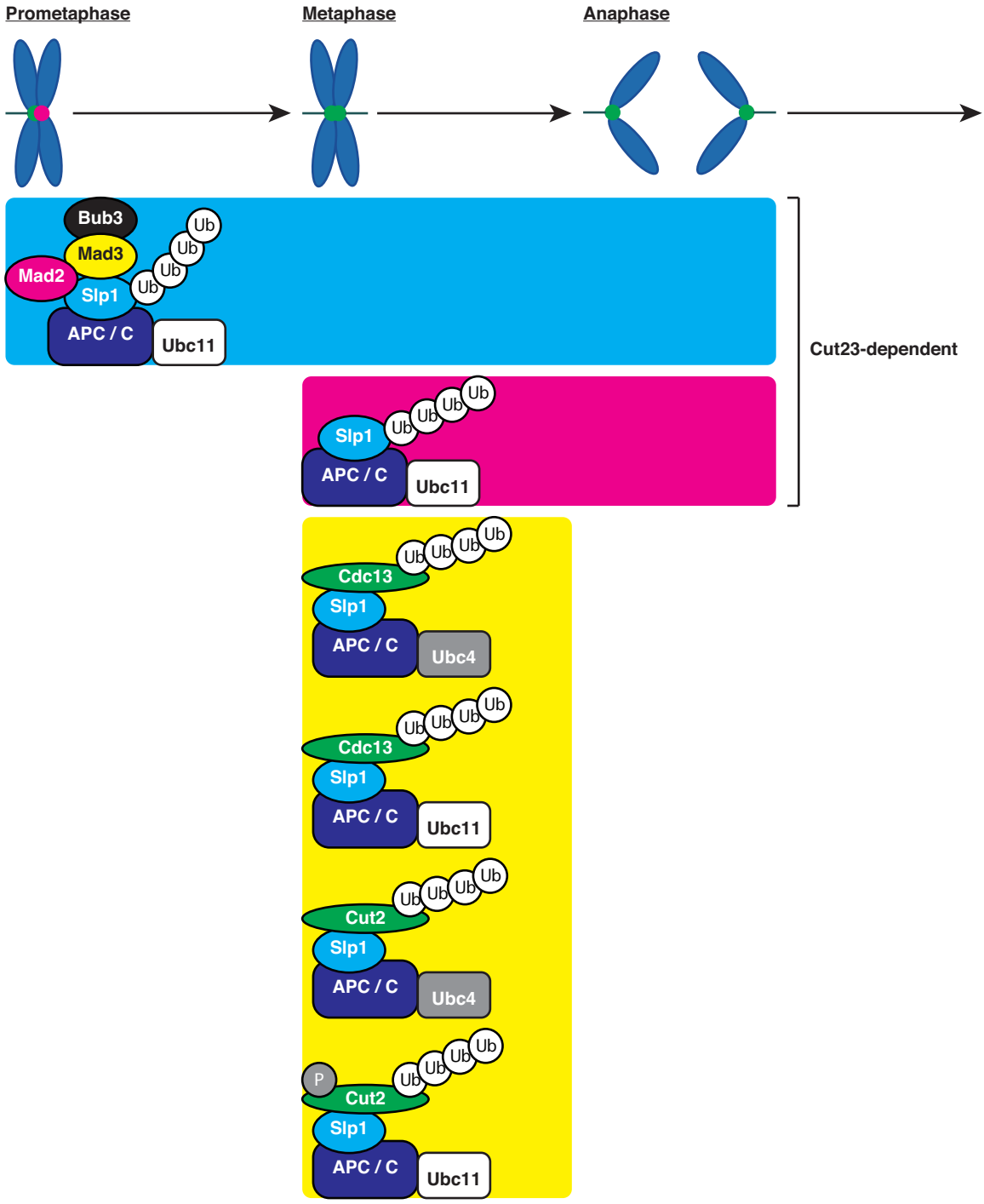


Figure 26 Graphical summary of the present research.
From early mitosis to anaphase, Slp1 is continuously ubiquitinated by Ubc11- and APC/$C^{MCC}$-dependent manner and then degraded. Ubiquitination of Slp1 by APC/$C^{Slp1}$ can also occur after the SAC is satisfied. Cut23 is essential for these two ubiquitination. Ubiquitination of Cdc13 in metaphase can be catalyzed by either Ubc4 or Ubc11. Ubiquitination of non-phosphorylated Cut2 seems to be preferentially mediated by Ubc4, while that of phosphorylated Cut2 by Ubc11.

through *in vitro* binding assay by use of human homologs, if this is also true of the fission yeast APC/C, the presumption could turn to be a persuasive argument.

On the other hand, B-type cyclin and securin are loaded to APC/C via binding with a coactivator (Schwab et al., 1997; Visintin et al., 1997; Fang et al., 1998b; Kramer et al., 1998; Burton and Solomon, 2001; Hilioti et al., 2001; Burton et al., 2005; Kraft et al., 2005; Pfleger and Kirschner, 2000). In these cases, the coactivator might function as a scaffold and localize substrates at accessible space for both E2s. This idea is particularly suppored by the stability of Cdc13 observed in Figure 21B. The separate responsibility for ubiquitination of Cut2 seen in the same experiment might be also attributed to the difference in spatial arrangements. Previous studies reported that ladder bands of Cut2 represent their phosphorylated forms and can be observed upon entry into mitosis (Funabiki et al., 1996b; Aoki et al., 2006). Based on these findings, the results observed in this thesis might suggest that Cut2 can be ubiquitinated in a number of ways and which way is selected from them would be probably determined by the form of Cut2, whether phosphorylated or not, or alternatively whether free or bound to Cut1; There exists a report suggesting that phosphorylation of Pds1 (a homolog of securin in the budding yeast) is required for its efficient binding to Esp1 (a homolog of separase in the budding yeast) (Agarwal and Cohen-Fix, 2002).

Besides, the preceding study has proposed that the SAC causes Cdc20 to bind to different sites on the APC/C and this alters APC/C substrate specificity (Izawa and Pines, 2011). The authors showed that Cdc20 incorporated into MCCs primarily required APC8 to bind to the APC/C, whereas Cdc20 bound to its substrate required APC3 and APC8. The observations, Figure 24 and 25, can be consistently explained by their model and could further revice it. Interacting with its substrate, the Cdc20 binds APC/C by APC3- and APC8-dependent manner. In this case, it is recognized as just a coactivator and only the substrate can be ubiquitinated. Meanwhile, when Cdc20 is free or incorporated into MCC, it interacts with APC/C only through the binding sites on the APC8 subunit. In this case, the Cdc20 can be recognized as a target for ubiquitination.

By the way, a few papers showed that the catalytic subcomplex composed of APC2 and APC11 can solely cooperate with an E2 enzyme to ubiquitinate substrates, securin and B-type cyclin, with very low activity (Gmachl et al., 2000; Tang et al., 2001; Vodermaier et al., 2003). These data were, however, incompatible with the results seen in Figure 19. The authors performed *in vitro* ubiquitination assays by use of recombinant proteins, and therefore it was conclude that they could occur *in vitro*, but do not reflect reactions *in vivo*, at least in the fission yeast cells.

### Ubiquitin topology

Valid speculations can be also led from researches about ubiquitin topology. According to them, frog and human UBE2C/UbcH10 preferentially forms polyubiquitin-chain linked through the 11th lysine residue of ubiqutin itself, K11, while there cannot be observed such bias in Ubc4/UbcH5-mediated ubiquitination (Kirkpatrick et al., 2006; Jin et al., 2008; Garnett et al., 2009; Williamson et al., 2009; Wu et al., 2010). Interestingly, in the budding yeast, which does not have a homolog of UbcH10, the APC/C predominantly generates Lys48-linked ubiquitin chains (Rodrigo-Brenni et al., 2010). A number of structural analyses indeed revealed that the K11-linked and other polyubiquitin-chains adopt distinct structures respectively (Cook et al., 1992; Varadan et al., 2002, 2004; Tenno et al., 2004; Ryabov and Fushman, 2006; Eddins et al., 2007; Sims and Cohen, 2009; Komander et al., 2009; Datta et al., 2009; Weeks et al., 2009; Bremm et al., 2010; Matsumoto et al., 2010; Virdee et al., 2010). Given this, the experimental data can be interpreted that *Sp*Ubc4 also has the ability to ubiquitinate Slp1, but the chain cannot become targeted for proteasomal proteolysis. Additionally, a recent study has suggested that multiple monoubiquitination can also become a degradation signal, at least for Cyclin B1 (Dimova et al., 2012).

A previous report intriguingly provided evidences that the N-terminal extension unique to UbcH10, a striking difference between the two E2s, restricts both polyubiquitination and multiubiquitination (Summers et al., 2008). Ectopic expression of UbcH10 lacking the N-terminal extension overrode an arrest imposed by SAC, suggesting that the N-terminal extension of UbcH10 might play a role in restricting ubiquitination activity when SAC is activated.

## Ubc11-catalyzed ubiquitination and MCCs disassembly

It was demonstrated that the defect of Ubc11 retained Slp1 bound to Mad2 even when the SAC was satisfied. The findings would suggest that it is the Ubc11-mediated ubiquitination that can trigger MCCs disassembly. And in fact, it have been generally accepted that APC/C-dependent ubiquitination reactions is required for MCCs disassembly, even though the target has not been identified yet (Reddy et al., 2007; Nilsson et al., 2008; Mansfeld et al., 2011; Jia et al., 2011; Foster and Morgan, 2012; Uzunova et al., 2012).

Now I would like to think about what the *bona fide* target, called "X" here for convenience, is. The critical point is that the X can be ubiquitinated during the SAC activation. In principle, the APC/C-dependent ubiquitination requires coactivators, by which each substrate can be recruited to APC/C and then ubiquitinated, and

it has been proposed that MCCs prevent the physical interaction between Slp1/Cdc20 and substrates. There, however, exist some exceptions, e.g., Nek2A, which binds directly to the APC/C and is subsequently ubiquitinated (Hayes et al., 2006). This leads to the speculation that the X is also equipped with the ability to bind to APC/C without coactivators. In this regard, paradoxically, the most convincing candidate is to be a component of MCCs. Considering the genetic interaction seen in Figure 11B, it turns to be a choice between the two: Mad2 or BubR1/Mad3. Alternatively, subunits of APC/C themselves are also significant candidates. In particular it has already reported that Cut4 can be ubiquitinated by Ubc11-dependent manner and ubiquitinated Cut4 is not incorporated into APC/C (Yamashita et al., 1996, 1999). Interestingly, the temperature-sensitivity of the *cut4-533* mutant can be also suppressed in the absence of the functional SAC (Kim et al., 1998). Other than this, the character of APC15 is fit with the X; Albeit dispensable for the activity of APC/C, it is required for MCCs disassembly (Mansfeld et al., 2011; Foster and Morgan, 2012; Uzunova et al., 2012).

On the other hand, how the ubiquitination contributes to MCCs disassembly also remains unclear. The simplest model is that this posttranslational modification induces the conformational change of the X and thereby promotes the release of Cdc20 from MCCs. An alternative possibility is that the protein Cdc48/p97/VCP is involved in this reaction. This enzyme is a highly conserved AAA ATPase and acts as a ubiquitin-selective chaperone that segregates ubiquitylated proteins from binding partners or immobile subcellular structures and thereby facilitates their proteasomal degradation (Rape et al., 2001; Ye et al., 2001; Rouiller et al., 2002; Braun et al., 2002; Shcherbik and Haines, 2007). Indeed, it has previously been suggested that *Sp*Cdc48 mediates the release of Cut1 from polyubiquitinated Cut2, which ensures the proteasomal degradation of only Cut2 (Ikai and Yanagida, 2006).

## Why is the regulation of Cdc20/Slp1 a dynamic system?

Previous studies and this thesis have indicated that Cdc20/Slp1 is continuously synthesized and degraded during the SAC activation (Pan and Chen, 2004; Nilsson et al., 2008; Ge et al., 2009; Foster and Morgan, 2012; Uzunova et al., 2012). It has been reported that in the budding yeast cells an excess of this coactivator could override the SAC to induce cell death and thus such regulation is important (Pan and Chen, 2004). The not-so-tight mitotic arrest observed in the *ubc11-P93L* cells (Figure 15 and 16) might be also attributed to an excess of Slp1 against the other components of MCCs and unprogrammed activation of APC/$C^{Slp1}$. Both translation and ubiquitination, however, requires ATP hydrolysis, which seems so wasteful. Nevertheless, why

has this dynamic system been adopted evolutionarily? One group has proposed that it enables the immediate destruction of substrates in response to the SAC satisfaction (Nilsson et al., 2008). In addtion to this, I raise an alternative possibility below.

A preceding research has suggested that Cdc20 requires the CCT chaperonin for its proper folding, without which it becomes dysfunctional (Camasses et al., 2003). This report prompts a strong suspicion that the ubiquitination or even incorporation into MCC denatures Cdc20 irreversibly. If this assumption reflects the fact, continuous synthesis and proteolysis of Cdc20 is conversely the unavoidable process. Besides, it enables not only the maintenance of SAC activation but also quality control of protein coincidentally and promotes energy savings.

## Perspective

As an achievement in the present research, I would like to especially highlight the novel discovery that each of the two E2 enzymes, *Sp*Ubc4 and *Sp*Ubc11, is responsible for collaborating with APC/C for a specific set of substrates. The data are, however, not sufficient for even answering to the above-discussed questions, and therefore further analyses must be performed. Notably, a series of *in vitro* ubiquitination assays can be highly informative experiments and might shed new light on the epoch-making researches about ubiquitin topology, termed "The ubiquitin code". A combination of *in vivo* ubiquitination assay, performed in Figure 21, and mass spectrometry analysis is most likely to yield a lot of beneficial information. It could raise candidates of the *bona fide* target required for MCCs disassembly, and might reveal unexpected role of APC/C or its cofactors. Indeed, it was found that 6 mM or higher concentrations of hydroxyurea, but not X-ray radiation, inhibits the growth of *ubc11-P93L* Δ*mad2* and *ubc11-P93L slp1-mr63* at 36°C, implying the involvement of Ubc11 in DNA replication checkpoint (Figure S1).

I hope some or all of the analyses mentioned above will contribute to the elucidation of the underlying biological significance of "The ubiquitin system", ordinarily observed in every eukaryotes.

# Acknowledgement

I greatly appreciate Prof. Tomohiro Matsumoto and Dr. Toshiyuki Habu for the tutelage, Dr. Andrea Baines, Dr. Kenji Kitamura, Dr. Taro Nakamura, Dr. Jun-ichi Nakayama, Dr. Hiroaki Seino, Dr. Chikashi Shimoda, Dr. Fumiaki Yamao, Dr. Mitsuhiro Yanagida and National BioResource Project[27] for reagents, Dr. Hiro Yamano, Dr. Tadashi Uemura, Dr. Osamu Chisaka, Dr. Jun Takeda, Dr. Tatsuki Kunoh, Dr. Kanji Furuya and colleagues of Radiation Biology Center for discussion and Ms Kyoko Matsui for technical assistance.

*March, 2013*

*Yasnori Holykoshi*

[27] http://yeast.lab.nig.ac.jp/nig/index_en.html

# References


Abrieu, A., Magnaghi-Jaulin, L., Kahana, J., Peter, M., Castro, A., Vigneron, S., Lorca, T., Cleveland, D. and Labbé, J. (2001). Mps1 Is a Kinetochore-Associated Kinase Essential for the Vertebrate Mitotic Checkpoint. Cell *106*, 83–93.

Agarwal, R. and Cohen-Fix, O. (2002). Phosphorylation of the mitotic regulator Pds1/securin by Cdc28 is required for efficient nuclear localization of Esp1/separase. Genes Dev *16*, 1371–82.

Aoki, K., Nakaseko, Y., Kinoshita, K., Goshima, G. and Yanagida, M. (2006). CDC2 Phosphorylation of the Fission Yeast Dis1 Ensures Accurate Chromosome Segregation. Curr Biol *16*, 1627–35.

Aristarkhov, A., Eytan, E., Moghe, A., Admon, A., Hershko, A. and Ruderman, J. (1996). E2-C, a cyclin-selective ubiquitin carrier protein required for the destruction of mitotic cyclins. Proc Natl Acad Sci U S A *93*, 4294–9.

Avery, O., Macleod, C. and McCarty, M. (1944). STUDIES ON THE CHEMICAL NATURE OF THE SUBSTANCE INDUCING TRANSFORMATION OF PNEUMOCOCCAL TYPES : INDUCTION OF TRANSFORMATION BY A DESOXYRIBONUCLEIC ACID FRACTION ISOLATED FROM PNEUMOCOCCUS TYPE III. J Exp Med *79*, 137–58.

Barisic, M., Sohm, B., Mikolcevic, P., Wandke, C., Rauch, V., Ringer, T., Hess, M., Bonn, G. and Geley, S. (2010). Spindly/CCDC99 Is Required for Efficient Chromosome Congression and Mitotic Checkpoint Regulation. Mol Biol Cell *21*, 1968–81.

Beach, D., Rodgers, L. and Gould, J. (1985). *RAN1*$^+$ controls the transition from mitotic division to meiosis in fission yeast. Curr Genet *10*, 297–311.

Bernard, P., Hardwick, K. and Javerzat, J. (1998). Fission Yeast Bub1 Is a Mitotic Centromere Protein Essential for the Spindle Checkpoint and the Preservation of Correct Ploidy through Mitosis. J Cell Biol *143*, 1775–87.

Berry, L., Feoktistova, A., Wright, M. and Gould, K. (1999). The *Schizosaccharomyces pombe dim1*$^+$ Gene Interacts with the Anaphase-Promoting Complex or Cyclosome (APC/C) Component *lid1*$^+$ and Is Required for APC/C Function. Mol Cell Biol *19*, 2535–46.

Blanco, M., Sánchez-Díaz, A., de Prada, J. and Moreno, S. (2000). APC$^{ste9/srw1}$ promotes degradation of mitotic cyclins in $G_1$ and is inhibited by cdc2 phosphorylation. EMBO J *19*, 3945–55.

Boutet, S., Disatnik, M., Chan, L., Iori, K. and Rando, T. (2007). Regulation of Pax3 by Proteasomal Degradation of Monoubiquitinated Protein in Skeletal Muscle Progenitors. Cell *130*, 349–62.

Braun, S., Matuschewski, K., Rape, M., Thoms, S. and Jentsch, S. (2002). Role of the ubiquitin-selective CDC48$^{UFD1/NPL4}$ chaperone (segregase) in ERAD of OLE1 and other substrates. EMBO J *21*, 615–21.

Bremm, A., Freund, S. and Komander, D. (2010). Lys11-linked ubiquitin chains adopt compact conformations and are preferentially hydrolyzed by the deubiquitinase Cezanne. Nat Struct Mol Biol *17*, 939–47.

Burton, J. and Solomon, M. (2001). D box and KEN box motifs in budding yeast Hsl1p are required for APC-mediated degradation and direct binding to Cdc20p and Cdh1p. Genes Dev *15*, 2381–95.

Burton, J. and Solomon, M. (2007). Mad3p, a pseudosubstrate inhibitor of APC$^{Cdc20}$ in the spindle assembly checkpoint. Genes Dev *21*, 655–67.

Burton, J., Tsakraklides, V. and Solomon, M. (2005). Assembly of an APC-Cdh1-Substrate Complex Is Stimulated by Engagement of a Destruction Box. Mol Cell *18*, 533–42.

Buschhorn, B., Petzold, G., Galova, M., Dube, P., Kraft, C., Herzog, F., Stark, H. and Peters, J. (2011). Substrate binding on the APC/C occurs between the coactivator Cdh1 and the processivity factor Doc1. Nat Struct Mol Biol *18*, 6–13.

Camasses, A., Bogdanova, A., Shevchenko, A. and Zachariae, W. (2003). The CCT Chaperonin Promotes Activation of the Anaphase-Promoting Complex through the Generation of Functional Cdc20. Mol Cell *12*, 87–100.

Carroll, C., Enquist-Newman, M. and Morgan, D. (2005). The APC Subunit Doc1 Promotes Recognition of the Substrate Destruction Box. Curr Biol *15*, 11–8.

Carroll, C. and Morgan, D. (2002). The Doc1 subunit is a processivity factor for the anaphase-promoting complex. Nat Cell Biol *4*, 880–7.

Carvallo, L., Muoz, R., Bustos, F., Escobedo, N., Carrasco, H., Olivares, G. and Larraín, J. (2010). Non-canonical Wnt Signaling Induces Ubiquitination and Degradation of Syndecan4. J Biol Chem *285*, 29546–55.

Chan, Y., Fava, L., Uldschmid, A., Schmitz, M., Gerlich, D., Nigg, E. and Santamaria, A. (2009). Mitotic control of kinetochore-associated dynein and spindle orientation by human Spindly. J Cell Biol *185*, 859–74.

Chao, W., Kulkarni, K., Zhang, Z., Kong, E. and Barford, D. (2012). Structure of the mitotic checkpoint complex. Nature *484*, 208–13.

Chen, R., Brady, D., Smith, D., Murray, A. and Hardwick, K. (1999). The Spindle Checkpoint of Budding Yeast Depends on a Tight Complex between the Mad1 and Mad2 Proteins. Mol Biol Cell *10*, 2607–18.

Chen, R., Shevchenko, A., Mann, M. and Murray, A. (1998). Spindle Checkpoint Protein Xmad1 Recruits Xmad2 to Unattached Kinetochores. J Cell Biol *143*, 283–95.

Chen, R., Waters, J., Salmon, E. and Murray, A. (1996). Association of Spindle Assembly Checkpoint Component XMAD2 with Unattached Kinetochores. Science *274*, 242–6.

Ciechanover, A., Elias, S., Heller, H. and Hershko, A. (1982). "Covalent Affinity" Purification of Ubiquitin-activating Enzyme. J Biol Chem *257*, 2537–42.

Ciechanover, A., Heller, H., Katz-Etzion, R. and Hershko, A. (1981). Activation of the heat-stable polypeptide of the ATP-dependent proteolytic system. Proc Natl Acad Sci U S A *78*, 761–5.

Ciosk, R., Zachariae, W., Michaelis, C., Shevchenko, A., Mann, M. and Nasmyth, K. (1998). An ESP1/PDS1 Complex Regulates Loss of Sister Chromatid Cohesion at the Metaphase to Anaphase Transition in Yeast. Cell *93*, 1067–76.

Clute, P. and Pines, J. (1999). Temporal and spatial control of cyclin B1 destruction in metaphase. Nat Cell Biol *1*, 82–7.

Cohen-Fix, O., Peters, J., Kirschner, M. and Koshland, D. (1996). Anaphase initiation in *Saccharomyces cerevisiae* is controlled by the APC-dependent degradation of the anaphase inhibitor Pds1p. Genes Dev *10*, 3081–93.

Cook, W., Jeffrey, L., Carson, M., Chen, Z. and Pickart, C. (1992). Structure of a Diubiquitin Conjugate and a Model for Interaction with Ubiquitin Conjugating Enzyme (E2). J Biol Chem *267*, 16467–71.

Cottarel, G. (1995). The *Saccharomyces cerevisiae HIS3* and *LYS2* genes complement the *Schizosaccharomyces pombe his5-303* and *lys1-131* mutations, respectively: new selectable markers and new multi-purpose multicopy shuttle vectors, pSP3 and pSP4. Curr Genet *28*, 380–3.

Courtheoux, T., Gay, G., Reyes, C., Goldstone, S., Gachet, Y. and Tournier, S. (2007). Dynein participates in chromosome segregation in fission yeast. Biol Cell *99*, 627–37.

da Fonseca, P., Kong, E., Zhang, Z., Schreiber, A., Williams, M., Morris, E. and Barford, D. (2011). Structures of APC/C$^{Cdh1}$ with substrates identify

Cdh1 and Apc10 as the D-box co-receptor. Nature *470*, 274–8.

Damagnez, V., Rolfe, M. and Cottarel, G. (1995). *Schizosaccharomyces pombe* and *Candida albicans* cDNA homologues of the *Saccharomyces cerevisiae UBC4* gene. Gene *155*, 137–8.

Datta, A., Hura, G. and Wolberger, C. (2009). The Structure and Conformation of Lys63-Linked Tetraubiquitin. J Mol Biol *392*, 1117–24.

De Antoni, A., Pearson, C., Cimini, D., Canman, J., Sala, V., Nezi, L., Mapelli, M., Sironi, L., Faretta, M., Salmon, E. and Musacchio, A. (2005). The Mad1/Mad2 Complex as a Template for Mad2 Activation in the Spindle Assembly Checkpoint. Curr Biol *15*, 214–25.

De Domenico, I., Vaughn, M., Li, L., Bagley, D., Musci, G., Ward, D. and Kaplan, J. (2006). Ferroportin-mediated mobilization of ferritin iron precedes ferritin degradation by the proteasome. EMBO J *25*, 5396–404.

den Elzen, N. and Pines, J. (2001). Cyclin A Is Destroyed in Prometaphase and Can Delay Chromosome Alignment and Anaphase. J Cell Biol *153*, 121–36.

Deveraux, Q., Ustrell, V., Pickart, C. and Rechsteiner, M. (1994). A 26 S Protease Subunit That Binds Ubiquitin Conjugates. J Biol Chem *269*, 7059–61.

Dimova, N., Hathaway, N., Lee, B., Kirkpatrick, D., Berkowitz, M., Gygi, S., Finley, D. and King, R. (2012). APC/C-mediated multiple monoubiquitylation provides an alternative degradation signal for cyclin B1. Nat Cell Biol *14*, 168–76.

Dobles, M., Liberal, V., Scott, M., Benezra, R. and Sorger, P. (2000). Chromosome Missegregation and Apoptosis in Mice Lacking the Mitotic Checkpoint Protein Mad2. Cell *101*, 635–45.

Dube, P., Herzog, F., Gieffers, C., Sander, B., Riedel, D., Müller, S., Engel, A., Peters, J. and Stark, H. (2005). Localization of the Coactivator Cdh1 and the Cullin Subunit Apc2 in a Cryo-Electron Microscopy Model of Vertebrate APC/C. Mol Cell *20*, 867–79.

Eddins, M., Varadan, R., Fushman, D., Pickart, C. and Wolberger, C. (2007). Crystal Structure and Solution NMR Studies of Lys48-linked Tetraubiquitin at Neutral pH. J Mol Biol *367*, 204–11.

Espeut, J., Cheerambathur, D., Krenning, L., Oegema, K. and Desai, A. (2012). Microtubule binding by KNL-1 contributes to spindle checkpoint silencing at the kinetochore. J Cell Biol *196*, 469–82.

Fang, G., Yu, H. and Kirschner, M. (1998a). The checkpoint protein MAD2 and the mitotic regulator CDC20 form a ternary complex with the anaphase-promoting complex to control anaphase initiation. Genes Dev *12*, 1871–83.

Fang, G., Yu, H. and Kirschner, M. (1998b). Direct Binding of CDC20 Protein Family Members Activates the Anaphase-Promoting Complex in Mitosis and G1. Mol Cell *2*, 163–71.

Fantes, P. (1979). Epistatic gene interactions in the control of division in fission yeast. Nature *279*, 428–30.

Foe, I., Foster, S., Cheung, S., DeLuca, S., Morgan, D. and Toczyski, D. (2011). Ubiquitination of Cdc20 by the APC Occurs through an Intramolecular Mechanism. Curr Biol *21*, 1870–7.

Foster, S. and Morgan, D. (2012). The APC/C Subunit Mnd2/Apc15 Promotes Cdc20 Autoubiquitination and Spindle Assembly Checkpoint Inactivation. Mol Cell *47*, 921–32.

Funabiki, H., Hagan, I., Uzawa, S. and Yanagida, M. (1993). Cell cycle-dependent Specific Positioning and Clustering of Centromeres and Telomeres in Fission Yeast. J Cell Biol *121*, 961–76.

Funabiki, H., Kumada, K. and Yanagida, M. (1996a). Fission yeast Cut1 and Cut2 are essential for sister chromatid separation, concentrate along the metaphase spindle and form large complexes. EMBO J *15*, 6617–28.

Funabiki, H., Yamano, H., Kumada, K., Nagao, K., Hunt, T. and Yanagida, M. (1996b). Cut2 proteolysis required for sister-chromatid seperation in fission yeast. Nature *381*, 438–41.

Funabiki, H., Yamano, H., Nagao, K., Tanaka, H., Yasuda, H., Hunt, T. and Yanagida, M. (1997). Fission yeast Cut2 required for anaphase has two destruction boxes. EMBO J *16*, 5977–87.

Garnett, M., Mansfeld, J., Godwin, C., Matsusaka, T., Wu, J., Russell, P., Pines, J. and Venkitaraman, A. (2009). UBE2S elongates ubiquitin chains on APC/C substrates to promote mitotic exit. Nat Cell Biol *11*, 1363–9.

Gassmann, R., Essex, A., Hu, J., Maddox, P., Motegi, F., Sugimoto, A., O'Rourke, S., Bowerman, B., McLeod, I., Yates, O., K, C., IM, D. and A (2008). A new mechanism controlling kinetochore-microtubule interactions revealed by comparison of two dynein-targeting components: SPDL-1 and the Rod/Zwilch/Zw10 complex. Genes Dev *22*, 2385–99.

Gassmann, R., Holland, A., Varma, D., Wan, X., Civril, F., Cleveland, D., Oegema, K., Salmon, E. and Desai, A. (2010). Removal of Spindly from microtubule-attached kinetochores controls spindle checkpoint silencing in human cells. Genes Dev *24*, 957–71.

Ge, S., Skaar, J. and Pagano, M. (2009). APC/C- and Mad2-mediated degradation of Cdc20 during spindle checkpoint activation. Cell Cycle *8*, 167–71.

Geley, S., Kramer, E., Gieffers, C., Gannon, J., Peters, J. and Hunt, T. (2001). Anaphase-promoting Complex/Cyclosome-dependent Proteolysis of Human Cyclin A Starts at the Beginning of Mitosis and Is Not Subject to the Spindle Assembly Checkpoint. J Cell Biol *153*, 137–48.

Gietz, D., St Jean, A., Woods, R. and Schiestl, R. (1992). Improved method for high efficiency transformation of intact yeast cells. Nucleic Acids Res *20*, 1425.

Glotzer, M., Murray, A. and Kirschner, M. (1991). Cyclin is degraded by the ubiquitin pathway. Nature *349*, 132–8.

Gmachl, M., Gieffers, C., Podtelejnikov, A., Mann, M. and Peters, J. (2000). The RING-H2 finger protein APC11 and the E2 enzyme UBC4 are sufficient to ubiquitinate substrates of the anaphase-promoting complex. Proc Natl Acad Sci U S A *97*, 8973–8.

Goldknopf, I. and Busch, H. (1977). Isopeptide linkage between nonhistone and histone 2A polypeptides of chromosomal conjugate-protein A24. Proc Natl Acad Sci U S A *74*, 864–8.

Gordon, C., McGurk, G., Wallace, M. and Hastie, N. (1996). A Conditional Lethal Mutant in the Fission Yeast 26 S Protease Subunit *mts3*$^{+}$ Is Defective in Metaphase to Anaphase Transition. J Biol Chem *271*, 5704–11.

Griffis, E., Stuurman, N. and Vale, R. (2007). Spindly, a novel protein essential for silencing the spindle assembly checkpoint, recruits dynein to the kinetochore. J Cell Biol *177*, 1005–15.

Grossberger, R., Gieffers, C., Zachariae, W., Podtelejnikov, A., Schleiffer, A., Nasmyth, K., Mann, M. and Peters, J. (1999). Characterization of the DOC1/APC10 Subunit of the Yeast and the Human Anaphase-promoting Complex. J Biol Chem *274*, 14500–7.

Guacci, V., Koshland, D. and Strunnikov, A. (1997). A Direct Link between Sister Chromatid Cohesion and Chromosome Condensation Revealed through the Analysis of *MCD1* in S. cerevisiae. Cell *91*, 47–57.

Haas, A. and Rose, I. (1982). The Mechanism of Ubiquitin Activating Enzyme. A KINETIC AND EQUILIBRIUM ANALYSIS. J Biol Chem *257*, 10329–37.

Haas, A., Warms, J. and Rose, I. (1983). Ubiquitin Adenylate: Structure and Role in Ubiquitin Activation. Biochemistry *22*, 4388–94.

Habu, T., Kim, S., Weinstein, J. and Matsumoto, T. (2002). Identification of a MAD2-binding protein, CMT2, and its role in mitosis. EMBO J *21*, 6419–28.

Hagting, A., Den Elzen, N., Vodermaier, H., Waizenegger, I., Peters, J. and Pines, J. (2002). Human securin proteolysis is controlled by the spindle checkpoint and reveals when the APC/C switches from activation by Cdc20 to Cdh1. J Cell Biol *157*, 1125–37.

Hall, M., Torres, M., Schroeder, G. and Borchers, C. (2003). Mnd2 and Swm1 Are Core Subunits of

the *Saccharomyces cerevisiae* Anaphase-Promoting Complex. J Biol Chem *278*, 16698–705.

Hames, R., Wattam, S., Yamano, H., Bacchieri, R. and Fry, A. (2001). APC/C-mediated destruction of the centrosomal kinase Nek2A occurs in early mitosis and depends upon a cyclin A-type D-box. EMBO J *20*, 7117–27.

Hardwick, K., Johnston, R., Smith, D. and Murray, A. (2000). *MAD3* Encodes a Novel Component of the Spindle Checkpoint which Interacts with Bub3p, Cdc20p, and Mad2p. J Cell Biol *148*, 871–82.

Hardwick, K. and Murray, A. (1995). Mad1p, a Phosphoprotein Component of the Spindle Assembly Checkpoint in Budding Yeast. J Cell Biol *131*, 709–20.

Hartwell, L. and Weinert, T. (1989). Checkpoints: Controls That Ensure the Order of Cell Cycle Events. Science *246*, 629–34.

Hayes, M., Kimata, Y., Wattam, S., Lindon, C., Mao, G., Yamano, H. and Fry, A. (2006). Early mitotic degradation of Nek2A depends on Cdc20-independent interaction with the APC/C. Nat Cell Biol *8*, 607–14.

He, X., Patterson, T. and Sazer, S. (1997). The *Schizosaccharomyces pombe* spindle checkpoint protein mad2p blocks anaphase and genetically interacts with the anaphase-promoting complex. Proc Natl Acad Sci U S A *94*, 7965–70.

Heinrich, S., Windecker, H., Hustedt, N. and Hauf, S. (2012). Mph1 kinetochore localization is crucial and upstream in the hierarchy of spindle assembly checkpoint protein recruitment to kinetochores. J Cell Sci *125*, 4720–7.

HERSHEY, A. and CHASE, M. (1952). INDEPENDENT FUNCTIONS OF VIRAL PROTEIN AND NUCLEIC ACID IN GROWTH OF BACTERIOPHAGE. J Gen Physiol *36*, 39–56.

Hershko, A., Ciechanover, A., Heller, H., Haas, A. and Rose, I. (1980). Proposed role of ATP in protein breakdown: Conjugation of protein with multiple chains of the polypeptide of ATP-dependent proteolysis. Proc Natl Acad Sci U S A *77*, 1783–6.

Hershko, A., Ganoth, D., Pehrson, J., Palazzo, R. and Cohen, L. (1991). Methylated Ubiquitin Inhibits Cyclin Degradation in Clam Embryo Extracts. J Biol Chem *266*, 16376–9.

Hershko, A., Ganoth, D., Sudakin, V., Dahan, A., Cohen, L., Luca, F., Ruderman, J. and Eytan, E. (1994). Components of a System That Ligates Cyclin to Ubiquitin and Their Regulation by the Protein Kinase cdc2. J Biol Chem *269*, 4940–6.

Hershko, A., Heller, H., Elias, S. and Ciechanover, A. (1983). Components of Ubiquitin-Protein Ligase System. RESOLUTION, AFFINITY PURIFICATION, AND ROLE IN PROTEIN BREAKDOWN. J Biol Chem *258*, 8206–14.

Hershko, A., Heller, H., Eytan, E., Kaklij, G. and Rose, I. (1984). Role of the $\alpha$-amino group of protein in ubiquitin-mediated protein breakdown. Proc Natl Acad Sci U S A *81*, 7021–5.

Hershko, A., Heller, H., Eytan, E. and Reiss, Y. (1986). The Protein Substrate Binding Site of the Ubiquitin-Protein Ligase System. J Biol Chem *261*, 11992–9.

Hershko, A., Leshinsky, E., Ganoth, D. and Heller, H. (1984). ATP-dependent degradation of ubiquitin-protein conjugates. Proc Natl Acad Sci U S A *81*, 1619–23.

Herzog, F., Primorac, I., Dube, P., Lenart, P., Sander, B., Mechtler, K., Stark, H. and Peters, J. (2009). Structure of the Anaphase-Promoting Complex/Cyclosome Interacting with a Mitotic Checkpoint Complex. Science *323*, 1477–81.

Hilioti, Z., Chung, Y., Mochizuki, Y., Hardy, C. and Cohen-Fix, O. (2001). The anaphase inhibitor Pds1 binds to the APC/C-associated protein Cdc20 in a destruction box-dependent manner. Curr Biol *11*, 1347–52.

Hirano, T., Funahashi, S., Uemura, T. and Yanagida, M. (1986). Isolation and characterization of *Schizosaccharomyces pombe cut* mutants that block nuclear division but not cytokinesis. EMBO J *5*, 2973–2979.

Hirano, T., Hiraoka, Y. and Yanagida, M. (1988). A Temperature-sensitive Mutation of the *Schizosaccharomyces pombe* Gene *nuc*$2^{+}$ That Encodes a

Nuclear Scaffold-like Protein Blocks Spindle Elongation in Mitotic Anaphase. J Cell Biol *106*, 1171–83.

Hiraoka, Y., Toda, T. and Yanagida, M. (1984). The *NDA3* gene of Fission Yeast Encodes $\beta$-Tubulin: A Cold-Sensitive *nda3* Mutation Reversibly Blocks Spindle Formation and Chromosome Movement in Mitosis. Cell *39*, 349–58.

Honda, K., Mihara, H., Kato, Y., Yamaguchi, A., Tanaka, H., Yasuda, H., Furukawa, K. and Urano, T. (2000). Degradation of human Aurora2 protein kinase by the anaphase-promoting complex-ubiquitin-proteasome pathway. Oncogene *19*, 2812–9.

Hough, R., Pratt, G. and Rechsteiner, M. (1986). Ubiquitin-Lysozyme Conjugates. IDENTIFICATION AND CHARACTERIZATION OF AN ATP-DEPENDENTPROTEASE FROM RABBIT RETICULOCYTE LYSATES. J Biol Chem *261*, 2400–8.

Hough, R. and Rechsteiner, M. (1984). Effects of temperature on the degradation of proteins in rabbit reticulocyte lysates and after injection into HeLa cells. Proc Natl Acad Sci U S A *81*, 90–4.

Howell, B., Hoffman, D., Fang, G., Murray, A. and Salmon, E. (2000). Visualization of Mad2 Dynamics at Kinetochores, along Spindle Fibers, and at Spindle Poles in Living Cells. J Cell Biol *150*, 1233–50.

Howell, B., McEwen, B., Canman, J., Hoffman, D., Farrar, E., Rieder, C. and Salmon, E. (2001). Cytoplasmic dynein/dynactin drives kinetochore protein transport to the spindle poles and has a role in mitotic spindle checkpoint inactivation. J Cell Biol *155*, 1159–72.

Howell, B., Moree, B., Farrar, E., Stewart, S., Fang, G. and Salmon, E. (2004). Spindle Checkpoint Protein Dynamics at Kinetochores in Living Cells. Curr Biol *14*, 953–64.

Hsu, J., Reimann, J., Sørensen, C., Lukas, J. and Jackson, P. (2002). E2F-dependent accumulation of hEmi1 regulates S phase entry by inhibiting $APC^{Cdh1}$. Nat Cell Biol *4*, 358–66.

Hwang, L. and Murray, A. (1997). A Novel Yeast Screen for Mitotic Arrest Mutants Identifies *DOC1*, a New Gene Involved in Cyclin Proteolysis. Mol Biol Cell *8*, 1877–87.

Ikai, N. and Yanagida, M. (2006). Cdc48 is required for the stability of Cut1/separase in mitotic anaphase. J Struct Biol *156*, 50–61.

Ikui, A., Furuya, K., Yanagida, M. and Matsumoto, T. (2002). Control of localization of a spindle checkpoint protein, Mad2, in fission yeast. J Cell Sci *115*, 1603–10.

Irniger, S., Piatti, S., Michaelis, C. and Nasmyth, K. (1995). Genes Involved in Sister Chromatid Separation Are Needed for B-type Cyclin Proteolysis in Budding Yeast. Cell *81*, 269–78.

Izawa, D. and Pines, J. (2011). How APC/C-Cdc20 changes its substrate specificity in mitosis. Nat Cell Biol *13*, 223–33.

Jablonski, S., Chan, G., Cooke, C., Earnshaw, W. and Yen, T. (1998). The hBUB1 and hBUBR1 kinases sequentially assemble onto kinetochores during prophase with hBUBR1 concentrating at the kinetochore plates in mitosis. Chromosoma *107*, 386–96.

Jaspersen, S., Charles, J. and Morgan, D. (1999). Inhibitory phosphorylation of the APC regulator Hct1 is controlled by the kinase Cdc28 and the phosphatase Cdc14. Curr Biol *9*, 227–36.

Jensen, R., Sprague, H. and I (1983). Regulation of yeast mating-type interconversion: Feedback control of *HO* gene expression by the mating-type locus. Proc Natl Acad Sci U S A *80*, 3035–9.

Jia, L., Li, B., Warrington, R., Hao, X., Wang, S. and Yu, H. (2011). Defining pathways of spindle checkpoint silencing: functional redundancy between Cdc20 ubiquitination and $p31^{comet}$. Mol Biol Cell *22*, 4227–4235.

Jin, L., Williamson, A., Banerjee, S., Philipp, I. and Rape, M. (2008). Mechanism of Ubiquitin-Chain Formation by the Human Anaphase-Promoting Complex. Cell *133*, 653–65.

Kallio, M., Beardmore, V., Weinstein, J. and Gorbsky, G. (2002). Rapid microtubule-independent dynamics of Cdc20 at kinetochores and centrosomes in mammalian cells. J Cell Biol *158*, 841–7.

Kang, J., Yang, M., Li, B., Qi, W., Zhang, C., Shokat, K., Tomchick, D., Machius, M. and Yu, H. (2008). Structure and Substrate Recruitment of the Human Spindle Checkpoint Kinase Bub1. Mol Cell *32*, 394–405.

Kawashima, S., Yamagishi, Y., Honda, T., Ishiguro, K. and Watanabe, Y. (2010). Phosphorylation of H2A by Bub1 Prevents Chromosomal Instability Through Localizing Shugoshin. Science *327*, 172–7.

Kim, S., Lin, D., Matsumoto, S., Kitazono, A. and Matsumoto, T. (1998). Fission Yeast Slp1: An Effector of the Mad2-Dependent Spindle Checkpoint. Science *279*, 1045–7.

King, E., Rachidi, N., Morrice, N., Hardwick, K. and Stark, M. (2007). Ipl1p-dependent phosphorylation of Mad3p is required for the spindle checkpoint response to lack of tension at kinetochores. Genes Dev *21*, 1163–8.

King, R., Peters, J., Tugendreich, S., Rolfe, M., Hieter, P. and Kirschner, M. (1995). A 20S Complex Containing CDC27 and CDC16 Catalyzes the Mitosis-Specific Conjugation of Ubiquitin to Cyclin B. Cell *81*, 279–88.

Kirkpatrick, D., Hathaway, N., Hanna, J., Elsasser, S., Rush, J., Finley, D., King, R. and Gygi, S. (2006). Quantitative analysis of *in vitro* ubiquitinated cyclin B1 reveals complex chain topology. Nat Cell Biol *8*, 700–10.

Komander, D., Reyes-Turcu, F., Licchesi, J., Odenwaelder, P., Wilkinson, K. and Barford, D. (2009). Molecular discrimination of structurally equivalent Lys 63-linked and linear polyubiquitin chains. EMBO Rep *10*, 466–73.

Kominami, K., Seth-Smith, H. and Toda, T. (1998). Apc10 and Ste9/Srw1, two regulators of the APC-cyclosome, as well as the CDK inhibitor Rum1 are required for $G_1$ cell-cycle arrest in fission yeast. EMBO J *17*, 5388–99.

Kops, G., van der Voet, M., van der Voet, M., Manak, M., van Osch, M., Naini, S., Brear, A., McLeod, I., Hentschel, D., Yates, v. d. H., S, S. and JV (2010). APC16 is a conserved subunit of the anaphase-promoting complex/cyclosome. J Cell Sci *123*, 1623–33.

Kraft, C., Vodermaier, H., Maurer-Stroh, S., Eisenhaber, F. and Peters, J. (2005). The WD40 Propeller Domain of Cdh1 Functions as a Destruction Box Receptor for APC/C Substrates. Mol Cell *18*, 543–53.

Kramer, E., Gieffers, C., Hölzl, G., Hengstschläger, M. and Peters, J. (1998). Activation of the human anaphase-promoting complex by proteins of the CDC20/Fizzy family. Curr Biol *8*, 1207–10.

Kramer, E., Scheuringer, N., Podtelejnikov, A., Mann, M. and Peters, J. (2000). Mitotic Regulation of the APC Activator Proteins CDC20 and CDH1. Mol Biol Cell *11*, 1555–69.

Kravtsova-Ivantsiv, Y., Cohen, S. and Ciechanover, A. (2009). Modification by Single Ubiquitin Moieties Rather Than Polyubiquitination Is Sufficient for Proteasomal Processing of the p105 NF-$\kappa$B Precursor. Mol Cell *33*, 496–504.

Lamb, J., Michaud, W., Sikorski, R. and Hieter, P. (1994). Cdc16p, Cdc23p and Cdc27p form a complex essential for mitosis. EMBO J *13*, 4321–8.

Lampson, M., Renduchitala, K., Khodjakov, A. and Kapoor, T. (2004). Correcting improper chromosome-spindle attachments during cell division. Nat Cell Biol *6*, 232–7.

Leverson, J., Joazeiro, C., Page, A., Huang, H., Hieter, P. and Hunter, T. (2000). The APC11 RING-H2 finger Mediates E2-Dependent Ubiquitination. Mol Biol Cell *11*, 2315–25.

Li, Y. and Benezra, R. (1996). Identification of a Human Mitotic Checkpoint Gene: *hsMAD2*. Science *274*, 246–8.

Lin, Y., Hwang, W. and Basavappa, R. (2002). Structural and Functional Analysis of the Human Mitotic-specific Ubiquitin-conjugating Enzyme, UbcH10. J Biol Chem *277*, 21913–21.

Lindon, C. and Pines, J. (2004). Ordered proteolysis in anaphase inactivates Plk1 to contribute to proper mitotic exit in human cells. J Cell Biol *164*, 233–41.

Liu, D., Vader, G., Vromans, M., Lampson, M. and Lens, S. (2009). Sensing Chromosome Bi-Orientation by Spatial Separation of Aurora B Kinase from Kinetochore Substrates. Science *323*, 1350–3.

Liu, D., Vleugel, M., Backer, C., Hori, T., Fukagawa, T., Cheeseman, I. and Lampson, M. (2010). Regulated targeting of protein phosphatase 1 to the outer kinetochore by KNL1 opposes Aurora B kinase. J Cell Biol *188*, 809–20.

London, N., Ceto, S., Ranish, J. and Biggins, S. (2012). Phosphoregulation of Spc105 by Mps1 and PP1 Regulates Bub1 Localization to Kinetochores. Curr Biol *22*, 900–6.

Longtine, M., McKenzie, D., DJ, S., NG, W., A, B., A, P., P, P. and JR (1998). Additional Modules for Versatile and Economical PCR-based Gene Deletion and Modification in *Saccharomyces cerevisiae*. Yeast *14*, 953–61.

Luo, X., Fang, G., Coldiron, M., Lin, Y., Yu, H., Kirschner, M. and Wagner, G. (2000). Structure of the Mad2 spindle assembly checkpoint protein and its interaction with Cdc20. Nat Struct Biol *7*, 224–9.

Luo, X., Tang, Z., Rizo, J. and Yu, H. (2002). The Mad2 Spindle Checkpoint Protein Undergoes Similar Major Conformational Changes Upon Binding to Either Mad1 or Cdc20. Mol Cell *9*, 59–71.

Luo, X., Tang, Z., Xia, G., Wassmann, K., Matsumoto, T., Rizo, J. and Yu, H. (2004). The Mad2 spindle checkpoint protein has two distinct natively folded states. Nat Struct Mol Biol *11*, 338–45.

Mansfeld, J., Collin, P., Collins, M., Choudhary, J. and Pines, J. (2011). APC15 drives the turnover of MCC-CDC20 to make the spindle assembly checkpoint responsive to kinetochore attachment. Nat Cell Biol *13*, 1234–43.

Mapelli, M., Filipp, F., Rancati, G., Massimiliano, L., Nezi, L., Stier, G., Hagan, R., Confalonieri, S., Piatti, S., Sattler, M. and Musacchio, A. (2006). Determinants of conformational dimerization of Mad2 and its inhibition by p31$^{comet}$. EMBO J *25*, 1273–84.

Mapelli, M., Massimiliano, L., Santaguida, S. and Musacchio, A. (2007). The Mad2 Conformational Dimer: Structure and Implications for the Spindle Assembly Checkpoint. Cell *131*, 730–43.

Matsumoto, M., Wickliffe, K., Dong, K., Yu, C., Bosanac, I., Bustos, D., Phu, L., Kirkpatrick, D., Hymowitz, S., Rape, M., Kelley, R. and Dixit, V. (2010). K11-Linked Polyubiquitination in Cell Cycle Control Revealed by a K11 Linkage-Specific Antibody. Mol Cell *39*, 477–84.

Matsumoto, T. (1997). A Fission Yeast Homolog of CDC20/p55$^{CDC}$/Fizzy Is Required for Recovery from DNA Damage and Genetically Interacts with p34$^{cdc2}$. Mol Cell Biol *17*, 742–50.

Matsuyama, A., Shirai, A. and Yoshida, M. (2008). A series of promoters for constitutive expression of heterologous genes in fission yeast. Yeast *25*, 371–6.

Matyskiela, M. and Morgan, D. (2009). Analysis of Activator-Binding Sites on the APC/C Supports a Cooperative Substrate-Binding Mechanism. Mol Cell *34*, 68–80.

Maundrell, K. (1990). *nmt1* of fission yeast. A HIGHLY TRANSCRIBED GENE COMPLETELY REPRESSED BY THIAMINE. J Biol Chem *265*, 10857–64.

Maundrell, K. (1993). Thiamine-repressible expression vectors pREP and pRIP for fission yeast. Gene *123*, 127–30.

Meadows, J., Shepperd, L., Vanoosthuyse, V., Lancaster, T., Sochaj, A., Buttrick, G., Hardwick, K. and Millar, J. (2011). Spindle Checkpoint Silencing Requires Association of PP1 to Both Spc7 and Kinesin-8 Motors. Dev Cell *20*, 739–50.

Michaelis, C., Ciosk, R. and Nasmyth, K. (1997). Cohesins: Chromosomal Proteins that Prevent Premature Separation of Sister Chromatids. Cell *91*, 35–45.

Millband, D. and Hardwick, K. (2002). Fission Yeast Mad3p Is Required for Mad2p To Inhibit the Anaphase-Promoting Complex and Localizes to Kinetochores in a Bub1p-, Bub3p-, and Mph1p-Dependent Manner. Mol Cell Biol *22*, 2728–42.

Miller, J., Summers, M., Hansen, D., Nachury, M., Lehman, N., Loktev, A. and Jackson, P. (2006). Emi1 stably binds and inhibits the anaphase-promoting complex/cyclosome as a pseudosubstrate inhibitor. Genes Dev *20*, 2410–20.

Miniowitz-Shemtov, S., Eytan, E., Ganoth, D., Sitry-Shevah, D., Dumin, E. and Hershko, A. (2012). Role of phosphorylation of Cdc20 in p31$^{comet}$-stimulated disassembly of the mitotic checkpoint complex. Proc Natl Acad Sci U S A *109*, 8056–60.

Nakamura, T., Nakamura-Kubo, M., Hirata, A. and Shimoda, C. (2001). The *Schizosaccharomyces pombe spo3*$^{+}$ Gene Is Required for Assembly of the Forespore Membrane and Genetically Interacts with *psy1*$^{+}$-encoding Syntaxin-like Protein. Mol Biol Cell *12*, 3955–72.

Nilsson, J., Yekezare, M., Minshull, J. and Pines, J. (2008). The APC/C maintains the spindle assembly checkpoint by targeting Cdc20 for destruction. Nat Cell Biol *10*, 1411–20.

Ohi, M., Feoktistova, A., Ren, L., Yip, C., Cheng, Y., Chen, J., Yoon, H., Wall, J., Huang, Z., Penczek, P., Gould, K. and Walz, T. (2007). Structural Organization of the Anaphase-Promoting Complex Bound to the Mitotic Activator Slp1. Mol Cell *28*, 871–85.

Okazaki, K., Okazaki, N., Kume, K., Jinno, S., Tanaka, K. and Okayama, H. (1990). High-frequency transformation method and library transducing vectors for cloning mammalian cDNAs by *trans*-complementation of *Schizosaccharomyces pombe*. Nucleic Acids Res *18*, 6485–9.

Osaka, F., Seino, H., Seno, T. and Yamao, F. (1997). A Ubiquitin-Conjugating Enzyme in Fission Yeast That Is Essential for the Onset of Anaphase in Mitosis. Mol Cell Biol *17*, 3388–97.

Pan, J. and Chen, R. (2004). Spindle checkpoint regulates Cdc20p stability in *Saccharomyces cerevisiae*. Genes Dev *18*, 1439–51.

Passmore, L. and Barford, D. (2005). Coactivator functions in a stoichiometric complex with anaphase-promoting complex/cyclosome to mediate substrate recognition. EMBO Rep *6*, 873–8.

Passmore, L., McCormack, E., Au, S., Paul, A., Willison, K., Harper, J. and Barford, D. (2003). Doc1 mediates the activity of the anaphase-promoting complex by contributing to substrate recognition. EMBO J *22*, 786–96.

Peters, J., King, R., Höög, C. and Kirschner, M. (1996). Identification of BIME as a Subunit of the AnaphasePpromoting Complex. Science *274*, 1199–201.

Pfleger, C. and Kirschner, M. (2000). The KEN box: an APC recognition signal distinct from the D box targeted by Cdh1. Genes Dev *14*, 655–65.

Pickart, C. and Rose, I. (1985). Functional Heterogeneity of Ubiquitin Carrier Proteins. J Biol Chem *260*, 1573–81.

Pinsky, B., Kung, C., Shokat, K. and Biggins, S. (2006). The Ipl1-Aurora protein kinase activates the spindle checkpoint by creating unattached kinetochores. Nat Cell Biol *8*, 78–83.

Pinsky, B., Nelson, C. and Biggins, S. (2009). Protein Phosphatase 1 Regulates Exit from the Spindle Checkpoint in Budding Yeast. Curr Biol *19*, 1182–7.

Posch, M., Khoudoli, G., Swift, S., King, E., Deluca, J. and Swedlow, J. (2010). Sds22 regulates aurora B activity and microtubule-kinetochore interactions at mitosis. J Cell Biol *191*, 61–74.

Prinz, S., Hwang, E., Visintin, R. and Amon, A. (1998). The regulation of Cdc20 proteolysis reveals a role for APC components Cdc23 and Cdc27 during S phase and early mitosis. Curr Biol *8*, 750–60.

Rape, M., Hoppe, T., Gorr, I., Kalocay, M., Richly, H. and Jentsch, S. (2001). Mobilization of Processed, Membrane-Tethered SPT23 Transcription Factor by CDC48$^{UFD1/NPL4}$, a Ubiquitin-Selective Chaperone. Cell *107*, 667–77.

Rape, M. and Kirschner, M. (2004). Autonomous regulation of the anaphase-promoting complex couples mitosis to S-phase entry. Nature *432*, 588–95.

Reddy, S., Rape, M., Margansky, W. and Kirschner, M. (2007). Ubiquitination by the anaphase-promoting complex drives spindle checkpoint inactivation. Nature *446*, 921–5.

Reimann, J., Freed, E., Hsu, J., Kramer, E., Peters, J. and Jackson, P. (2001a). Emi1 Is a Mitotic Regulator that Interacts with Cdc20 and Inhibits the Anaphase Promoting Complex. Cell *105*, 645–55.

Reimann, J., Gardner, B., Margottin-Goguet, F. and Jackson, P. (2001b). Emi1 regulates the anaphase-promoting complex by a different mechanism than Mad2 proteins. Genes Dev *15*, 3278–85.

Rieder, C., Cole, R., Khodjakov, A. and Sluder, G. (1995). The Checkpoint Delaying Anaphase in Response to Chromosome Monoorientation Is Mediated by an Inhibitory Signal Produced by Unattached Kinetochores. J Cell Biol *130*, 941–8.

Rieder, C., Schultz, A., Cole, R. and Sluder, G. (1994). Anaphase Onset in Vertebrate Somatic Cells Is Controlled by a Checkpoint That Monitors Sister Kinetochore Attachment to the Spindle. J Cell Biol *127*, 1301–10.

Rodrigo-Brenni, M., Foster, S. and Morgan, D. (2010). Catalysis of Lysine 48-Specific Ubiquitin Chain Assembly by Residues in E2 and Ubiquitin. Mol Cell *39*, 548–559.

Rosenberg, J., Cross, F. and Funabiki, H. (2011). KNL1/Spc105 Recruits PP1 to Silence the Spindle Assembly Checkpoint. Curr Biol *21*, 942–7.

Rouiller, I., DeLaBarre, B., May, A., Weis, W., Brunger, A., Milligan, R. and Wilson-Kubalek, E. (2002). Conformational changes of the multifunction p97 AAA ATPase during its ATPase cycle. Nat Struct Biol *9*, 950–7.

Ryabov, Y. and Fushman, D. (2006). Interdomain Mobility in Di-Ubiquitin Revealed by NMR. Proteins *63*, 787–96.

Salimian, K., Ballister, E., Smoak, E., Wood, S., Panchenko, T., Lampson, M. and Black, B. (2011). Feedback Control in Sensing Chromosome Biorientation by the Aurora B Kinase. Curr Biol *21*, 1158–65.

Samejima, I. and Yanagida, M. (1994). Bypassing Anaphase by Fission Yeast *cut9* Mutation: Requirement of *cut9*$^{+}$ to Initiate Anaphase. J Cell Biol *127*, 1655–70.

Scaërou, F., Starr, D., Piano, F., Papoulas, O., Karess, R. and Goldberg, M. (2001). The ZW10 and Rough Deal checkpoint proteins function together in a large, evolutionarily conserved complex targeted to the kinetochore. J Cell Sci *114*, 3103–14.

Schwab, M., Lutum, A. and Seufert, W. (1997). Yeast Hct1 Is a Regulator of Clb2 Cyclin Proteolysis. Cell *90*, 683–93.

Schwab, M., Neutzner, M., Möcker, D. and Seufert, W. (2001). Yeast Hct1 recognizes the mitotic cyclin Clb2 and other substrates of the ubiquitin ligase APC. EMBO J *20*, 5165–75.

Seino, H., Kishi, T., Nishitani, H. and Yamao, F. (2003). Two Ubiquitin-Conjugating Enzymes, UbcP1/Ubc4 and UbcP4/Ubc11, Have Distinct Functions for Ubiquitination of Mitotic Cyclin. Mol Cell Biol *23*, 3497–505.

Seufert, W. and Jentsch, S. (1990). Ubiquitin-conjugating enzymes UBC4 and UBC5 mediate selective degradation of short-lived and abnormal proteins. EMBO J *9*, 543–50.

Shaeffer, J. (1994). Monoubiquitinated $\alpha$ Globin Is an Intermediate in the ATP-dependent Proteolysis of $\alpha$ Globin. J Biol Chem *269*, 22205–10.

Shah, J., Botvinick, E., Bonday, Z., Furnari, F., Berns, M. and Cleveland, D. (2004). Dynamics of Centromere and Kinetochore Proteins; Implications for Checkpoint Signaling and Silencing. Curr Biol *14*, 942–52.

Shcherbik, N. and Haines, D. (2007). Cdc48p$^{Npl4p/Ufd1p}$ Binds and Segregates Membrane-Anchored/Tethered Complexes via a Polyubiquitin Signal Present on the Anchors. Mol Cell *25*, 385–97.

Shepperd, L., Meadows, J., Sochaj, A., Lancaster, T., Zou, J., Buttrick, G., Rappsilber, J., Hardwick, K. and Millar, J. (2012). Phosphodependent Recruitment of Bub1 and Bub3 to Spc7/KNL1 by Mph1

Kinase Maintains the Spindle Checkpoint. Curr Biol *22*, 891–9.

Shirayama, M., Zachariae, W., Ciosk, R. and Nasmyth, K. (1998). The Polo-like kinase Cdc5p and the WD-repeat protein Cdc20p/fizzy are regulators and substrates of the anaphase promoting complex in *Saccharomyces cerevisiae*. EMBO J *17*, 1336–49.

Sims, J. and Cohen, R. (2009). Linkage-Specific Avidity Defines the Lysine 63-Linked Polyubiquitin-Binding Preference of Rap80. Mol Cell *33*, 775–83.

Sironi, L., Mapelli, M., Knapp, S., De Antoni, A., Jeang, K. and Musacchio, A. (2002). Crystal structure of the tetrameric Mad1-Mad2 core complex: implications of a 'safety belt' binding mechanism for the spindle checkpoint. EMBO J *21*, 2496–506.

Sørensen, C., Lukas, C., Kramer, E., Peters, J., Bartek, J. and Lukas, J. (2001). A Conserved Cyclin-Binding Domain Determines Functional Interplay between Anaphase-Promoting Complex-Cdh1 and Cyclin A-Cdk2 during Cell Cycle Progression. Mol Cell Biol *21*, 3692–703.

Starr, D., Williams, B., Hays, T. and Goldberg, M. (1998). ZW10 Helps Recruit Dynactin and Dynein to the Kinetochore. J Cell Biol *142*, 763–74.

Stewart, S. and Fang, G. (2005). Destruction Box-Dependent Degradation of Aurora B Is Mediated by the Anaphase-Promoting Complex/Cyclosome and Cdh1. Cancer Res *65*, 8730–5.

Sudakin, V., Chan, G. and Yen, T. (2001). Checkpoint inhibition of the APC/C in HeLa cells is mediated by a complex of BUBR1, BUB3, CDC20, and MAD2. J Cell Biol *154*, 925–36.

Sudakin, V., Ganoth, D., Dahan, A., Heller, H., Hershko, J., Luca, F., Ruderman, J. and Hershko, A. (1995). The Cyclosome, a Large Complex Containing Cyclin-Selective Ubiquitin Ligase Activity, Targets Cyclins for Destruction at the End of Mitosis. Mol Biol Cell *6*, 185–97.

Suijkerbuijk, S., Vleugel, M., Teixeira, A. and Kops, G. (2012). Integration of Kinase and Phosphatase Activities by BUBR1 Ensures Formation of Stable Kinetochore-Microtubule Attachments. Dev Cell *23*, 745–55.

Summers, M., Pan, B., Mukhyala, K. and Jackson, P. (2008). The Unique N Terminus of the UbcH10 E2 Enzyme Controls the Threshold for APC Activation and Enhances Checkpoint Regulation of the APC. Mol Cell *31*, 544–56.

Takayama, Y., Mamnun, Y., Trickey, M., Dhut, S., Masuda, F., Yamano, H., Toda, T. and Saitoh, S. (2010). Hsk1- and SCF$^{Pof3}$-Dependent Proteolysis of *S. pombe* Ams2 Ensures Histone Homeostasis and Centromere Function. Dev Cell *18*, 385–96.

Takayama, Y., Sato, H., Saitoh, S., Ogiyama, Y., Masuda, F. and Takahashi, K. (2008). Biphasic Incorporation of Centromeric Histone CENP-A in Fission Yeast. Mol Biol Cell *19*, 682–90.

Tanaka, K., Yonekawa, T., Kawasaki, Y., Kai, M., Furuya, K., Iwasaki, M., Murakami, H., Yanagida, M. and Okayama, H. (2000). Fission Yeast Eso1p Is Required for Establishing Sister Chromatid Cohesion during S Phase. Mol Cell Biol *20*, 3459–69.

Tang, Z., Li, B., Bharadwaj, R., Zhu, H., Ozkan, E., Hakala, K., Deisenhofer, J. and Yu, H. (2001). APC2 Cullin Protein and APC11 RING Protein Comprise the Minimal Ubiquitin Ligase Module of the Anaphase-promoting Complex. Mol Biol Cell *12*, 3839–51.

Tang, Z., Shu, H., Oncel, D., Chen, S. and Yu, H. (2004). Phosphorylation of Cdc20 by Bub1 Provides a Catalytic Mechanism for APC/C Inhibition by the Spindle Checkpoint. Mol Cell *16*, 387–97.

Tange, Y. and Niwa, O. (2008). *Schizosaccharomyces pombe* Bub3 Is Dispensable for Mitotic Arrest Following Perturbed Spindle Formation. Genetics *179*, 785–92.

Taylor, S., Ha, E. and McKeon, F. (1998). The Human Homologue of Bub3 Is Required for Kinetochore Localization of Bub1 and a Mad3/Bub1-related Protein Kinase. J Cell Biol *142*, 1–11.

Taylor, S. and McKeon, F. (1997). Kinetochore Localization of Murine Bub1 Is Required for Normal Mitotic Timing and Checkpoint Response to Spindle Damage. Cell *89*, 727–35.

Teichner, A., Eytan, E., Sitry-Shevah, D., Miniowitz-Shemtov, S., Dumin, E., Gromis, J. and Hershko, A. (2011). p31$^{comet}$ promotes disassembly of the mitotic checkpoint complex in an ATP-dependent process. Proc Natl Acad Sci U S A *108*, 3187–92.

Tenno, T., Fujiwara, K., Tochio, H., Iwai, K., Morita, E., Hayashi, H., Murata, S., Hiroaki, H., Sato, M., Tanaka, K. and Shirakawa, M. (2004). Structural basis for distinct roles of Lys63- and Lys48-linked polyubiquitin chains. Genes Cells *9*, 865–75.

Thornton, B., Ng, T., Matyskiela, M., Carroll, C., Morgan, D. and Toczyski, D. (2006). An architectural map of the anaphase-promoting complex. Genes Dev *20*, 449–60.

Thrower, J., Hoffman, L., Rechsteiner, M. and Pickart, C. (2000). Recognition of the polyubiquitin proteolytic signal. EMBO J *19*, 94–102.

Tian, W., Li, B., Warrington, R., Tomchick, D., Yu, H. and Luo, X. (2012). Structural analysis of human Cdc20 supports multisite degron recognition by APC/C. Proc Natl Acad Sci U S A *109*, 18419–24.

Tugendreich, S., Tomkiel, J., Earnshaw, W. and Hieter, P. (1995). CDC27Hs Colocalizes with CDC16Hs to the Centrosome and Mitotic Spindle and Is Essential for the Metaphase to Anaphase Transition. Cell *81*, 261–8.

Uhlmann, F., Lottspeich, F. and Nasmyth, K. (1999). Sister-chromatid separation at anaphase onset is promoted by cleavage of the cohesin subunit Scc1. Nature *400*, 37–42.

Uhlmann, F., Wernic, D., Poupart, M., Koonin, E. and Nasmyth, K. (2000). Cleavage of Cohesin by the CD Clan Protease Separin Triggers Anaphase in Yeast. Cell *103*, 375–86.

Uzunova, K., Dye, B., Schutz, H., Ladurner, R., Petzold, G., Toyoda, Y., Jarvis, M., Brown, N., Poser, I., Novatchkova, M., Mechtler, K., Hyman, A., Stark, H., Schulman, B. and Peters, J. (2012). APC15 mediates CDC20 autoubiquitylation by APC/C$^{MCC}$ and disassembly of the mitotic checkpoint complex. Nat Struct Mol Biol *19*, 1116–23.

Vanoosthuyse, V. and Hardwick, K. (2009). A Novel Protein Phosphatase 1-Dependent Spindle Checkpoint Silencing Mechanism. Curr Biol *19*, 1176–81.

Vanoosthuyse, V., Meadows, J., van der Sar, S., Millar, J. and Hardwick, K. (2009). Bub3p Facilitates Spindle Checkpoint Silencing in Fission Yeast. Mol Biol Cell *20*, 5096–105.

Varadan, R., Assfalg, M., Haririnia, A., Raasi, S., Pickart, C. and Fushman, D. (2004). Solution Conformation of Lys$^{63}$-linked Di-ubiquitin Chain Provides Clues to Functional Diversity of Polyubiquitin Signaling. J Biol Chem *279*, 7055–63.

Varadan, R., Walker, O., Pickart, C. and Fushman, D. (2002). Structural Properties of Polyubiquitin Chains in Solution. J Mol Biol *324*, 637–47.

Vink, M., Simonetta, M., Transidico, P., Ferrari, K., Mapelli, M., De Antoni, A., Massimiliano, L., Ciliberto, A., Faretta, M., Salmon, E. and Musacchio, A. (2006). In Vitro FRAP Identifies the Minimal Requirements for Mad2 Kinetochore Dynamics. Curr Biol *16*, 755–66.

Virdee, S., Ye, Y., Nguyen, D., Komander, D. and Chin, J. (2010). Engineered diubiquitin synthesis reveals Lys29-isopeptide specificity of an OTU deubiquitinase. Nat Chem Biol *6*, 750–7.

Visintin, R., Prinz, S. and Amon, A. (1997). *CDC20* and *CDH1*: A Family of Substrate-Specific Activators of APC-Dependent Proteolysis. Science *278*, 460–3.

Vodermaier, H., Gieffers, C., Maurer-Stroh, S., Eisenhaber, F. and Peters, J. (2003). TPR Subunits of the Anaphase-Promoting Complex Mediate Binding to the Activator Protein CDH1. Curr Biol *13*, 1459–68.

Wassmann, K. and Benezra, R. (1998). Mad2 transiently associates with an APC/p55Cdc complex during mitosis. Proc Natl Acad Sci U S A *95*, 11193–8.

WATSON, J. and CRICK, F. (1953). MOLECULAR STRUCTURE OF NUCLEIC ACIDS: A structure for Deoxyribose Nucleic Acid. Nature *171*, 737–8.

Weeks, S., Grasty, K., Hernandez-Cuebas, L. and Loll, P. (2009). Crystal structures of Lys-63-linked tri- and di-ubiquitin reveal a highly extended chain architecture. Proteins *77*, 753–9.

Welburn, J., Vleugel, M., Liu, D., Yates, L., MA, F., T, C. and IM (2010). Aurora B Phosphorylates Spatially Distinct Targets to Differentially Regulate the Kinetochore-Microtubule Interface. Mol Cell *38*, 383–92.

Westhorpe, F., Tighe, A., Lara-Gonzalez, P. and Taylor, S. (2011). p31$^{comet}$-mediated extraction of Mad2 from the MCC promotes efficient mitotic exit. J Cell Sci *124*, 3905–16.

Williams, B., Karr, T., Montgomery, J. and Goldberg, M. (1992). The *Drosophila l(1)zw10* Gene Product, Required for Accurate Mitotic Chromosome Segregation, Is Redistributed at Anaphase Onset. J Cell Biol *118*, 759–73.

Williamson, A., Wickliffe, K., Mellone, B., Song, L., Karpen, G. and Rape, M. (2009). Identification of a physiological E2 module for the human anaphase-promoting complex. Proc Natl Acad Sci U S A *106*, 18213–8.

Windecker, H., Langegger, M., Heinrich, S. and Hauf, S. (2009). Bub1 and Bub3 promote the conversion from monopolar to bipolar chromosome attachment independently of shugoshin. EMBO Rep *10*, 1022–8.

Wu, T., Merbl, Y., Huo, Y., Gallop, J., Tzur, A. and Kirschner, M. (2010). UBE2S drives elongation of K11-linked ubiquitin chains by the Anaphase-Promoting Complex. Proc Natl Acad Sci U S A *107*, 1355–60.

Xia, G., Luo, X., Habu, T., Rizo, J., Matsumoto, T. and Yu, H. (2004). Conformation-specific binding of p31$^{comet}$ antagonizes the function of Mad2 in the spindle checkpoint. EMBO J *23*, 3133–43.

Yamada, H., Kumada, K. and Yanagida, M. (1997). Distinct subunit functions and cell cycle regulated phosphorylation of 20S APC/cyclosome required for anaphase in fission yeast. J Cell Sci *110 ( Pt 15)*, 1793–804.

Yamada, H., Matsumoto, S. and Matsumoto, T. (2000). High dosage expression of a zinc finger protein, Grt1, suppresses a mutant of fission yeast *slp1*$^{+}$, a homolog of CDC20/p55CDC/Fizzy. J Cell Sci *113 ( Pt 22)*, 3989–99.

Yamagishi, Y., Yang, C., Tanno, Y. and Watanabe, Y. (2012). MPS1/Mph1 phosphorylates the kinetochore protein KNL1/Spc7 to recruit SAC components. Nat Cell Biol *14*, 746–52.

Yamaguchi, S., Okayama, H. and Nurse, P. (2000). Fission yeast Fizzy-related protein srw1p is a $G_1$-specific promoter of mitotic cyclin B degradation. EMBO J *19*, 3968–77.

Yamamoto, T., Watanabe, S., Essex, A. and Kitagawa, R. (2008). SPDL-1 functions as a kinetochore receptor for MDF-1 in *Caenorhabditis elegans*. J Cell Biol *183*, 187–94.

Yamano, H., Gannon, J. and Hunt, T. (1996). The role of proteolysis in cell cycle progression in *Schizosaccharomyces pombe*. EMBO J *15*, 5268–79.

Yamashita, Y., Nakaseko, Y., Kumada, K., Nakagawa, T. and Yanagida, M. (1999). Fission yeast APC/cyclosome subunits, Cut20/Apc4 and Cut23/Apc8, in regulating metaphase-anaphase progression and cellular stress responses. Genes Cells *4*, 445–63.

Yamashita, Y., Nakaseko, Y., Samejima, I., Kumada, K., Yamada, H., Michaelson, D. and Yanagida, M. (1996). 20S cyclosome complex formation and proteolytic activity inhibited by the cAMP/PKA pathway. Nature *384*, 276–9.

Yang, M., Li, B., Tomchick, D., Machius, M., Rizo, J., Yu, H. and Luo, X. (2007). p31$^{comet}$ Blocks Mad2 Activation through Structural Mimicry. Cell *131*, 744–55.

Ye, Y., Meyer, H. and Rapoport, T. (2001). The AAA ATPase Cdc48/p97 and its partners transport proteins from the ER into the cytosol. Nature *414*, 652–6.

Yin, H., Gui, Y., Du, G., Frohman, M. and Zheng, X. (2010). Dependence of Phospholipase D1 Multimonoubiquitination on Its Enzymatic Activity and Palmitoylation. J Biol Chem *285*, 13580–8.

Yoon, H., Feoktistova, A., Wolfe, B., Jennings, J., Link, A. and Gould, K. (2002). Proteomics Analysis Identifies New Components of the Fission and Budding Yeast Anaphase-Promoting Complexes. Curr Biol *12*, 2048–54.

Yu, H., King, R., Peters, J. and Kirschner, M. (1996). Identification of a novel ubiquitin-conjugating enzyme involved in mitotic cyclin degradation. Curr Biol *6*, 455–66.

Yu, H., Peters, J., King, R., Page, A., Hieter, P. and Kirschner, M. (1998). Identification of a Cullin Homology Region in a Subunit of the Anaphase-Promoting Complex. Science *279*, 1219–22.

Zachariae, W., Schwab, M., Nasmyth, K. and Seufert, W. (1998a). Control of Cyclin Ubiquitination by CDK-Regulated Binding of Hct1 to the Anaphase Promoting Complex. Science *282*, 1721–4.

Zachariae, W., Shevchenko, A., Andrews, P., Ciosk, R., Galova, M., Stark, M., Mann, M. and Nasmyth, K. (1998b). Mass Spectrometric Analysis of the Anaphase-Promoting Complex from Yeast: Identification of a Subunit Related to Cullins. Science *279*, 1216–9.

Zachariae, W., Shin, T., Galova, M., Obermaier, B. and Nasmyth, K. (1996). Identification of Subunits of the Anaphase-Promoting Complex of *Saccharomyces cerevisiae*. Science *274*, 1201–4.

Zich, J., Sochaj, A., Syred, H., Milne, L., Cook, A., Ohkura, H., Rappsilber, J. and Hardwick, K. (2012). Kinase Activity of Fission Yeast Mph1 is Required for Mad2 and Mad3 to Stably Bind the Anaphase Promoting Complex. Curr Biol *22*, 296–301.

Zou, H., McGarry, T., Bernal, T. and Kirschner, M. (1999). Identification of a Vertebrate Sister-Chromatid Separation Inhibitor Involved in Transformation and Tumorigenesis. Science *285*, 418–22.

## Supplemental Information

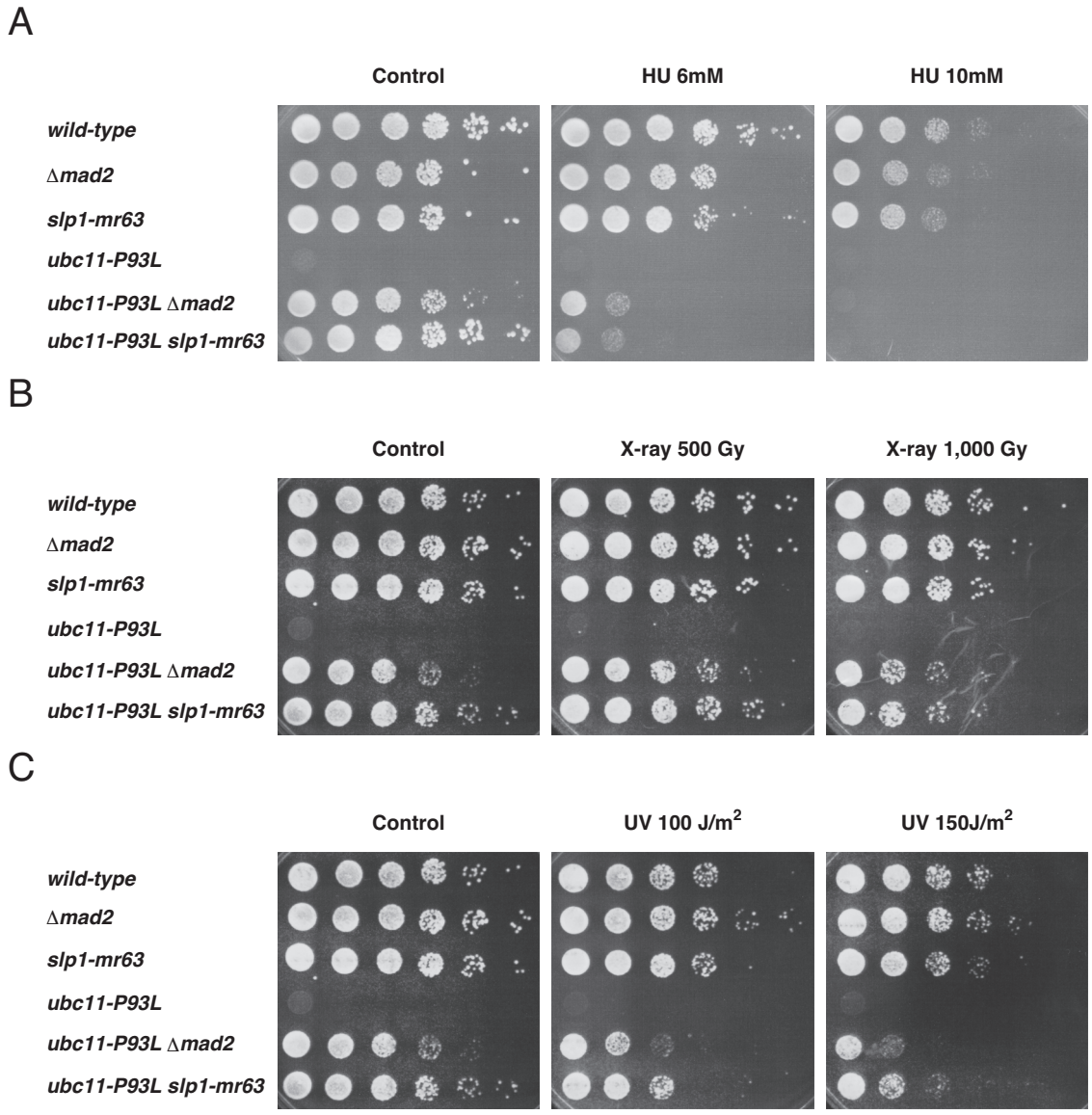


Figure S 1 The sensitivity of *ubc11-P93L* mutants to DNA damage agents.
The wild-type strain, Δ*mad2*, *slp1-mr63*, *ubc11-P93L*, *ubc11-P93L* Δ*mad2* and *ubc11-P93L slp1-mr63* strains were examined for their sensitivity to DNA damage agents. The plates were incubated at 36°C for 4 days. (A) The sensitivity to hydroxyurea (HU). They were grown in liquid YEA and spotted on YEA media containing indicated concentration of HU. (B) The sensitivity to X-ray radiation. They were grown in liquid YEA, irradiated with indicated doses of X-ray and then spotted on YEA media. (C) The sensitivity to ultraviolet (UV) radiation. They were grown in liquid YEA, spotted on YEA media and thereafter irradiated with indicated doses of UV.